

# Chemical Strategies To Design Textured Materials: from Microporous and Mesoporous Oxides to Nanonetworks and Hierarchical Structures

Galo J. de A. A. Soler-Illia,<sup>†</sup> Clément Sanchez,<sup>\*,†</sup> Bénédicte Lebeau,<sup>‡</sup> and Joël Patarin<sup>‡</sup>

Laboratoire de Chimie de la Matière Condensée, CNRS UMR 7574, Université Pierre et Marie Curie, 4 Place Jussieu, 75252 Paris Cedex 05, France, and Laboratoire de Matériaux Minéraux, CNRS UMR CNRS-A 7016, ENSCMu, 3 rue A. Werner, 68093 Mulhouse Cedex

Received May 6, 2002

## Contents

1. Introduction	4093	5. Perspectives and Concluding Remarks	4132
2. Crystalline Microporous Materials	4095	6. References	4134
2.1. Introduction	4095		
2.2. Porous Solids	4095		
2.3. Zeolites and Related Microporous Solids	4095		
2.3.1. Definition and Structural Delimitation	4095		
2.3.2. Synthesis Strategies of Microporous Crystalline Phases	4096		
2.3.3. Formation Mechanisms of Microporous Crystalline Phases	4097		
2.3.4. Properties and Applications of Zeolitic Materials	4098		
3. Mesoporous Materials: Using Supramolecular Templates To Enhance Pore Size	4099		
3.1. Introduction	4099		
3.2. Synthesis Tools for Mesostructure Production	4100		
3.2.1. Synthesis Strategies	4100		
3.2.2. Self-Assembling Templates	4102		
3.3. Silica-Based Structures	4107		
3.3.1. Evolution of the Research	4107		
3.3.2. Formation of the Inorganic Network	4108		
3.3.3. Formation Mechanisms	4110		
3.3.4. Stability of the Inorganic Network	4114		
3.3.5. Thermal Treatment and Porosity	4114		
3.4. Non-Silica Mesostructured Materials	4114		
3.4.1. Synthesis Strategies for Non-Silica Oxide-Based Structures: Evolution of the Research	4115		
3.4.2. Control of the Formation of the Inorganic Network	4115		
3.4.3. Formation Mechanisms	4123		
3.4.4. Stability of the Inorganic Network: from Consolidated Hybrids to Mesoporous Phases	4127		
4. Multiscale Texturation	4128		
4.1. Phase Separation, Cooperative Autoassembly, and Topological Defects	4128		
4.2. Micromolding and Cooperative Self-Assembly	4129		
4.3. Biotemplates and Cooperative Self-Assembly	4130		
4.4. Organogel/Metal Oxide Hybrids	4130		

## 1. Introduction

Nanosciences will be, as biology, one of the fields that will contribute to a high level of scientific and technological development along the 21st century. Nanostructured inorganic, organic, or hybrid organic–inorganic nanocomposites present paramount advantages to facilitate integration and miniaturization of the devices (nanotechnologies), thus affording a direct connection between the inorganic, organic, and biological worlds. The ability to assemble and organize inorganic, organic, and even biological components in a single material represents an exciting direction for developing novel multifunctional materials presenting a wide range of novel properties.<sup>1</sup>

Soft chemistry based processes (i.e., chemistry at low temperatures and pressures, from molecular or colloidal precursors) clearly offer innovative strategies to obtain tailored nanostructured materials. The mild conditions of sol–gel chemistry provide reacting systems mostly under kinetic control. Therefore, slight changes of experimental parameters (i.e., pH, concentrations, temperatures, nature of the solvent, counterions) can lead to substantial modifications of the resulting supramolecular assemblies. This may give rise to inorganic or hybrid solids with enormous differences in morphology and structure and, hence, in their properties.<sup>2–4</sup> However, the resulting nanostructures, their degree of organization, and thus their properties certainly depend on the chemical nature of their organic and inorganic components, but they also rely on the synergy between these components. Thus, the tuning of the nature, the extent, the accessibility, and the curvature of the hybrid interfaces is a key point in the design of new nanostructured materials. The growth of soft chemistry derived inorganic or hybrid networks templated by organized surfactant assemblies (*structure directing agents*) allowed construction of a new family of nanostructured materials in the mesoscopic scale (2–100 nm): the best example is the ever-growing family of meso-organized hybrids or mesoporous inorganic materials.<sup>5–17</sup>

Moreover, recently, micromolding methods have been developed, in which the use of emulsion drop-

\* Author to whom correspondence should be addressed [telephone +33 (0) 144275534; fax +33 (0) 144274769; e-mail clem@ccr.jussieu.fr].

<sup>†</sup> Laboratoire de Chimie de la Matière Condensée.

<sup>‡</sup> Laboratoire de Matériaux Minéraux.



The first contact Galo Juan de Avila Arturo Soler-Illia (born in Buenos Aires, May 31, 1970) had with chemistry was when he burned his parents' dining table with sulfuric acid, at the age of five. Since then, he obtained his Licenciatura en Quimica (1989/1993) at the University of Buenos Aires (UBA), where he also received his Ph.D. in chemistry (1994/1998), supervised by Dr. M. A. Blesa, in the precipitation mechanisms of mixed metal oxide precursors from solution. During his postdoctoral research in Paris with Dr. Clément Sanchez, he worked in nanocomposite hybrid materials, particularly in the synthesis and formation mechanisms of transition metal oxide-based mesostructured and mesoporous phases. He also worked in applications for mesoporous thin films for St Gobain Recherche, Paris. At present, he is moving to the Chemistry Unit of the Comisión Nacional de Energía Atómica, in Buenos Aires, Argentina, as a CONICET staff scientist. His main current interests are the development of novel nano- and mesostructured multifunctional materials, as well as the exploration of their complex synthesis routes, which combine sol-gel chemistry and self-assembly. He has been fellow of CONICET, UBA, and Fundación Antorchas. He is coauthor of about 30 publications and illustrations for 3 books. He is a member of the MRS, CONICET (Argentina), and Gabbos.

lets, latex beads, bacterial threads, colloidal templates, or organogelators leads to control of the shapes of complex objects in the micrometer scale.<sup>18–25</sup>

These synthesis procedures are inspired by those observed to take place in natural systems. Indeed, for some hundreds of million years, nature has been producing extremely performing materials (magnetotactical bacteria, ferritine, teeth, bone, shells, etc.) by making use of highly selective structures. The construction of these complex structures is promoted by specific chemical links, as well as by a rich and varied set of conformations and topologies. For example, it is well-known that the highly efficient recognition processes in biology (e.g., antibody/antigen or enzymatic behavior) depend on the spatial distribution (tertiary structures) at the nanometric level, as well as on the molecular scale interactions. Learning the "savoir faire" of these particular living systems and organisms from understanding their rules and transcription modes could lead us to be able to design and build novel materials. These new compounds will bear improved or entirely new capabilities, far more efficient than the conventional materials that we are able to synthesize nowadays. An ambitious project has been undertaken by several research groups with diverse origin (biologists, chemists, physicists, ...), who aim to understand the construction processes of mineral objects that take place within hybrid interfaces that play a structuring and functional role. The first results, concerning the tailored design and construction of mineral-based or organomineral hybrid-based frameworks, are indeed



Clément Sanchez, born in 1949, is Director of Research at the French Council Research (CNRS) and has a teaching professor position at l'Ecole Polytechnique (Palaiseau). He received an engineer degree from l'Ecole Nationale Supérieure de Chimie de Paris in 1978 and a thèse d'état (Ph.D.) in physical chemistry from the University of Paris VI in 1981. He did postdoctoral work at the University of California, Berkeley, and is currently performing research at the University Pierre and Marie Curie in Paris. He specializes in the field of chemistry and physical properties of transition metal oxide gels. He currently heads a research group of about 10 scientists working on sol-gel chemistry of transition metal alkoxides and synthesis of new hybrid organic inorganic materials. His main interests are the study of the relationship between optical, mechanical properties and hybrid material structures. More recently he has focused a part of his research on the study of self-assembly processes to build hybrid organic-inorganic materials textured at different length scales. He was organizer of several international meetings [The First European Meeting on Hybrid Materials, (1993); Materials Research Symposia: Better Ceramics Through Chemistry VI (1994); Hybrid Organic-Inorganic Materials B.C.T.C. VII (1996); Hybrid Materials (1998); and Hybrid Organic-Inorganic Materials (2000 and 2002)]. He is also a member of the Materials Research Society and the Société Chimique de France. Since 2001 he has been Editor in Chief of the *New Journal of Chemistry* (RSC). He is the author or coauthor of over 250 scientific publications and 15 patents. He has also given over 50 invited lectures in international meetings. He has taken the direction of the "Laboratoire de Chimie de la Matière Condensée" (University of Paris 6) since 1999.



Since 1998, Bénédicte Lebeau has been a Centre National de la Recherche Scientifique (CNRS) research scientist at the Laboratoire de Matériaux Minéraux in Mulhouse (Université de Haute Alsace, France). Her current research is focused on the synthesis of highly ordered porous silica and aluminosilicate materials. Her primary interest is the modification of these solids by covalent coupling of organic functions on the inorganic network. She carried out graduate work with Dr. Clément Sanchez at the University Pierre and Marie Curie in Paris, specializing in the synthesis and characterization of sol-gel hybrid materials for optics applications. After earning her Ph.D. degree in 1995, she worked on the control of the morphology of hydroxyapatite crystals in the Dr. Sanchez's research group as a Rhodia-Lafarge-Bouygue postdoctoral fellow, after which she carried out postdoctoral research in the biomimetism area with Prof. Stephen Mann at the University of Bath, U.K.



Joël Patarin is a director of research at the National Center of Scientific Research (CNRS) and head director of the Laboratory of Inorganic Materials at the Chemistry School, Université de Haute-Alsace, Mulhouse (France). His research focuses on the synthesis of porous inorganic materials with controlled pore size such as crystalline microporous solids [zeolites and related materials (gallophosphates, zincophosphates, ...)] and organized mesoporous solids. In particular, he was involved in the synthesis of the large-pore gallophosphate cloverite whose structure displays a three-dimensional channel system with pore openings delimited by 20-membered rings. In the past few years, his group has devoted a major effort in the synthesis of these porous solids in fluoride medium. Patarin studied chemistry at Nantes University, completing his diploma thesis on the synthesis of titanosilicates in 1985. He obtained a CNRS position as researcher the same year and joined the group of Professor R. Wey at the Laboratory of Inorganic Materials of Mulhouse. In particular, he worked on the synthesis of iron-containing zeolites and obtained his Ph.D. degree in 1988. In 1995, he prepared his habilitation to follow researches and was named director of research in 1997. Since 1999, he has been the head director of the laboratory. Dr. Patarin is the author or coauthor of over 100 research papers, 13 patents, and more than 130 communications. He is a member of the editorial board of *Microporous and Mesoporous Materials*, a member of the International Zeolite Association, and a member of the French Zeolite Group. Dr. Patarin can be reached at the Laboratoire des Matériaux Minéraux, Ecole Nationale Supérieure de Chimie de Mulhouse, Université de Haute-Alsace, 3 rue Alfred Werner, 68093 Mulhouse, France, and by e-mail at J.Patarin@uha.fr.

encouraging. These efforts should permit improved understanding of the complex mechanisms involved in biomineralization processes that remain currently unknown.<sup>9,26–30</sup>

Zeolites and related porous solids, silica, and hybrid mesostructured composites, obtained by combination of all these methods, are the best examples of the state of the art of these approaches.<sup>5,13,17,27,30,31–34</sup> Without doubt, these strategies will give birth to a constellation of innovative advanced materials with promising applications in many fields: optics, electronics, ionics, mechanics, membranes, protective coatings, catalysis, sensors, and biological applications (immobilization, recognition, drug delivery, etc.).<sup>35</sup>

## 2. Crystalline Microporous Materials

### 2.1. Introduction

A great number of natural materials are characterized by a negatively charged mineral framework, bearing cavities, cages, or tunnels where water molecules or inorganic cations (as charge-compensating ions) are occluded. Among these solids, zeolites (from the greek, *zein*, to boil, and *lithos*, stone) define the great family of crystalline microporous

aluminosilicates, presenting pore sizes of  $d < 1$  nm. The applications of these microporous materials are widespread. Although mostly aimed at industrial catalytic processes (i.e., chemical and petroleum industries), zeolites also hold their place in everyday life (phosphate-free cleaning products, isolating purposes, etc.). Indeed, these solids are very efficient as selective ion-exchange agents and sorbents, due to the high mobility of water and cations and their high and well-defined porosity. These remarkable properties explain the interest of hundreds of research groups worldwide, in the quest for the study and development of novel materials with controlled porosity.

The first synthesis procedures involved aluminosilicate gels as precursors and strong alkaline conditions, using a great variety of mineral bases. A great number of novel structures (aluminosilicates or related materials such as phosphate-based microporous solids, etc.) have been obtained by introducing organic molecules (generally N-based compounds) into the reaction mixtures. These organic moieties act as *molecular templates*, around which the inorganic phase is built. There is a close relationship between the morphology of the organic template and the morphology of the cavities or channels of the inorganic structure. In this way, it is possible to synthesize an amazing set of microporous solids, with crystalline walls of variable composition and microstructure, from organomineral gels.

### 2.2. Porous Solids

According to the classification made by IUPAC,<sup>36</sup> porous solids can be arranged in three main categories, depending on their pore size (diameter,  $d$ ), in micro- ( $d < 2$  nm), meso- ( $2 \text{ nm} < d < 50$  nm), and macroporous materials ( $d > 50$  nm). Some illustrative examples are given in Figure 1. In this section, we will focus on microporous materials, particularly on zeolites. Further on, we will discuss silica- and non-silica-based mesoporous solids,<sup>37</sup> which present sharp pore distributions.

### 2.3. Zeolites and Related Microporous Solids

#### 2.3.1. Definition and Structural Delimitation

Zeolites constitute by themselves one of the most important families of crystalline microporous solids. The original name was initially given to natural aluminosilicates belonging to the class of tectosilicates. The latter are built up from a three-dimensional array of tetrahedral units  $\text{TO}_4$  ( $\text{T} = \text{Si}, \text{Al}$ ), each oxygen atom bridging two tetrahedra. However, the main difference between zeolites and the other members of the tectosilicate family (feldspar) is the presence of channels and cavities of molecular dimensions, which are in contact with the external medium. To preserve electroneutrality, alkaline (or alkaline-earth) cations are present within these cavities, as well as water. The general formula of these aluminosilicates can be considered to be  $\text{M}_{2/n}\text{O}, \text{Al}_2\text{O}_3, x\text{SiO}_2, y\text{H}_2\text{O}$ , where M is one cation of valence  $n$  and  $x \geq 2$ .

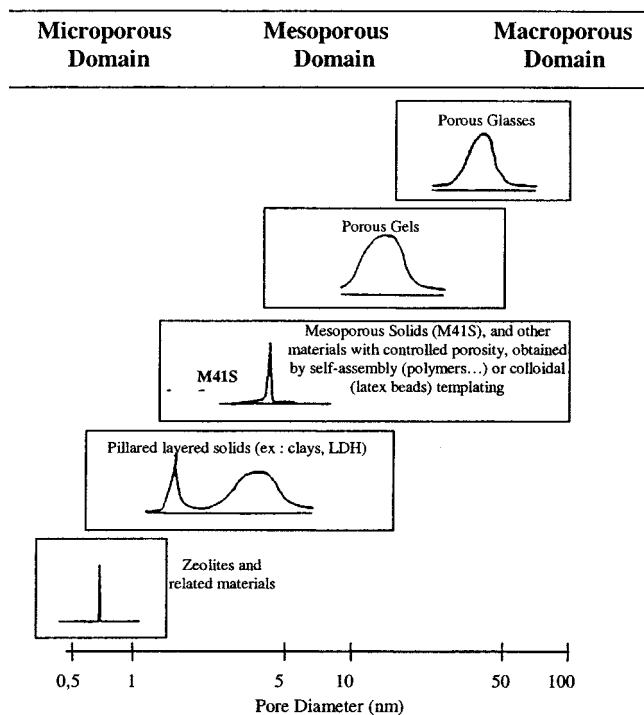


**Figure 1.** Examples of micro-, meso-, and macroporous materials, showing pore size domains and typical pore size distributions.

In the past 60 years, there has been a sustained interest in the synthesis of these materials, in view of their properties and their applications in catalysis or sorption. The first synthesis procedures were performed by alkaline treatment of aluminosilicate gels, in the presence of mineral bases. The introduction of nitrogen-containing bases (or alkylammonium cations) in the reaction mixtures provided an interesting breakthrough. New zeolite-type structures were created, as well as new families of materials, bearing or not an isostructural relationship with zeolites. This is the case of the microporous aluminophosphate molecular sieves, developed by Union Carbide,  $\text{AlPO}_4\text{-n}$ ,<sup>38</sup> or derived materials, obtained by incorporation of Si,<sup>39</sup> Me (Me = Co, Fe, Mg, Mn, Zn), or El (El = As, B, Be, Ga, Ti, Li).<sup>40</sup> The classification of these compounds is sketched in Figure 2. After

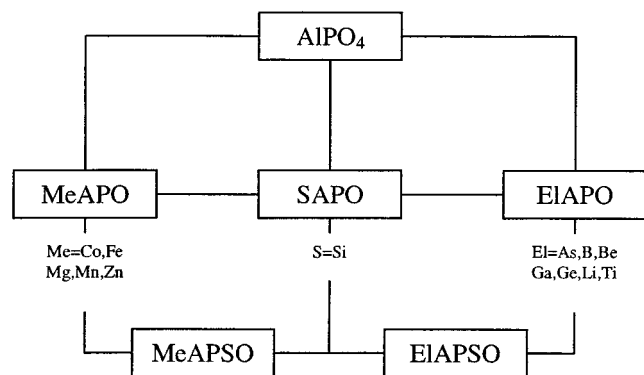


**Figure 2.** Classification of aluminophosphate and derived phases (adapted from Flanigan et al.<sup>40</sup>).

these findings, the family of crystalline microporous phosphates grew considerably. Some examples include gallophosphates,<sup>41–43</sup> zincophosphates,<sup>44,45</sup> be-

ryllophosphates,<sup>46</sup> vanadophosphates,<sup>47</sup> and ferrophosphates.<sup>48</sup> In some of these microporous phosphates, the backbone element T (T = Ga, Fe, ...) associated with P can be tetra-, penta- or hexacoordinated.

The expression “zeolite” has nowadays a broader meaning, to include all microporous silica-based solids presenting crystalline walls, including those materials where a fraction of Si atoms has been substituted by another element, T, such as a trivalent (T = Al, Fe, B, Ga, ...) or a tetravalent (T = Ti, Ge, ...) metal. The following categories have been established, as a function of the Si/T ratio: zeolites, Si/T < 500; and zeosils, Si/T > 500; these compounds are essentially Si-based, but, contrary to clathrasils, the porosity of these materials is accessible. Both zeosils and clathrasils define the family of porosil silica-based materials.

The crystalline microporous phosphates are identified as “related microporous solids”.

In summary, microporous solids are distinguished by a three-dimensional framework, resulting from corner-connected  $\text{TO}_4$  units (T = Si, Al, P, Ge, Ga, ...); oxygen atoms bridge two metal centers; and channels or cavities of molecular dimensions, capable of communicating with the outside.

Actual structures can deviate from these ideal definitions, due to the presence of  $\text{TX}_4$ ,  $\text{TX}_5$ , or  $\text{TX}_6$  polyhedra (X = O, F) or nonbridging oxygen atoms (for example, terminal  $-\text{OH}$  groups).

A three-letter code is attributed to each structure, defined by the Structure Commission of the International Zeolite Association (IZA).<sup>49</sup> As an example, faujasite and their synthetic equivalents X and Y correspond to the structural-type FAU. Nowadays, zeolitic frameworks are classified in 135 different structure types.<sup>50</sup>

### 2.3.2. Synthesis Strategies of Microporous Crystalline Phases

**Synthesis Methods.** Crystalline molecular sieves are generally obtained by hydrothermal crystallization of a heterogeneous gel, which consists of a liquid and a solid phase. The reaction media contain the following: sources of the cation(s) that form the framework (T = Si, Al, P, ...); sources of mineralizing agents ( $\text{HO}^-$ ,  $\text{F}^-$ ); mineral cations or organic species (cations or neutral molecules); and solvent (generally water).

Zeolite synthesis is generally performed in alkaline media,  $T < 200$  °C. In the case of aluminophosphate families, and derived compounds (SAPO, MeAPO, etc.), the reaction pH is between 3 and 10. Anions such as hydroxide or fluoride collaborate in the dissolution of the reactive silica moieties in the gel and their transfer to the growing crystals. In addition,  $\text{F}^-$  anions can play the role of a costructuring agent, by stabilizing certain building blocks of the inorganic network.<sup>51</sup>

Nonaqueous routes have also been explored; they may involve a nonaqueous solvent as ethylene glycol<sup>52,53</sup> or dry synthesis methods.<sup>54</sup> However, traces of water may be present in the solvents.<sup>53</sup> Water can also be generated in situ, upon evolution of the reacting systems.<sup>54,55</sup>

**Table 1. Templating Agents Used in the Synthesis of Porosils (SiO<sub>2</sub> Polymorphs)**

organic template	Porosil structural code	organic template	Porosil structural code
1-aminoadamantane	DDR	<i>N</i> -benzyl-1-azonium[2.2.2]bicyclooctane	IFR
<i>N,N,N</i> -trimethyl-1-adamantammonium cations	AFI	1,3,3,6,6-pentamethyl-6-azonium[3.2.1]bicyclooctane	ITE
dibenzyl-dimethylammonium cations	BEA	cobalticinium cations	NON
ethylene glycol or trioxane	SOD	3,5-dimethyl- <i>N,N</i> -diethylpiperidinium cations	MEL
tetrapropylammonium cations	MFI	4,4'-trimethylenedipiperidine	MTW
diethylamine	TON	quinuclidinium cations	AST
di- <i>n</i> -propylamine	MTT	tetramethylammonium cations	MTN

**Zeolite Formation and Growth.** A great number of studies have been focused on the crystallization mechanism of zeolites. Two main hypotheses have been proposed. The first one, originally presented by Flanigen and co-workers,<sup>56</sup> suggested that crystallization takes place by a reorganization of the gel network; this process is not mediated by the liquid phase. This pioneering model has been practically abandoned and displaced by the hypothesis of Barrer and colleagues,<sup>57</sup> who supposed that the formation of zeolite crystals takes place in solution. In this model, the nucleation and growth of crystalline nuclei are a result of condensation reactions between soluble species, the gel performing a limited role as a reservoir of matter.

### 2.3.3. Formation Mechanisms of Microporous Crystalline Phases

**Building Unit Model.** Barrer and co-workers suggested that the elaborate zeolite frameworks were made up from more complex building blocks, which were present in solution: the secondary building units (SBU).<sup>57</sup> Sixteen different kinds of SBU have been identified from structural studies.<sup>49</sup> This model settles an interesting point of view: solids may be built up from preformed building blocks. A major limitation of this approach is that not all of the proposed SBUs have been found in solution. However, these building blocks could be present in concentrations below detection limits; these minor quantities could suffice to trigger the generation of microporous frameworks. Alternative models have been developed to rationalize the formation of aluminosilicates,<sup>58–60</sup> gallophosphates,<sup>43</sup> and aluminophosphates,<sup>61,62</sup> based on molecular modeling coupled to structural analysis.

**Organic Templating Agents.** As previously stated, the use of organic species as templating agents has widened the number and nature of microporous crystalline solid phases. So far, amines and related compounds (quaternary ammonium cations), linear or cyclic ethers, and coordination compounds (organometallic complexes) have been the most commonly used organic templates. The template is supposed to keep its integrity in the synthesis medium (chemical and thermal stability). Under an alternative approach, the template species can be generated in situ by controlled decomposition of organic precursors. This has been advantageously used to prepare novel microporous aluminophosphates in the presence of alkylformamides. The partial degradation of these compounds leads to the corresponding alkylamines, which are kept in the cavities of the material.<sup>62,63</sup>

Table 1 presents some templating agents of widespread use in the synthesis of porosils, as well as their standard codes.

**Role of the Organic Species.** The organic species are frequently occluded in the microporous voids of the synthesized material, contributing to the stability of the mineral backbone. The guest–framework stabilizing interactions can be of Coulombic, H-bonding, or van der Waals type. However, guest–guest interactions can also contribute to the total energy. This is the case of 18-crown-6/Na<sup>+</sup> complexes, in the synthesis of EMC-2 zeolite,<sup>64</sup> or of the *p*-dioxane/Na<sup>+</sup> complex, in the synthesis of MAZ-like zeolites.<sup>65</sup> The trapped organic moieties perform several roles:

- Coulombic balance of the negatively charged framework (e.g., aluminosilicates).
- filling of the microporous cavities.
- structuring by the “template effect”; that is, the mineral species present a degree of preorganization around the organic molecules, and/or the crystal growth is oriented by the shape and symmetry of the template.
- chemical action, by modifying the properties of the solution or the resulting gel (the organic species is mostly hydrophobic).
- thermodynamic action, by stabilizing a given building block of the mineral framework.

Silica-based molecular sieves and silica-rich zeolites ( $5 < \text{Si/Al} < \infty$ ) are the simplest systems in which these “template effects” have been observed.

**Template Effect of the Organic Species.** In most cases, an adequate matching exists between the geometries of the organic species and those of the microporous cage or channel network. The molecules play thus a real *template effect*, around which the mineral framework is built. The local structuring of water might be an important issue; in fact, a close analogy between clathrates (arrangements constituted mainly by water structured around other molecules) and the family of clathrasils can be noted. This is the case of tetramethylammonium clathrate [(CH<sub>3</sub>)<sub>4</sub>NOH·5H<sub>2</sub>O], which presents the sodalite-like structure. This zeolite has been also obtained in the presence of tetramethylammonium (TMA<sup>+</sup>) cations. In the case of structurally related solids (SOD type), such as zincophosphate (Zn, O, P framework) and aluminophosphate (Al, O, P framework), TMA<sup>+</sup> cations are also perfectly adapted to the sodalite-like cage size (Figure 3). Wiebke<sup>66</sup> has synthesized a new family of mixed clathrate–silicate materials, reinforcing the analogy between the two families of compounds. In clathrates, water is structured around big cations or anions, presenting low



**Figure 3.** TMA<sup>+</sup> cations occluded into the sodalite cage (cage  $\beta$ ). In this scheme, the network-forming elements T (T = Si, Al, ...) are located at the corners, defined by the intersection of three edges. O atoms can be found at the center of each edge.

charge and hydrophobic character. These nonpolar or slightly polar molecules [a typical example is (C<sub>3</sub>H<sub>7</sub>)<sub>4</sub>N<sup>+</sup>] are rejected by the solvent and isolated in polyhedral cavities.

The presented analogies between clathrates and silicates, including the existence of mixed compounds and the structuring of water in the presence of hydrophobic molecules, led to the elaboration of a porous mineral framework in terms of a “replication” water–inorganic species process. The latter is then followed by condensation of the resulting organic–inorganic species. This template effect will be illustrated by an example: silicalite-1 (MFI structural type).

Two main components constitute the MFI structure (MFI for Mobil Five): ZSM-5, where the Si/Al ratio varies between 10 and 500, and silicalite-1, a pure siliceous form (Si/Al > 500). MFI structure<sup>67</sup> is characterized by the presence of two types of interconnected channels, the opening of which is delimited by 10 tetrahedral units (Figure 4). Silicalite-1 can be obtained in the presence of a great variety of organic species. However, the pure phase can be obtained only by performing the synthesis in the presence of tetrapropylammonium cations (TPA<sup>+</sup>) cations. In the as-synthesized solids, four TPA<sup>+</sup> per unit cell are occluded within the inorganic framework, at the intersection of both systems of channels (**Figure 4C**). It is clear that there is a geometrical tuning between these cations and the channel system, as only one cation per intersection is present.

Solid-state NMR studies of the reaction gels along the synthesis performed by Burkett and co-workers<sup>68</sup>

confirmed the van der Waals interactions between the TPA<sup>+</sup> and the inorganic silica species. The experiments were carried out using <sup>1</sup>H–<sup>29</sup>Si cross-polarization (CP) techniques, and the reaction mixtures were prepared in the presence of D<sub>2</sub>O. An organomineral entity was evidenced, even in the absence of any crystalline phase, by the substitution of the water belonging to the (hydrophobic) solvation layer of TPA<sup>+</sup> by silica-containing moieties. This “replication” of the water structure by a silica “copy” should be favorable from a thermodynamical point of view, the van der Waals interactions and the de-structuring of the water molecules contributing to the enthalpic and entropic terms, respectively. The assembly of the organomineral entities and the growth of the nuclei thus formed should lead to silicalite-1. The different steps involved in the formation of this solid phase are schematized in Figure 5. These authors have shown that the crystallization did not take place in the presence of tetraethanolammonium cations (geometrically similar to TPA<sup>+</sup>). In this case, the strong H-bonding interactions that take place between the ethanol groups and water molecules hinder the “replication” process.

More recently, this mechanism has been validated by de Moor and co-workers using small (SAXS)-, wide (WAXS)-, and ultrasmall (USAXS)-angle X-ray Scattering.<sup>69</sup> Other authors have independently demonstrated the formation of an organomineral species containing 33 Si atoms, bent around TPA<sup>+</sup>, and presenting a connectivity scheme similar to that found in the MFI structure.<sup>70</sup>

#### 2.3.4. Properties and Applications of Zeolitic Materials

Because of their perfectly controlled porous structure with molecular size pores, zeolitic materials are genuine shape-selective molecular sieves. The presence of charge compensation cations (alkaline, alkaline-earth, protons, etc.) within the porosity of the inorganic frameworks gives to these materials ionic exchange and catalytic properties, which are widely used in the industry. Moreover, the hydrophobic (zeosils, SiO<sub>2</sub>) or hydrophilic (aluminosilicates) nature of the tailorable inorganic framework make these solids useful as specific adsorbents of organic molecules or water in the gas or liquid phase. The three main applications of zeolitic materials are adsorption and drying, catalysis, and detergency.

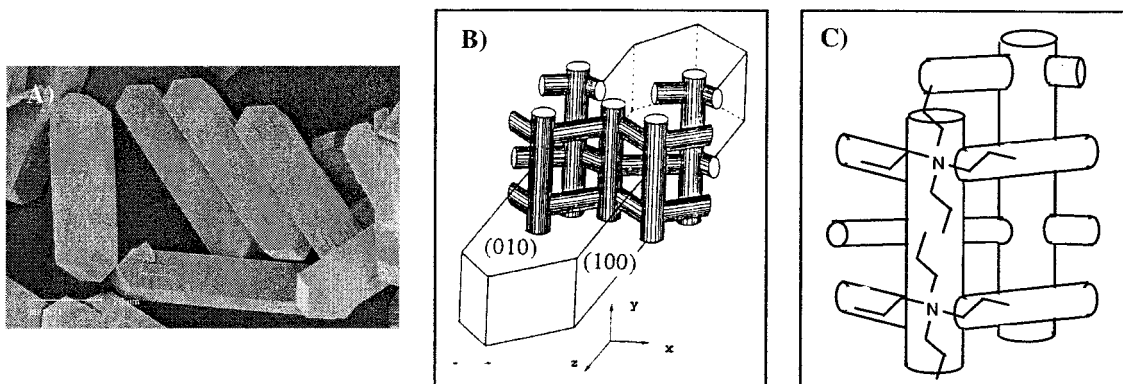


**Figure 4.** Structure-type MFI: (a) crystals of silicalite-1; (b) overview of the channel system; (c) scheme of the location of the TPA<sup>+</sup> cations at the channel intersection.

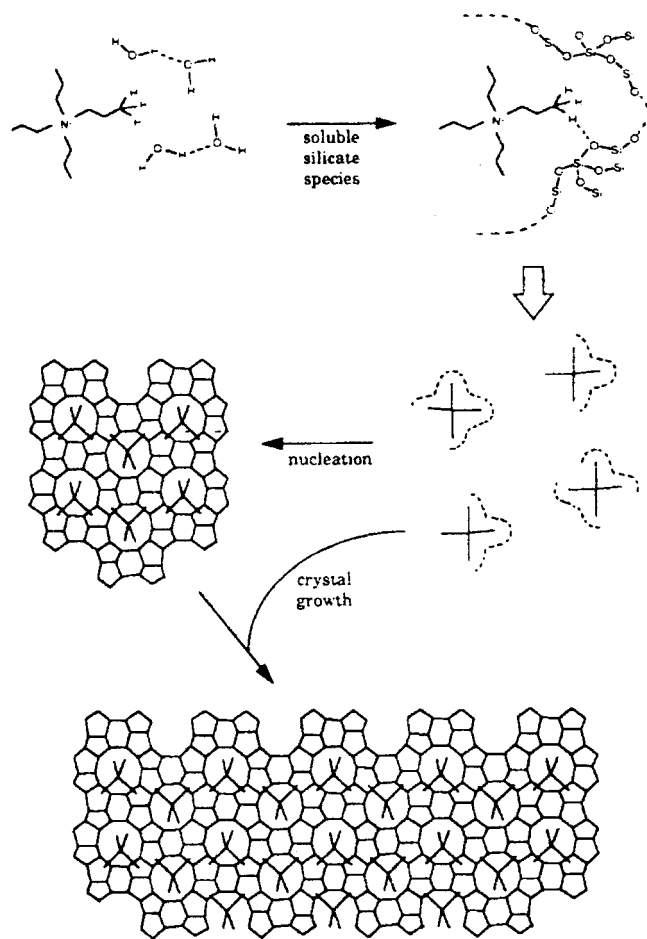


**Figure 5.** Scheme of the proposed formation mechanism of silicalite-1 (adapted from ref 68).

To illustrate these applications, one can quote adsorption of water molecules in double-glazing, gas drying, catalytic cracking (production of fuel, increase of the gasoline octane number), and non-phosphate-containing laundry soaps (trapping of calcium and magnesium). The world consumption ( $10^3$  tons) and distribution (vol %) of use of these materials in 1988 are given in Figure 6.<sup>71</sup> Recent data<sup>72</sup> related to synthetic zeolite production show that the tonnages for the three main applications have greatly increased in the past 10 years. Indeed, in 1998 they rose  $1.05 \times 10^6$ ,  $1.6 \times 10^5$ , and  $1 \times 10^5$  tons for detergency, catalysis, and adsorption drying, respectively. Detergency represents  $\sim 70\%$  of the market; some laundry soaps can contain up to 40 wt % of zeolite A (structure-like LTA).

Numerous other applications, less important in tonnage and mainly based on the use of natural zeolites, have been also developed: wastewater treatment, treatment of nuclear effluents, pet food, or soil improvement.

Recent patents have claimed the use of these materials for antibacterial properties<sup>73,74</sup> or as combustion delaying agents.

In catalysis, most of the zeolites are used in refining and petrochemical material. In petroleum refining, the main applications are fluid catalytic cracking (FCC), hydrocracking, isomerization of products from the decomposition of C5–C6 cuts, and

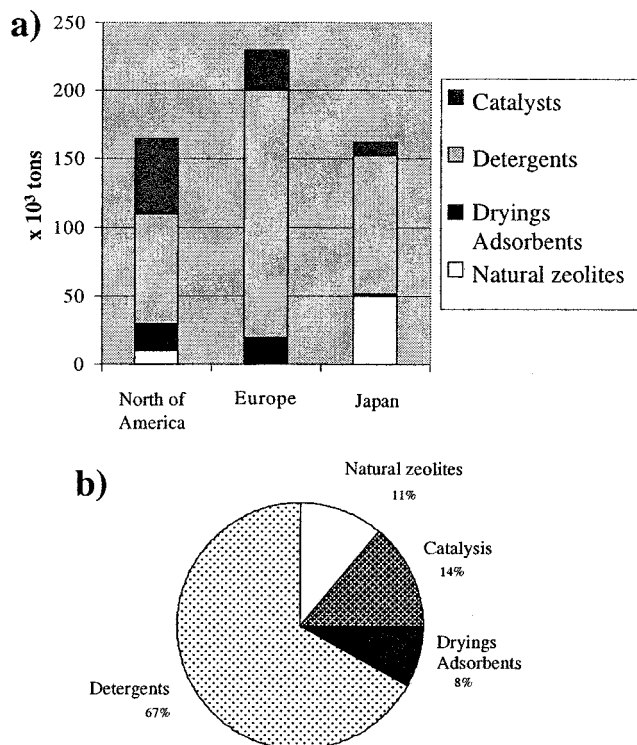


**Figure 6.** Consumption ( $\times 10^3$  tons) (a) and distribution in vol % of the use of zeolitic materials in the world in 1988 (b) (adapted from ref 71).

dewaxing. In petrochemicals, developed reactions are aromatic transformations (isomerization, alkylation, disproportionation, and transalkylation reactions).

The use of zeolites in fine chemistry processes is and will be more and more important. Indeed, homogeneous catalysis processes (contrary to heterogeneous catalysis processes) act usually in a static bed, limit or avoid corrosion problems, and allow return to the catalyst.

In this area, among the reactions catalyzed by zeolites, one can quote double-bond isomerization, skeleton isomerization, dehydration, dehydrogenation, halogenation, acylation or alkylation of aromatic compounds, selective oxidation, selective hydrogenation, etc.<sup>75–77</sup> One of the most remarkable examples in the past decade is the industrial development of TS-1 (silica-rich and titanium-doped MFI zeolite)<sup>78</sup> as a catalyst for phenol hydroxylation.<sup>79</sup>

It is noteworthy that among the 135 types of identified zeolites, only about a dozen are used in the industry or have a high industrial potential. Table 2 presents a list of the main zeolitic materials. Recently, a more detailed review on the applications of these solids in catalysis has been published.<sup>80</sup>

### 3. Mesoporous Materials: Using Supramolecular Templates To Enhance Pore Size

#### 3.1. Introduction

Regardless of the great amount of work dedicated to zeolites and related crystalline molecular sieves, the dimensions and accessibility of pores were restrained to the sub-nanometer scale. This limited the application of these pore systems to small molecules.

**Table 2. Zeolitic Structures Used or with a High Industrial Potential (Adapted from Reference 62)**

structural type	application
LTA	detergency, drying, and separation
FAU, MOR	adsorption and catalysis
LTL	catalysis: aromatization
MFI	adsorption and catalysis
BEA	catalysis
CHA (silicoaluminophosphate)	catalysis: conversion of methanol into olefins
FER	catalysis: framework isomerization of <i>n</i> -butenes
AEL (silicoaluminophosphate), TON	catalysis: isomerization of paraffins; decrease of the flowing point for diesel oils
MTW	catalysis

During the past decade, an important effort has been focused on obtaining molecular sieves showing larger pore size.

The introduction of supramolecular assemblies (micellar aggregates, rather than molecular species) as templating agents permitted a new family of mesoporous silica and aluminosilicate compounds (M41S) to be obtained, first developed by a research group at Mobil Oil.<sup>81,82</sup> These solid phases are characterized by ordered mesopores presenting sharp pore size dispersions.

The M41S family includes a bidimensional hexagonal phase (MCM-41, for Mobil Composition of Matter), a cubic phase, MCM-48, and several lamellar phases; particularly, MCM-50 is reported to be thermally stable.

The synthesis of large-pore molecular sieves was not the only consequence of this discovery. This breakthrough permitted confirmation of several ideas and concepts proposed by a large community of researchers, focused on biomineralization processes. As described by S. Mann<sup>27</sup> the importance of this new “organized matter soft chemistry synthesis” is continuously increasing. The synthesis of inorganic or hybrid materials presenting complex architectures over a multiscale range should be possible by controlling construction, morphology, and hierarchy in precipitation reactions. Another relevant outcome is the approach experienced by the communities studying biomineralization and the synthesis and design of advanced materials. The close relationships between biology and “chemistry of organized matter” converge in the terms *molecular tectonics* or *nanotectonics*. Nature employs macromolecules and microstructures to control the nucleation and growth of mineral compounds or organomineral hybrid composites; similar approaches are nowadays being developed in the synthesis of advanced materials.

In particular, a permanent effort is made to develop textured inorganic or hybrid phases. These materials are potential candidates for a variety of applications, in the fields of catalysis,<sup>34</sup> optics, photonics, sensors, separation, drug delivery,<sup>83</sup> sorption, acoustic or electrical insulation, ultralight structural materials,<sup>24,25</sup> etc.

In the case of porous materials, increasing the pore size has been one of the goals of structural control, to permit the penetration of large size molecules into the host porous structure. Macroporous materials

(i.e.,  $\varnothing_{\text{pore}} > 50$  nm) are particularly interesting, due to their improved transport properties. Organized macroporous arrays should present optimal fluxes, and diffusion should not be a limiting issue for these materials. This is a central point for any processes concerning accessibility, such as catalysis, sorption, delivery, or sensors.

The choice of the organic template to spatially control the mineralization process along various scales, ranging from the angstroms to micrometers, is a key issue in the synthesis of textured or porous materials. In the case of mesoporous oxides, the templating relies on supramolecular arrays: micellar systems formed by surfactants or block copolymers.<sup>81,82</sup>

In the following sections, we will describe the chemical tools that are necessary to construct silica- and non-silica-based organized hybrid or inorganic structures by soft chemistry processes. The most relevant work produced in this field from 1992 to the present will be reviewed and thoroughly discussed.

## 3.2. Synthesis Tools for Mesostructure Production

### 3.2.1. Synthesis Strategies

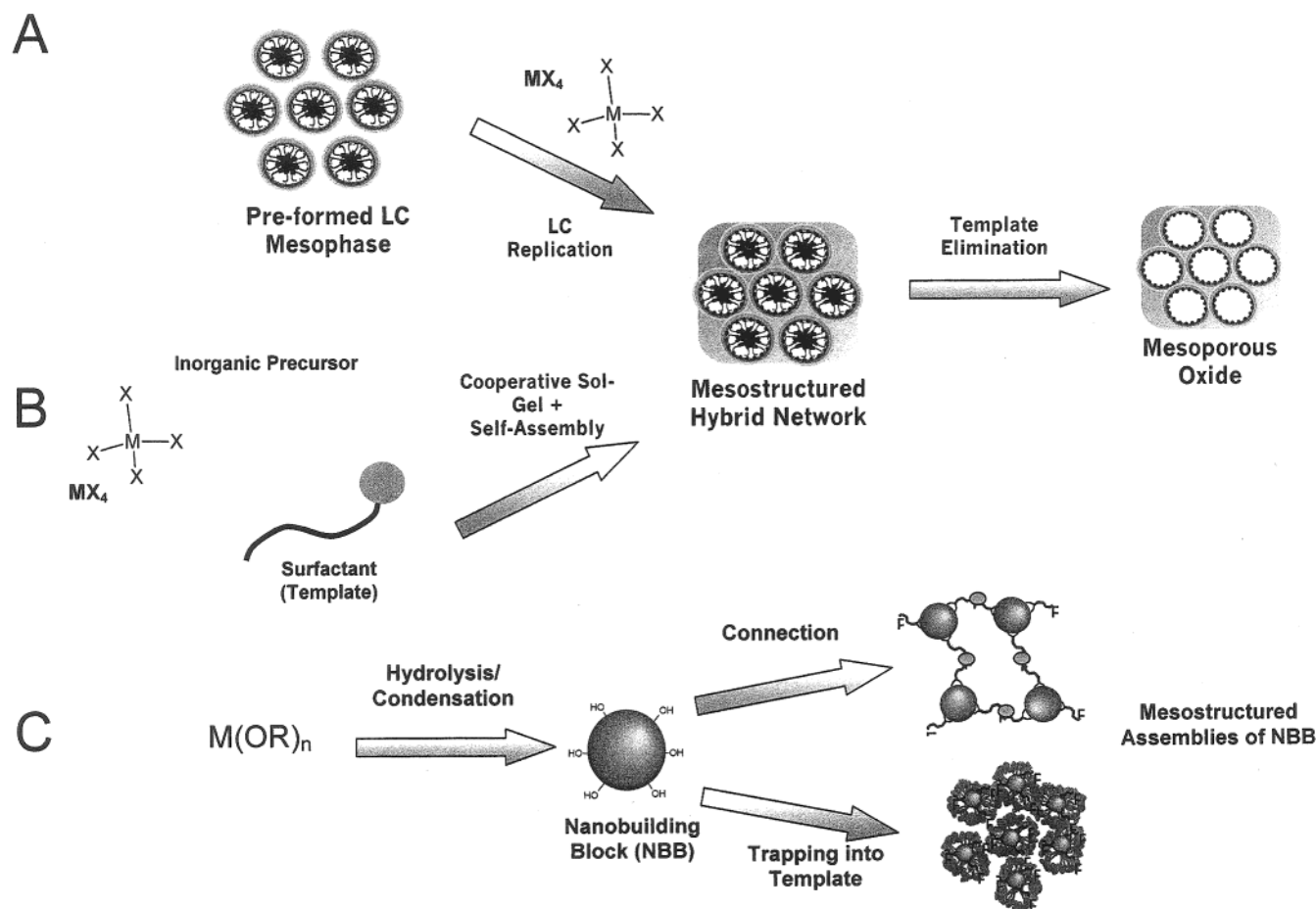
“Chimie Douce” (soft chemistry) is indeed an interesting starting point for the development of a “biomimetic approach” of mesostructured materials, in view of the typical synthesis conditions: low temperatures; coexistence of inorganic, organic, and even biologically attractive moieties; widespread choice of precursors (monomers or condensed species); and possibilities of controlled shaping (i.e., powders, gels, films, ...). Exploration in this field is persistently growing, and a number of biomimetic synthesis strategies have been recently developed.<sup>27,28</sup> The large set of *smart materials*, ranging from nanostructured materials (such as ordered dispersions of inorganic bricks in hybrid matrices, mesostructured inorganic networks, or dual networks) to more complex materials having hierarchical architectures, reported during the past 10 years, is testimony to the scientific success of this field.<sup>2–14</sup>

Figure 7 presents an illustration of the main general synthesis strategies used to construct these materials. In all of these synthesis strategies, the chemical, spatial, and structural properties of the texturing agent, or the “reaction pockets”, must be thoroughly adjusted by controlling the rates of chemical reactions, the nature of the interfaces, and the encapsulation of the growing inorganic phase. An adequate tailoring of the organomineral interface is of utmost importance to obtain well-defined textured phases. The chemical, spatial, and temporal control of this “hybrid interface” is a major task in the challenge of developing cooperatively assembled inorganic–organic integrated systems.

These synthesis strategies (Figure 7) can be categorized following two principal approaches:

(1) The molecular/supramolecular templates are present in the synthesis media from the beginning; the self-assembly process of the templates is followed by (or synchronized with) the formation of the





**Figure 7.** Main synthetic approaches for mesostructured materials. The mesostructure can be previously formed (route A), or a cooperative process (route B) can take place. Route C makes use of preformed nanobuilding blocks (NBB).

mineral network, deposited around the “self-assembled substrate”. “Inorganic replication” occurs at accessible interfaces built by preorganized or self-assembled molecular or supramolecular templates, which create the mesostructure in the material. These templates can be organic compounds (surfactant molecules, amphiphilic block copolymers, dendrimers, etc.) or biomolecules, forming micellar assemblies and/or liquid crystal mesophases. They can also be preformed objects having submicronic, micronic, or macroscopic sizes, colloids (latex, silica), bacteria or virus, or even mesoporous silica frameworks that can be used as a template (nano- or microcasting) to embed any other component or material, being commonly used examples (route A).

In many cases a “cooperative self-assembly” can take place in situ between the templates and the mineral network precursors yielding the organized architectures (route B).

(2) In the second approach, a nanometric inorganic component is formed (by inorganic polymerization or precipitation reactions). Nanoparticle formation can take place not only in solution but also in micelle interiors, emulsions, or vesicles, leading to complex shaped materials. The control of the dynamics of precipitation of this nanometric building block (NBB) is a key point when syntheses are performed under these conditions. These NBB can be subsequently assembled and linked by organic connectors or by taking advantage of organic functions dangling on the

particle surface (route C). The synthetic strategies and routes using NBB leading to ordered or disordered hybrid networks have been recently reviewed.<sup>4</sup>

All of these strategies based on transcription, synergic assembly, and morphosynthesis can also be simultaneously combined (integrative synthesis) to give rise to hierarchical materials.<sup>27</sup> We will briefly discuss the main parameters that control mesostructured assemblies in the following paragraphs.

The key feature in the synthesis of mesostructured materials is to achieve a well-defined segregation of organic (generally hydrophobic) and inorganic (hydrophilic) domains at the nanometric scale; here, the nature of the hybrid interface plays a fundamental role. The most relevant thermodynamic factors affecting the formation of a hybrid interface have been first proposed by Monnier et al.<sup>84</sup> and discussed in depth by Huo et al.<sup>33</sup> in their description of the “charge matching” model (see section 3.3.4). The free energy of mesostructure formation ( $\Delta G_{\text{ms}}$ ) is composed of four main terms, which represent, respectively, the contributions of the inorganic–organic interface ( $\Delta G_{\text{inter}}$ ), the inorganic framework ( $\Delta G_{\text{inorg}}$ ), the self-assembly of the organic molecules ( $\Delta G_{\text{org}}$ ), and the contribution of the solution ( $\Delta G_{\text{sol}}$ ).

$$\Delta G_{\text{ms}} = \Delta G_{\text{inter}} + \Delta G_{\text{inorg}} + \Delta G_{\text{org}} + \Delta G_{\text{sol}} \quad (1)$$

In the classical liquid crystal templating (route A), the contribution due to the organization of the

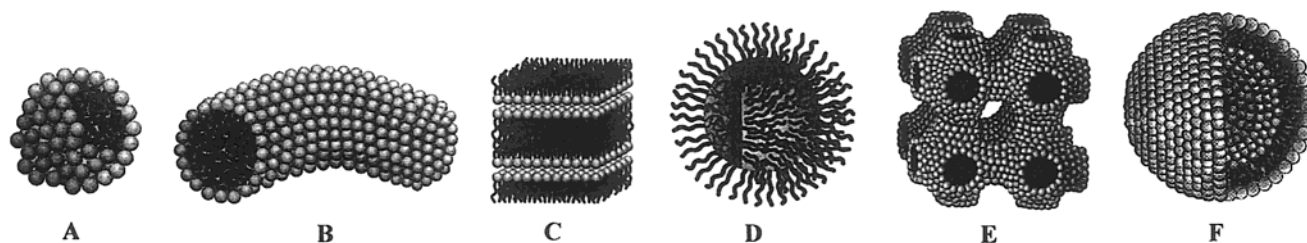


**Figure 8.** Micellar structures (A = sphere, B = cylinder, C = planar bilayer, D = reverse micelles, E = bicontinuous phase, F = liposomes). Reprinted with permission from ref 88. Copyright 1994 John Wiley and Sons, Inc.

amphiphilic molecules prevails over the other interactions. In the cooperative assembly route (B), template concentrations may be well below those necessary for obtaining liquid crystalline assemblies or even micelles. Thus, the creation of a well-defined and compatible hybrid interface between the inorganic walls and the organic templates (i.e.,  $\Delta G_{\text{inter}}$ ) is central to the generation of a well-ordered hybrid structure with adequate curvature. This has been demonstrated for silica systems in strongly alkaline media (pH 13) at ambient temperature, where extended silica polymerization is not possible (i.e.,  $|\Delta G_{\text{inorg}}| \rightarrow 0$ ). In these conditions, hydrolysis and inorganic condensation are separate events.<sup>85</sup> The formation of the inorganic phase can be subsequently triggered as a subsequent process, directed to different mesophases. A similar strategy has been applied for the construction of titania–surfactant hybrid assemblies in strongly acidic medium (vide infra).

From the kinetic point of view, the formation of an organized hybrid mesostructure is the result of the delicate balance of two competitive processes: phase separation/organization of the template and inorganic polymerization. This issue, well-known in microscale phase segregation,<sup>86</sup> is essential when one is working with systems where inorganic condensation is fast. In conditions where condensation is slow (i.e., pH near the  $\text{pH}_{\text{iep}}$  of silica), the kinetic constants ( $k_i$ ) of the different processes should be ordered as follows:

$$k_{\text{inter}} > k_{\text{org}} > k_{\text{inorg}} \quad (2)$$

Thus, the formation of ordered phases is controlled by the self-assembly involving the hybrid interface. Enhanced hydrolysis by addition of  $\text{F}^-$  anions<sup>87</sup> helps to obtain well-defined mesostructures even in conditions where condensation is faster (pH, presence of  $\text{F}^-$ , which also induces condensation).

Hence, two aspects are essential to fine-tune the self-assembly and the construction of the inorganic framework: the reactivity of the inorganic precursors (polymerization rate, isoelectric point, etc.) and the interactions to generate a well-defined hybrid interface. These central points are not only relevant for mesostructured silica but can also be translated into the domain of the more reactive non-silica systems, as will be shown in the next section.

### 3.2.2. Self-Assembling Templates

The main organic templates used in the elaboration of mesostructured hybrids or mesoporous solids can be classified in three categories: molecular-based

organized systems (MOS), polymeric templates, and other texturing agents.

**Molecular-Based Organized Systems.** *Surfactant-Based MOS.* Structuring is the consequence of the combination of steric effects and repulsive forces, yielding a different result in pure or multicomponent media. In particular, in liquid media, the presence of components with a strong anisotropy may induce an organization on the nano- to micrometric scale, in the form of nanometric aggregates (micelles), extended layers (membranes), or solvent-containing bilayers (liposomes). Amphiphilic or surfactant molecules, displaying a polar head and a nonpolar tail, tend to aggregate in solvents where one of these domains is insoluble. This “frustrated” situation forces the amphiphilic molecule to adopt a compromise situation, from the energetic point of view, and aggregates are formed. Beyond the critical micellar concentration (cmc), the amphiphilic molecules form micelles in solvents of a marked polar or nonpolar character.

A combination of molecular geometry and intermolecular (solvophilic/phobic, Coulombic, H-bonding) and entropic interactions drives these solutions to self-assemble into colloidal systems, presenting different microstructures: spherical, cylindrical, planar, cellular,<sup>88</sup> etc. The assembly depends on the nature and morphology of the discrete molecules. The numerous micellar assemblies and aggregates, constituted by the association of amphiphilic molecules, linked by weak forces (van der Waals, H-bonds, electrostatic, etc.) rather than by covalent bonds, are collectively known as association colloids or molecular organized systems.

The architecture of the final materials (“the manner in which coexisting phases are arranged in space”<sup>89</sup>) will directly rely on the nature of the surfactant molecules, that is, the morphology of the micellar aggregates and the interactions at the inorganic–organic interface (solvent–micelle interaction, in the case of solutions). Thus, knowledge of the polar head geometry and charge of the surfactants is essential.

*Role of Surfactant Geometry.* Micellar aggregates organize according to different shapes (spherical or cylindrical micelles, lamellae, ...), permitting the coexistence of two incompatible phases. Some typical micellar structures are presented in Figure 8. In some colloidal systems, a more complex behavior has been evidenced, and other arrangements, such as the spongelike bicontinuous structure (Figure 8E), are possible.

**Table 3.  $g$  Parameter of Different Micellar Structures (According to References 90–92)**

$g = v/l_c a_0$	structures	examples
$g < 0.33$	spherical micelles	single chain lipids with a large polar head (soaps or ionic detergents)
$g = 0.33-0.5$	cylindrical micelles	single chain lipids with a small polar head (soaps or ionic detergents in concentrated electrolyte solutions)
$g = 0.5-1$	bilayer (vesicles)	double-chain lipids
$g = 1-2$	bilayer (membranes)	
$g = 2-3$	inverse cylindrical micelles	double-chain lipids and a small polar head
$g > 3$	inverse spherical micelles	

Upon progressive increase of surfactant concentration in the aqueous solution, a number of phases appear, always following the same order: “direct” spheres, “direct” cylinders, lamellae, “inverse” cylinders, and “inverse” spheres; this order corresponds to a monotonic variation of the interfacial curvature.

Different models have been proposed to explain these experimental facts, the main parameters taken into account being (1) the hydrophobic interactions between organic chains, (2) geometric restrictions due to molecular packing, (3) molecule exchange between aggregates, (4) enthalpy and entropy of packing, and (5) electrostatic repulsion between polar heads.

A relatively simple model proposed by Israelachvili and colleagues,<sup>90,91</sup> based on geometrical considerations, explains and predicts the resulting self-assembled structures of each type. This model considers a hydrophobic liquid-like core, the contribution of which is merely due to geometrical constraints. These geometrical considerations rely on the ratio of the polar head surface to the hydrophobic volume. The amphiphilic molecules are thus modeled like a conical fragment (the hydrophobic part) attached to a spherical (hydrophilic) head. Two main shapes are possible (Figure 9): direct conical, or *ice-cream cone* (one hydrophobic chain), and inverse conical, or *champagne cork* (two hydrophobic chains).

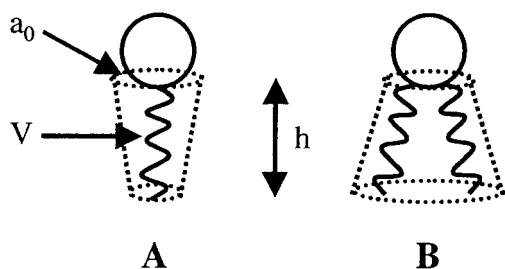


**Figure 9.** Schematic representation of amphiphilic molecules, adopting conical shape (*ice-cream cone*, A) or inverse conical (*champagne cork*, B).

The steric hindrance of the hydrophobic chain is characterized by the ratio  $v/l$ , where  $v$  is the chain volume and  $l$  is the chain length; in the case of the polar head, its contribution is given by the effective optimal surface,  $a_0$ . To ensure chain fluidity,  $l$  must verify that  $l < l_c$ , where  $l_c$  is the length of the fully extended chain;  $l_c$  can be easily estimated as a function of the number of C atoms in the chain,  $n$ . The value of the packing parameter,  $g = v/l_c a_0$ , links the molecular structure of the amphiphilic molecule to the architecture of the aggregates. The limiting values of  $g$  can be easily calculated for an aggregate of known geometry, by using the condition of chain fluidity ( $l < l_c$ ) and an estimation of the aggregation number (number of molecules forming

the micelle). The latter can be obtained from two relationships: the aggregate surface to  $a_0$  and the aggregate volume to  $v$ . Table 3 summarizes the different micellar structures compatible with a given  $g$ .<sup>90–93</sup>

Huo et al.<sup>94</sup> were the first to take into account the  $g$  parameter to explain the formation of different surfactant-templated oxide mesostructures. In principle, the structure of the mesophase depends on the packing properties of the surfactant molecules, hence, on the value of  $g$ . The validity of this concept has been illustrated by a complete study, which took into account various parameters, such as surfactant nature, pH, presence of cosolvents or cosurfactants, and their influence on the observed phase transitions, for fixed synthesis conditions. For silica systems, it has been shown that an increase of  $g$  (i.e., a decrease in the curvature of the micellar motif) leads to phase transitions along the sequence micellar cubic ( $Pm3n$ ) → hexagonal ( $P6m$ ) → bicontinuous cubic ( $Ia3d$ ) → lamellar.<sup>95</sup>

**Role of the Polar Head Charge.** Both surfactant and inorganic soluble species direct the synthesis of mesostructured MCM-41-type materials. The hybrid solids thus formed are strongly dependent on the interaction between surfactants and the inorganic precursors. In the case of ionic surfactants, the formation of the mesostructured material is mainly governed by electrostatic interactions. In the simplest case, the charges of the surfactant ( $S$ ) and the mineral species ( $I$ ) are opposite, in the synthesis conditions (pH). Two main *direct* synthesis routes have been identified:  $S^+I^-$  and  $S^-I^+$ .<sup>96,97</sup> Two other synthesis paths, considered to be *indirect*, also yield hybrid mesophases from the self-assembly of inorganic and surfactant species bearing the same charge: counterions get involved as charge compensating species. The  $S^+X^-I^+$  path takes place under acidic conditions, in the presence of halogenide anions ( $X^- = Cl^-, Br^-$ ); the  $S^-M^+I^-$  route is characteristic of basic media, in the presence of alkaline cations ( $M^+ = Na^+, K^+$ ). The different possible hybrid inorganic–organic interfaces are schematized in Figure 10.

Other synthesis routes rely on nonionic surfactants, where the main interactions between the template and the inorganic species are H-bonding or dipolar, giving birth to the so-called neutral path:  $S^0I^0$ ,<sup>98,99</sup>  $N^0I^0$ ,<sup>100,101</sup> and  $N^0F-I^+$ .<sup>102</sup>

Table 4 gives different examples of mesostructured inorganic materials obtained following the above-mentioned paths.<sup>33,94,103–114</sup>

**Organogelator-Based MOS Systems.** Organogelators (low-weight organic molecules) are able to form thermoreversible physical gels in a variety of solvents in very low concentrations ( $\sim 10^{-3}$  mol dm<sup>-3</sup>,  $< 1\%$  w/w). The solvent molecules are immobilized, and

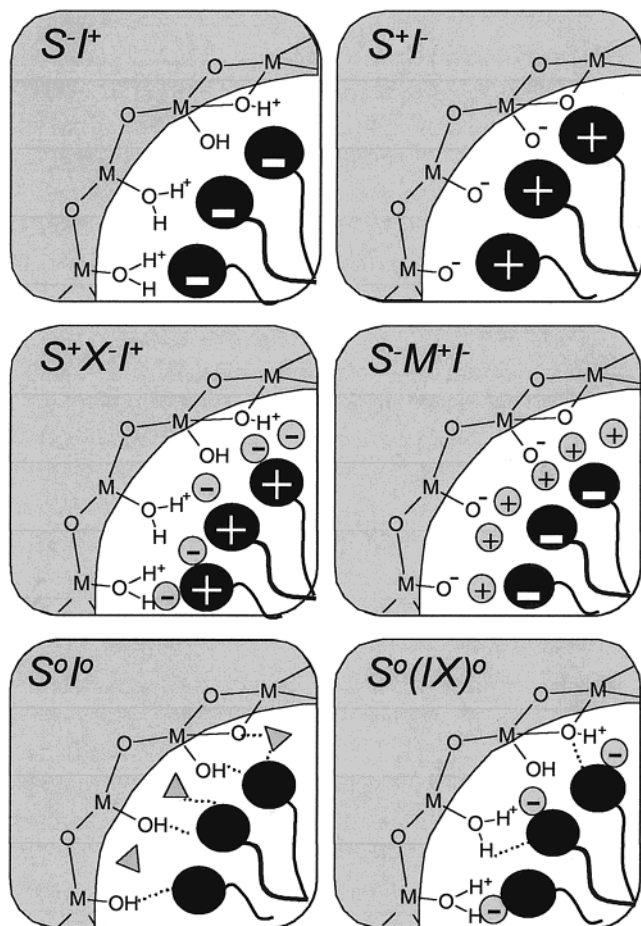


**Figure 10.** Schematic representation of the different types of silica-surfactant interfaces. S represents the surfactant molecule and I, the inorganic framework.  $M^+$  and  $X^-$  represent the corresponding counterions. Solvent molecules are not shown, except for the  $I^0S^0$  case (triangles); dashed lines correspond to H-bonding interactions. For a detailed explanation, refer to the text.

strongly anisotropic structures are formed, mostly in the shape of fibers, but also as ribbons, platelets, or cylinders.<sup>115–118</sup>

Several families of organogelators exist; however, the physical-chemical phenomena leading to the gelation of organic liquid phases is not yet well understood, and most organogelators have been serendipitously discovered. These molecules are mostly classified according to the main forces present in the gel formation step, although different interactions can be responsible for the organization at the supramolecular level: H-bonding, van der Waals forces, dipole-dipole interactions, charge transfer, electrostatic interactions, coordination bonds, etc.

Figure 11 presents some typical examples of organogelators belonging to the different families: capable of performing H-bonding, based on a steroidal or organometallic skeleton, or other molecules such as phthalocyanines or 2,3-bis-*n*-decyloxyanthracene (DDOA).

Recent AFM studies demonstrated the role of the solvent in the formation of fibrous organogels, based in cholesterol derivatives. These gels are composed by fibers imprisoning  $\sim 30\%$  of the solvent molecules; every organogelator molecule is thus able to “fix”

**Table 4.** Examples of Mesostuctured Inorganic Materials Showing Different Interactions between the Surfactant and the Inorganic Framework

surfactant type	interaction type	example materials (structure) <sup>a</sup>	ref		
cationic $S^+$	$S^+I^-$	silica: MCM-41 (hex)	37		
		MCM-48 (cub)	37		
		MCM-50	37		
		tungsten oxide (lam, hex)	33, 103		
		Sb oxide (V) (lam, hex, cub)	33		
		tin sulfur (lam)	33, 104		
	aluminum phosphate (lam, hex)	105, 106			
	$S^+X^-I^+$	silica: SBA-1 (cub Pm3a)	33		
		SBA-2 (hex 3D)	33, 94		
		SBA-3 (hex)	33		
zinc phosphate (lam)		33			
$S^+F^-I^0$	zirconium oxide (lam, hex)	108			
	titanium dioxide (hex)	283			
anionic $S^-$	$S^-I^+$	silica (hex)	102		
		Mg, Al, Ga, Mn, Fe, Co, Ni, Zn (lam) oxides	33		
		lead oxide (lam, hex)	33		
		aluminum oxide (hex)	109		
		tin oxide (hex)	110		
		titanium oxide (hex)	111		
		zinc oxide (lam)	33		
		alumina (lam)	33		
		neutral $S^0$ or $N^0$	$S^0I^0$	silica: HMS (hex)	99
				MSU-X (hex)	100
$N^0I^0$	silica (lam, cub, hex)		112		
	Ti, Al, Zr, Sn (hex) oxides		100, 110		
$N^0X^-I^+$	silica: SBA-15 (hex)		107		
	silica (Hex)		102		
$(N^0M^{n+})I^0$	silica (Hex)		148		
	Nb, Ta (hex) oxide		113, 114		
$S^-M^+I^-$					

<sup>a</sup> hex, hexagonal; lam, lamellar; cub, cubic.

$\sim 10^3$  solvent molecules. The rest of the solvent is placed between these fibers, bearing a weak interaction with the organogelators; this “weakly bonded” solvent may also be a cosolvent, not capable of forming gels.<sup>118</sup>

Organogels are already being used in the photographic, cosmetic, oil, and food industries. Being able to reversibly form fibrous networks, with well-defined geometry and shape, they have been recently used as templates for the synthesis of nano- and microstructured materials, as will be shown below.

**Polymeric Templates. Dendrimers.**<sup>119–121</sup> Dendrimers are macromolecules composed of monomers that are associated in a fractal-like manner around a multifunctional central core. Two synthesis approaches (convergent or divergent) have been described. After successive reactions, an *n*th-generation polymer (Figure 12) is obtained, resulting in a highly branched arrangement of functionalized chains of overall spherical shape. The terminal functions in the periphery can be adequately tailored, as well as the nature of the inner cavities, closer to the dendrimer core.

Dendrimers are polymers of very well-defined structure, isomolecular and multifunctional, presenting characteristic solubility, viscosity, and thermal stability. This high structural definition, associated with their flexibility in size and functions, makes dendrimers a very promising template for the synthesis of novel materials. The most interesting studies should aim to the synthesis of new hybrid

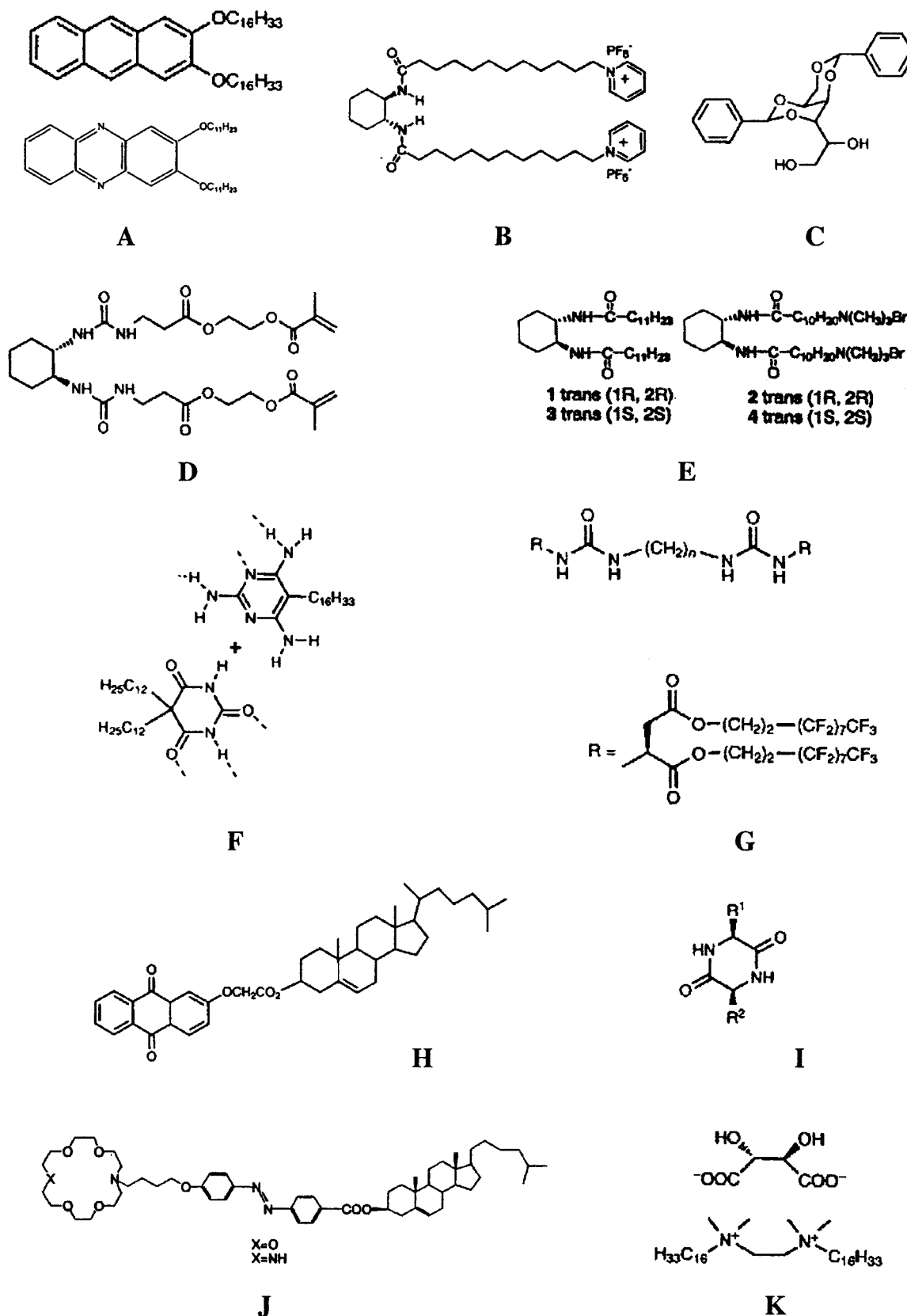


**Figure 11.** Examples of organogelators. Description and examples are given in the text.

nanocomposites; all of these strategies can in principle be transposed for industrial purposes to hyperbranched polymers, which are cheaper, although not so monodisperse.

Dendrimers have already found numerous applications including metal complexation<sup>122</sup> and also use

as catalysts,<sup>123</sup> and their incorporation within silica allows production of supported catalysts,<sup>124</sup> chromatographic supports,<sup>125</sup> or porous membranes.<sup>2c</sup>

Recently, dendrimers have been used as building blocks for nanostructured materials<sup>126</sup> and as templates to prepare mesoporous silica.<sup>127</sup>

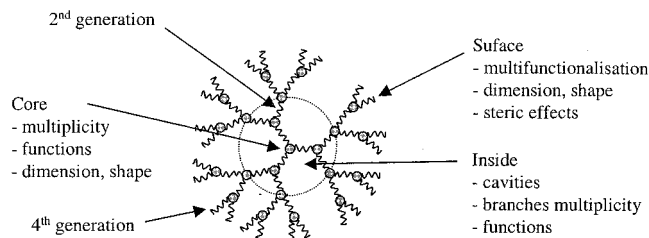


**Figure 12.** Schematic representation of a dendrimer.

**Block Copolymers.** Amphiphilic block copolymers (ABC) represent a new class of functional polymers, with a strong application potential, mainly due to the high energetic and structural control that can be exerted on the material interfaces. The chemical structure of ABCs can be programmed to tailor interfaces between materials of totally different chemical natures, polarities, and cohesion energies.<sup>128</sup> ABCs are able to self-assemble in varied morphologies (Figure 13), like their molecular counterparts,

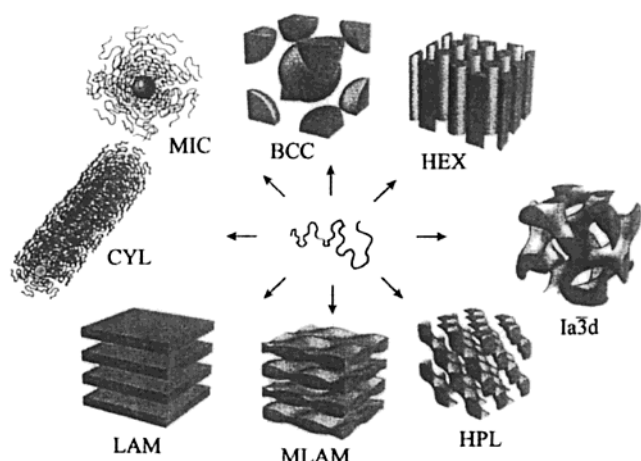


**Figure 13.** Main morphologies of ABC polymers: spherical micelles (MIC), cylindrical micelles (CYL), lamellar structures (LAM), modulated lamellar (MLAM), hexagonal pinhole layers (HPL), gyroids (*Ia3d*), ordered cylinders (HEX), and body-centered cubic (BCC). Reprinted from ref 129. Copyright 1998 Wiley-VCH.

the “traditional” surfactants. Polymer organized systems (POS) formed by ABC polymers are excellent templates for the structuring of inorganic networks; they have been also used for growth control of discrete mineral particles.<sup>8,129</sup> Diblock (AB) or triblock (ABA) block copolymers are generally used, in which A represents a hydrophilic block [polyethylene oxide (PEO) or polyacrylic acid (PAA)] and B, a hydrophobic block [polystyrene (PS), polypropylene oxide (PPO), polyisoprene (PI), or polyvinylpyridine (PVP)].

Biological systems make use of amphiphilic polymeric systems, such as proteins and polysaccharides, to solve problems of heterophase stabilization. Nowadays, a great variety of polymers based on nucleic acids, amino acids, and saccharides are being developed by biological and biochemical methods. These macromolecules, which are used for medicinal applications, could also be applied as building blocks or templates of advanced mesostructured materials. A very interesting example has been recently presented, where synthetic polypeptide-based ABCs are

capable of acting simultaneously as templates and catalysts of the formation of an ordered silica framework.<sup>130</sup>

**Other Texturing Agents. Colloidal Crystals.** Colloidal suspensions of polystyrene (PS) spheres (“colloidal latex”) can lead to ordered structures in the submicronic range upon slow sedimentation followed by solvent evaporation. The optical properties of these systems, known as “colloidal crystals”, have been thoroughly studied.<sup>131</sup> These “organic opals” have been also studied as templates, to yield macroporous materials.<sup>24,25</sup> The interstitial space between the spheres is first impregnated with an inorganic sol (generally obtained by the hydrolysis–condensation of inorganic precursors, such as alkoxides, or related compounds). A second step implies the elimination of the organic template, by heating or washing. This permits in turn the revelation of a tridimensional porous network, the periodicity of which can be controlled by controlling the size of the PS spheres. Three-dimensional ordered macroporous titania (anatase) structures have also been obtained by a cooperative method, where the fabrication of the templating agent and the impregnation are carried out simultaneously.<sup>132</sup>

Monodisperse hexagonal mesoporous silica spheres have been prepared by micromolding in inverted polymer opals. The inverted polymer opal was made by first the infiltration of monomer within the voids of a silica opal. After polymerization, the silica spheres were removed by etching with HF.<sup>133</sup> The uniform and interconnected voids of the porous polymer can be subsequently used to generate a wide variety of highly monodisperse inorganic, polymeric, and metallic solid and core–shell colloids, as well as hollow colloids with controllable shell thickness, as colloidal crystals.<sup>134</sup>

**Biological Systems.** Biological systems such as proteins or other supramolecularly organized entities (viruses, bacteria) can also be used in order to obtain textured or structured inorganic frameworks. Some recent works describe the use of these systems as direct templates of the mineral phase (tobacco mosaic virus, *Bacillus subtilis*, other bacterial threads, cells, etc.) or as host cavities to control the growth of inorganic objects (ferritine).<sup>23,135–138</sup>

At the macroscopic level, the organic matrix of a cuttlebone of a *Sepia officinalis* (cuttlefish) was used as a template to make macroporous chitin–silica composites.<sup>138</sup> Butterfly wings and spider silk have been also used to template siliceous matrix produced by chemical vapor deposition.<sup>139</sup>

**Phase Separation.** Texturation methods that take advantage of phase separation processes have also been described.<sup>24,140,141</sup> In this approach, the precipitation of the inorganic phase is performed within a water/oil or polar/nonpolar solvent microemulsion. The inorganic phase, often hydrophilic, is formed in the polar phase of the emulsion. Recently, thermodynamically stable microemulsions have been prepared with amphiphilic block copolymers and used to produce mesostructured cellular foam materials with uniformly sized and shaped pores.<sup>142</sup>

Mixtures of hydrosoluble/hydrophobic polymers have also been used as preformed templates to generate a hierarchically controlled morphology.<sup>86</sup> Microstructural control is attained by controlling gelation and precipitation processes; the phase separation step is via a spinodal decomposition.

In contrast, mineral gels (based on silica or organosilanes) can also be used in the growth and orientation control of organic nanocrystals. The linear and nonlinear optical properties of these materials are nowadays being studied.<sup>143</sup>

### 3.3. Silica-Based Structures

#### 3.3.1. Evolution of the Research

Silica-based materials are the most studied systems, for several reasons: a great variety of possible structures (flexibility of tetracoordinated Si), a precise control of the hydrolysis–condensation reactions (due to a lower reactivity), enhanced thermal stability of the obtained amorphous networks (no crystallization upon thermal treatment), and strong grafting of organic functions. In addition, a great number of structures found in nature presenting complex architectures (the case of diatoms or radiolaria) are silica-based.

The discovery of mesoporous silica or aluminosilicate molecular sieves in 1992 had an enormous impact in different domains, such as catalysis, adsorption, optics, and electronics. The novel M41S family was originally obtained by hydrothermal synthesis, in basic media, from inorganic gels containing silicate (or aluminosilicate), in the presence of quaternary trimethylammonium cations,  $C_nH_{2n+1}(CH_3)_3N^+$  ( $C_nTMA^+$ ,  $8 < n < 18$ ),  $C_{16}TMABr$  (CTAB) being the most usual surfactant. An alternative method was presented by a Japanese group in 1990, the same year as Mobil's patent. The intercalation of  $C_nTMA^+$  ( $n = 12, 14, 16, \text{ or } 18$ ) in the interlamellar space of a hydrated silicate, *kanemite* ( $NaHSi_2O_5 \cdot 3H_2O$ ) gave rise to the series of folded sheet mesoporous (FSM) materials;<sup>144</sup> analogously to MCM-41, FSM-16 is prepared from CTAB. More recently, Di Renzo et al.<sup>145</sup> showed that the first examples of low-density mesoporous materials had already been patented in the early 1970s;<sup>146</sup> these silica materials present characteristics similar to those of MCM-41. Recently, a pseudomorphic synthesis based on the dissolution–reprecipitation of silica microspheres in alkaline media in the presence of  $C_{16}TMABr$  allows one to produce morphologically controlled MCM-41.<sup>147</sup>

The use of nonionic surfactants as templating agents opened new opportunities in this field.<sup>98,99</sup> Hexagonal mesoporous silica (HMS) compounds are obtained at neutral pH, according to a new synthesis path,  $S^{OT}$ ,<sup>98,99</sup> using primary amines  $C_nH_{2n+1}NH_2$  ( $n = 8–18$ ) as amphiphilic molecules. Nitrogen NMR studies demonstrate that the amines are not protonated under the synthesis conditions. The interaction between inorganic precursors and amines seems to depend essentially on H-bonding. Diamines  $H_2H(C_nH_{2n})NH_2$  ( $n = 8–12$ ) are a particularly interesting template to prepare lamellar structures capable of resisting the extraction of the organic component.

Indeed, these multilayer geometries can be arranged into globular vesicles. The walls are formed by a lamellar stacking, between which a microporosity is developed. Mesoporous silica (MSU-X) has also been synthesized using PEO-based polymers as templates, of the general formula  $R-(OCH_2CH_2)_nOH$  ( $R = \text{alkyl chain}$ ).<sup>100,101</sup> The presence of  $M^{2+}$  ions attached to the ethylene oxide groups seems to enhance the ordering.<sup>148</sup>

A great deal of work has been devoted to pore size control. Beck et al. were able to tailor the pore size from 15 to 45 Å by varying the chain length of  $C_nTMA^+$  cations between 8 and 18 carbon atoms. The addition of organic molecules such as 1,3,5-trimethylbenzene<sup>82</sup> or alkanes<sup>149</sup> permitted increased pore size up to 100 Å. These swelling agents are soluble in the hydrophobic part of the micelle, increasing the volume of the template. This method, albeit simple in appearance, is difficult to put into practice, lacks reproducibility, and yields less organized mesophases. As an alternative to the swelling agent, an effective method relies on prolonged hydrothermal treatment in  $TMA^+$  solutions; this procedure improves the pore organization, as well as increasing the pore size.<sup>150</sup>

However, the pore size of MCM-41 and related materials is restricted by the size of the micellar templates; a natural extension to increase the pore size consists of making use of larger molecules such as polymers or more complex texturing agents (other organic or biological templates). The utilization of ABCs for larger pore sizes has been demonstrated and thoroughly discussed by Antonietti and colleagues.<sup>8,129</sup> Following this approach, Stucky and co-workers (who had developed the synthesis of the SBA silica series in acidic media<sup>33,94</sup>) have developed synthesis methods that yield large-pore (up to 300 Å) mesoporous silica.<sup>107</sup> The group of S. Mann made use of bacterial threads to create a macroporous hexagonal texture in silica.<sup>23</sup> These synthesis paths that rely on preformed templates are interesting in multiscale templating (vide infra).<sup>19,23,151</sup> Mann pioneered the preparation of functional siliceous materials with ordered and bimodal porosity. Antonietti and colleagues shortly after reported the synthesis of mesoporous silica with large pores and bimodal pore size distribution by templating of polymer lattices.<sup>152</sup> The use of colloidal crystals made of polystyrene beads as a template for three-dimensional well-organized macroporous inorganic network<sup>18,153</sup> promoted also the development of inorganic materials with polymodal porosity.<sup>22</sup> The multiscale porosity design was also well illustrated by the use of polydimethylsilane stamps as template<sup>151</sup> or the use of zeolite nanoparticles as building-blocks (Table 5).<sup>154</sup>

Mesostructured silica has also been obtained using synthetic polypeptides as templates. After having studied the role of silicate in silica biomineralization in *Tethya aurantia* sponges, Morse et al. synthesized Cys-Lys block copolymers, capable of mimicking the properties of silicate in<sup>130,155</sup> the copolypeptides self-assembly in structured aggregates that hydrolyze the silica source [tetraethoxysilane (TEOS)]. Simultaneously, these aggregates direct an organized

**Table 5. Main Research Concerning the Synthesis of Micro-, Meso-, and Macrostructured Silica in the Presence of Organic Templates**

framework	structuring agents	structure <sup>a</sup>	porosity	ref
SiO <sub>2</sub> and SiO <sub>2</sub> /Al <sub>2</sub> O <sub>3</sub>	C <sub>n</sub> TMA <sup>+</sup>	hex, lam, cub	15–100 Å	82
SiO <sub>2</sub>	C <sub>n</sub> TMA <sup>+</sup>	hex (FSM)	20–40 Å	144
	C <sub>n</sub> NH <sub>2</sub> , C <sub>n</sub> EO	hex (HMS, MSU)	20–50 Å	98–101
	ABC	disordered	70–150 Å	8–129
	ABC (P123)	hex (SBA-15)	100–300 Å	107
	latex	hc	200–500 Å	19
	bacterial threads	hex	bimodal	23
	latex/ABC	disordered	bimodal	152
	latex/C <sub>16</sub> TMABr	hc/hex	bimodal	22
	electrolyte/ABC	foam/hex	bimodal	317
	PDMS/latex/ABC	–/hc/cub	polymodal	151
	latex/zeolites	hc/MFI	bimodal	154
	co-polyptide	spheres/columns		130
	microemulsion	disordered		140
organogelator	hollow fiber		500 Å 330	
functionalized SiO <sub>2</sub> indirect path	C <sub>16</sub> TMABr	hex	20 Å	159, 160
functionalized SiO <sub>2</sub> direct path	C <sub>16</sub> TMABr	hex	20 Å	162

<sup>a</sup> hex, hexagonal; lam, lamellar; hc, compact hexagonal; cub, cubic; MFI, zeolite-type structure.

structure. Moreover, a controlled oxidation of –SH groups belonging to the Cys fragments permits varied final structures: from hard silica spheres (totally reduced Cys) to well-defined silica columns (totally oxidized form of the copolymer). These results illustrate the importance of the self-assembled copolymer architecture in the obtained tertiary structure and thus in the morphology.

In the synthesis of template-mediated siliceous materials with complex architecture, the use of soft templates has been extended to microemulsions<sup>140</sup> and organogelators.<sup>156</sup>

**Porous Organically Modified Silica Matrices.** Apart from the synthesis optimization and the quest for new architectures in MCM-41 and related solids, an important effort has been set to develop materials with well-defined functionalities. Once the pore size and shape have been mastered, it is the turn of adding functions to the internal surface of these pores, to modify the surface properties or to provide a particular property to the material.<sup>157,158</sup> The first approach is to postfunctionalize a mesoporous oxide phase (calcined or extracted, to eliminate the template), by grafting organic<sup>159,160</sup> or organometallic groups.<sup>161</sup> Mann et al. have shown that the grafting can be directly made by co-condensation of an organosilane and a silicon alkoxide, in the presence of surfactants.<sup>162</sup> This synthesis route presents several advantages, such as the high control of the concentration and dispersion of the grafted functions.<sup>157,163</sup>

The most representative research works concerning the synthesis of meso- and macrostructured hybrid silicas are presented in Table 5.

### 3.3.2. Formation of the Inorganic Network

**Pure Silica Frameworks: Role of the Hybrid Interface.** MCM-41-type materials are characterized by a regular hexagonal arrangement of cylindrical pores, presenting a sharp pore distribution. The inorganic walls are generally microporous (nonorganized microporosity) and constituted by amorphous silica.

Originally, the M41S family was synthesized from different silica sources (such as TEOS, Ludox colloidal silica, fumed silica, sodium silicate), a cationic surfactant (C<sub>16</sub>TMABr), a base (NaOH, TMAOH), and water.

In these alkaline conditions, the interactions between surfactant molecules (S<sup>+</sup>) and the inorganic framework (I<sup>–</sup>) are mainly electrostatic (S<sup>+</sup>I<sup>–</sup>). Analogous solids can be synthesized in acidic media (SBA-1, SBA-3). In this case, the mineral–template interactions are different, and a more relaxed hybrid interface (S<sup>+</sup>X<sup>–</sup>I<sup>+</sup> type) is created, where the charge-compensating anion X<sup>–</sup> (for example, Cl<sup>–</sup> from HCl, used to adjust pH) permits an electrostatic coupling between the equally charged surfactant and inorganic species.<sup>96</sup>

These procedures have been extended to nonionic surfactants. The HMS family is obtained by precipitation at neutral pH, using TEOS as the silica source and primary amines as templates.<sup>98,99</sup> In these conditions, the formation of the silica network is probably catalyzed by the amine functions [amines are excellent catalysts of Si(IV) hydrolysis and condensation]. The MSU-x family of mesoporous silica has been prepared by hydrolysis–condensation of TEOS in strong acidic media, in the presence of PEO-based templates.<sup>100,101</sup> In these systems, thicker walls (and hence an improved thermal stability) are obtained as a consequence of both acid catalysis and the interactions between the template and the inorganic framework.

Fluoride is a well-known catalyst for hydrolysis and polymerization of silica species<sup>15</sup> and has been used in the synthesis of mesoporous silica materials under various conditions to improve structural order.<sup>100,102,164</sup> A two-step process based on the use of fluoride has been developed to produce mesoporous siliceous materials. This synthetic pathway presents the advantages of being easy and highly reproducible.<sup>165,166</sup> A one-step synthesis leading to highly ordered materials has been developed in a wide pH range (0–9).<sup>167</sup>



Antonietti and colleagues proposed a synthesis path that relies on ABC polymeric templates.<sup>8,129</sup> The syntheses are generally carried out in acid media, using silicon alkoxide precursors. The formation of the mineral network may take place either in the hydrophilic domains or at the interface of the self-assembled block copolymer. The utilization of ABCs permits increased pore size in about an order of magnitude and thicker walls, enhancing thermal and mechanical stability. Moreover, macroscopic monoliths (from millimeters to centimeters) can be obtained by this pathway, due to the enhanced ductility and elasticity imparted by the polymer. Following this approach, Stucky and colleagues synthesized mesoporous silica presenting large size pores, up to 300 Å.<sup>107</sup> Even larger pores can be created by resorting to more complex organic or biological texturing agents (see below).<sup>151,154</sup>

**Doped Silica and Silica-Based Mixed Structures.** The first synthesis methods of mesoporous materials were aimed at silicates and aluminosilicates, as a consequence of their potential implications in the catalysis field. This initial effort was soon followed by the synthesis of other mixed oxides, such as vanadosilicates, borosilicates, zirconosilicates, titanosilicates, and gallosilicates.<sup>168–172</sup> The insertion of metal cations into the silica framework can be attained either by a postsynthesis treatment or by the mixing of the adequate precursors in the initial reacting systems.

The interest of doping relies in the creation of novel catalytic materials. The incorporation of metal centers seems simple. However, a deeper analysis of the abundant methods described so far in the literature reveals a lack of reproducibility of the obtained materials, namely in terms of the effective incorporation of the heteroelement into the silica framework and its localization and dispersion throughout the material. Other important gaps are the nature of the mesostructure and the stability of the material. A synthesis method based on a “retarding agent”, triethanolamine (TEA), circumvents these limitations.<sup>173</sup> By making use of atrane complexes as inorganic precursors, it has been possible to obtain doped M-MCM-41 (M = B, Al, Sn, Zn, Ti, Zr, V, Mo, Mn, Fe, Co, and Ni) with an M/Si ratio improved by an order of magnitude.

It has also been shown that improved dopant ratios for trivalent cations can be attained by resorting to a neutral  $S^{0T^0}$  synthesis path, rather than an electrostatic approach.<sup>174</sup> In these cases, the incorporation of the M(III) is strongly dependent on the synthesis conditions, particularly on pH.

Recently, various methods to dope siliceous MCM-41 matrices with titanium have been compared.<sup>175</sup> The direct synthesis route generally leads to a less ordered porous network. Postsynthesis doping of Ti allows high Ti loadings. The incorporation of Ti by impregnation results in a phase separation. Although a small decrease in pore diameter is observed, the MCM-41 structure is preserved when titanium is postgrafted. The resulting solids present an even dispersion of titanium centers.

**Hybrid Compounds.** The high control of MCM-41 and related phases (in terms of highly accessible surface, a wide choice of pore size, and pore uniformity and distribution) makes these materials particularly interesting as supports. Organic functions can be grafted onto the oxide walls, leading to hybrid mesostructured materials, with tunable surfaces. This is an indeed promising issue in the design of advanced integrated materials, such as catalysts, membranes, sensors, and nanoreactors.<sup>176</sup>

An important number of techniques have been developed or adapted to add organic functions to the walls of mesoporous silica,<sup>157</sup> combining the properties of a mesoporous inorganic structure with the surface organic groups. The mineral framework ensures an ordered structure in the mesoscale, thermal and mechanical stability. The organic species integrated to the material permit fine control of the interfacial and bulk properties, such as hydrophobicity, porosity, accessibility, optical, electrical, or magnetic properties. The incorporation of the organic functions can in principle be carried out in two ways: (a) by covalent binding on the inorganic walls of the material (post-treatment) and (b) by direct incorporation of the organic functions, upon the synthesis process (one-pot).

In the first approach, organochlorosilanes or organoalkoxysilanes have been widely used to graft specific organic groups, by condensation reactions with silanol or Si–O–Si groups of the silica framework (Figure 14 a).<sup>159,160,177</sup> The mesoporous hosts

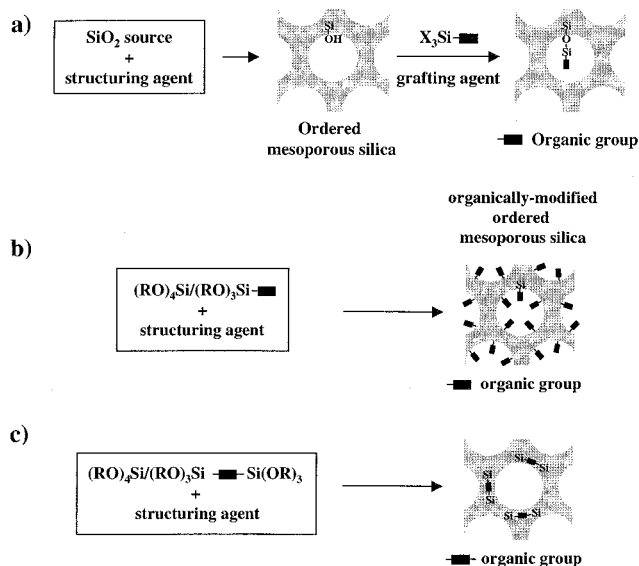


**Figure 14.** Incorporation of organic functions in mesoporous silica: (a) surface grafting of organic functions on the mesopore walls by postsynthesis; direct incorporation of organic functions by co-condensation of organosilanes (b) or bridging silsesquioxanes (c).

must be thoroughly dried before the addition of the organosilane precursors to avoid their autocondensation in the presence of water. The concentration and distribution control of the organic functions is restricted by the surface silanols and their accessibility. The grafting ratio depends on the precursor reactivity, being also limited by diffusion and steric factors.

An alternative approach for pore functionalization relies on a direct synthesis, based on the co-condensation of siloxane and organosiloxane precursors in situ to yield modified MCM-41 in one step (Figure 14b).<sup>162,178</sup> Whereas siloxane precursors ensure the formation of the mineral network, organosiloxane moieties play a double role: they contribute as building blocks of the inorganic structure and they provide the organic groups. This one-pot pathway presents several advantages, such as high modification ratios, homogeneous incorporation, and short preparation times.<sup>163</sup> However, the choice of the modified precursor is constrained by the synthesis conditions. Alkaline media, hydrothermal conditions, and solvent extraction limit the choice to organic fragments presenting Si–C bonds stable to nucleophilic attack. Bridged silsesquioxanes [(RO)<sub>3</sub>Si–R'–Si(OR)<sub>3</sub>] have also been utilized in this kind of synthesis, also yielding organically modified mesoporous silica, also known as periodic mesoporous organosilicas (PMO).<sup>179–182</sup> In these materials, the organic groups (R') are homogeneously incorporated inside the mesoporous walls, which permits the addition of new functions without pore blocking (Figure 14c). Moreover, these structures present an extremely well-defined mesostructure. A great variety of bridging groups have been incorporated, such as  $-(\text{CH}_2)_n-$  or  $-\text{C}_6\text{H}_4-$ . Mesoporous particles presenting different mesostructures (2D-hex, 3D-hex, and micellar cubic *Pm3n*) and controlled morphology (rodlike, spherical, and decaoctahedral, respectively) have been obtained by resorting to  $\text{R}' = -\text{CH}_2\text{CH}_2-$  in different synthesis conditions.<sup>183</sup> When R' is a *p*-disubstituted phenyl, particularly well-ordered materials have been synthesized, which combine mesopores with walls presenting a layered structure in the molecular range (5.7 Å), giving rise to a hierarchically ordered mesostructure in a one-pot synthesis. In this case, the phenyl–phenyl interactions are believed to be responsible for the crystalline arrangements of the pore walls.<sup>184</sup> Bulky groups able to chelate metal centers, such as 1,4,8,11-tetraazacyclotetradecane (cyclam), have been incorporated in the walls of large-pore Pluronic-templated silica.<sup>185</sup>

### 3.3.3. Formation Mechanisms

After the discovery of M41S and related solids, an important number of research teams focused on the understanding of their formation mechanisms.<sup>186</sup> Most of the work was devoted to MCM-41 silica in alkaline medium, using cationic alkylammonium halide templates. In this section, we will present a critical review of these advances. Although there is a sustained interest in the formation paths of mesostructured silica films, we will not present the works devoted to film formation, as a detailed discussion is out of the scope of this review. The essential features of the evaporation-induced self-assembly approach have been addressed by Brinker and colleagues,<sup>187</sup> and we will describe some interesting applications for non-silica systems in the corresponding section.

Several models of MCM-41 formation have been proposed,<sup>5</sup> a very important task in order to rationalize the nature and structure of the obtained materi-

als. Finding a correlation between the synthesis method and the final structure is a key point to the design of mesoporous materials, an indeed more elegant strategy than the usual combinatorial/analytical approach.

All models proposed so far are based on one principle: surfactant molecules play a central role in directing the formation of the inorganic mesostructure from soluble mineral species.

The principal sources of discrepancy between different models concern the condensation extent and structure of the mineral precursor, the structure of the hybrid surfactant/mineral precursor species involved in the self-assembly process and, thus, the nature of the surfactant–inorganic precursor interaction at the hybrid interface. The latter parameter seems to be the key factor, the modification of which implies obtaining a great variety of mesoporous structures. From a general point of view, the formation mechanism of mesostructured phases, based on the specific electrostatic interaction between an inorganic precursor (*I*) and the surfactant polar head (*S*) was formalized by Huo et al.<sup>96</sup> The reaction path involving cationic surfactants and negatively charged silica species is called the  $\text{S}^+I^-$  path. Analogously, the  $\text{S}^-I^+$ ,  $\text{S}^+X^-I^+$  (where  $X^-$  is a counteranion), and  $\text{S}^-M^+I^-$  (where  $M^+$  is a metallic cation) paths were established. This is an indeed useful classification (see Table 4), particularly when other types of interactions are also involved.

**Liquid Crystal Templating (LCT) Approach.** The obtained mesostructure for M41S materials depends in principle on the surfactant concentration and hydrophobic chain length and on the presence of organic swelling agents, dissolved in the hydrophobic spaces. This analogy with liquid crystal mesophases led Beck and co-workers to initially propose mechanisms in which the texturing effect was provided by a liquid crystalline phase. Following this line of thought, two LCT pathways for MCM-41 formation were proposed (Figure 15): (I) Silicate precursors fill

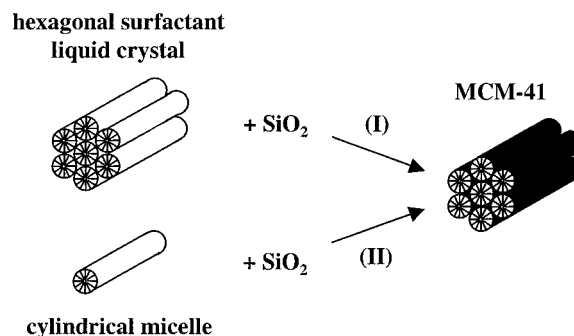


**Figure 15.** Schematic pathways proposed by Beck et al.<sup>82</sup> for MCM-41 formation.

the water-rich spaces of the hydrophilic domains of a preformed lyotropic LC hexagonal phase and settle on the polar heads, located at the external surface of the micelles. (II) The inorganic species direct the self-assembly process of the surfactant, forming hybrid hexagonal coarrangements.

In both cases, the negatively charged mineral moieties ( $\text{pH} > \text{pH}_{\text{iep}}$  for silica; iep = isoelectric point)

interact preferentially with the ammonium polar heads of the surfactant, which are positively charged. Subsequent condensation leads to a continuous inorganic phase. This initial mechanism proposed by Mobil was, however, reworked, on the basis of further experimental evidence: the surfactant concentration is well below the one required for LC formation, and on the basis of  $^{14}\text{N}$  NMR studies, Davis and colleagues showed that the hexagonal LC phase is not formed during the synthesis of MCM-41.<sup>188</sup> It was instead proposed that under the synthesis conditions reported by the Mobil team, the formation of MCM-41 begins with the deposition of a silicate layer (consisting of two or three monolayers) on the surface of isolated rodlike micelles. These “rods” are randomly ordered, eventually surrounded by a hexagonal silica mesostructure. Heating and aging of this material complete silicate condensation, leading to the MCM-41 structure.

However, in different synthesis conditions, the pioneer Mobil mechanism has been recently validated.<sup>112</sup>

The second LCT mechanism has been vaguely postulated as a self-assembly process of the ammonium polar heads and the mineral moieties, based on the favorable electrostatic interactions. The silicate/surfactant “supermolecules” are probably less soluble than the surfactant molecules, which induces the separation of an LC phase at concentrations lower than the cmc of the surfactant.

Steel et al. performed  $^{14}\text{N}$  NMR studies, which led them to propose that surfactants directly self-assemble in hexagonal LC phases upon silicate addition.<sup>189</sup> Silicate species are initially organized in layers. Aging of the reaction mixtures induces folding and rearrangement of these sheets around rodlike micelles, this transformation leading to MCM-41 mesostructures.

**Cooperative Self-Assembly Pathway.** Researchers at the University of Santa Barbara proposed a third mechanism, suggesting that the MCM-41 phase might be derived from a lamellar phase, observed by XRD in the initial mixtures.<sup>84,190</sup> The formation of this lamellar phase would be favored by the electrostatic matching between the highly charged anionic silicate species and the positively charged surfactants. Once the silica condensation is triggered, the negative charge density is reduced, leading to an increase of the optimal surface per polar group. This new situation leads in turn to a charge rearrangement; to keep the electroneutrality, the silica/surfactant ratio must increase. As a consequence, the interface begins to develop a more marked curvature, causing the lamellar  $\rightarrow$  hexagonal transition. This argument is supported by experimental observations in which *kanemite*, a layered hydrated sodium silicate, is used as an inorganic precursor for the synthesis of a mesostructured phase.<sup>144</sup> The lamellar  $\rightarrow$  hexagonal transition was also observed in the so-called FSM materials, prepared by intercalation of alkylammonium surfactants into kanemite. After the ionic exchange, the silica layers fold around the surfactant, leading to a hexagonal phase. The final material displays a

structure very similar to that of MCM-41. However, the proposed mechanism is still a matter of debate. By using in-situ XRD, Lindén et al.<sup>191</sup> showed that hexagonal silica-CTAB mesostructures are directly obtained by precipitation in alkaline media. Using a similar technique (energy dispersive XRD) O'Hare and co-workers confirmed that a lamellar insertion product ( $\text{C}_{16}\text{TMA}^+$  into kanemite) is the first solid formed in the synthesis of two-dimensional hexagonal FSM-16-type materials. At the synthesis pH, dissolution-precipitation processes take place and govern the observed transition. In contrast, no ordered precursors were found in the synthesis conditions for 2D-hex MCM-41.<sup>192</sup>

An important advance in the understanding of the formation mechanisms of MCM-41 was accomplished with the works of Firouzi et al.<sup>193</sup> Under synthesis conditions where extended silica condensation is hindered (low temperature, pH  $\sim$ 14), a cooperative self-assembly of silicates and surfactants has been demonstrated by NMR and X-ray scattering (Figure 16). This group unambiguously demonstrated that a micellar solution of cetyltrimethylammonium bromide ( $\text{C}_{16}\text{TMABr}$ ) was transformed in a hexagonal phase in the presence of silicate anions, which exchange with the surfactant counteranions (bromide). This leads to a silicatropic LC phase (SLC), constituted by silicate-covered cylindrical micelles. The micelles act as a template source, the charged silicates behaving in some way as polyelectrolytes. These observations are consistent with the well-known effect of electrolytes that tend to shift the phase boundaries of micellar systems. The SLC presents a behavior similar to that observed in lyotropic systems, even though for lower surfactant concentrations, and in the presence of reactive anions such as silicate. Heating of the SLC phase triggers the irreversible condensation of the silicate species, leading to MCM-41.

Firouzi et al.<sup>85</sup> also demonstrated that in high pH conditions, a preferential interaction between the trimethylammonium head and  $[\text{Si}_8\text{O}_{20}]^{8-}$  silicate anions (D4R, double four-ring) was present, in addition to the electrostatic charge balance. This interaction is so strong that a solution containing an alkyltrimethylammonium surfactant can force the formation of D4R species, even for silica concentrations where D4R species are not likely to form. The close relationship between the projected surfaces of the polar head and a D4R anion (0.098 vs 0.094 nm<sup>2</sup>, respectively) was suggested to be the driving force for this behavior.

**Silicate-Template Interactions: Hybrid Polyelectrolyte Model.** Several of the proposed mechanisms postulate an ionic exchange in solution between the silicate species and the counteranions at the micellar surface.<sup>194,195</sup> This exchange can be a driving force for micelle elongation into rodlike arrangements that lead to the LC phase. The silicate/counterion exchanges taking place on the micellar surface have been recently studied by Zana and colleagues<sup>196,197</sup> by fluorescence techniques, using molecular probes such as pyrene or dipyranylpropane. This study permitted improved understanding

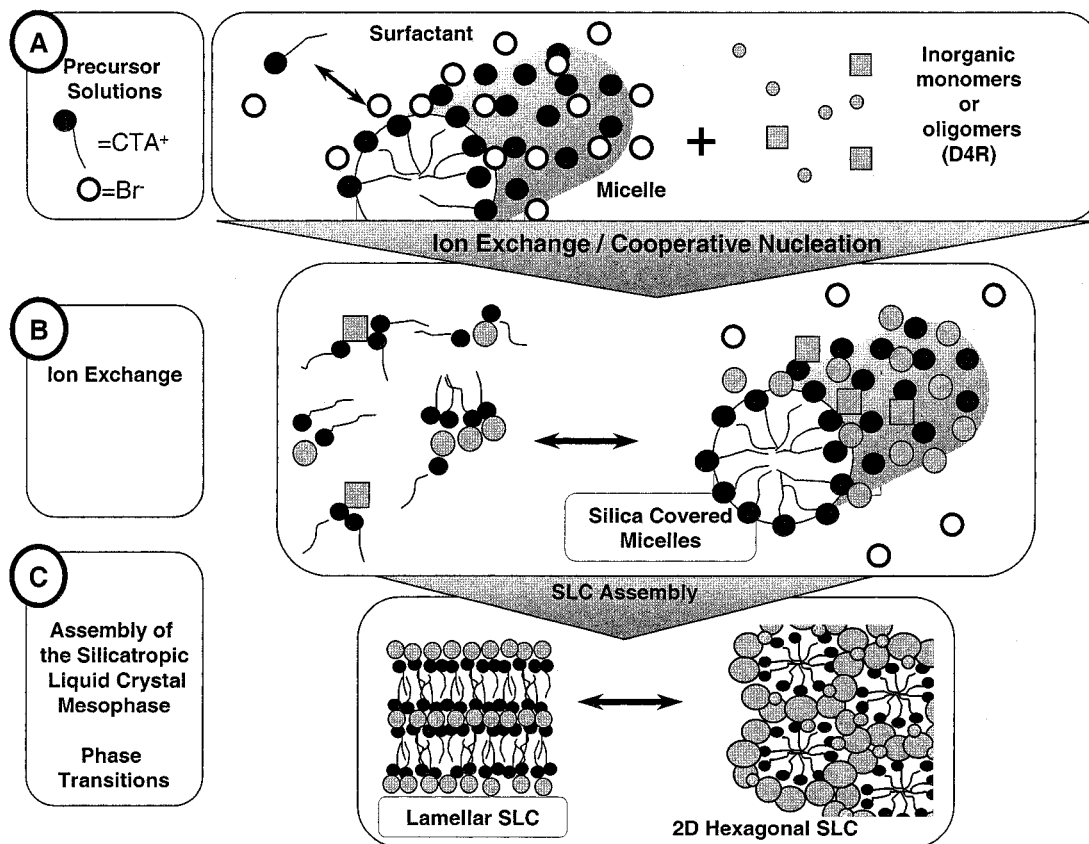


**Figure 16.** Schematic pathways of the “surfactant–silica” cooperative organization mechanism proposed by Firouzi et al. (adapted from ref 193).

of the modifications that are induced by the mineral species on the behavior of micelles in solution, under the synthesis conditions for MCM-41. Fluorescence measurements in highly alkaline medium (pH 13.6) and before silica polymerization (pH 11.6) demonstrated that the exchange of the counteranions on the micellar surface is quite poor. In consequence, this process in solution is not likely to be the determining step in the whole process of mesophase formation.

In view of these results, a new model was proposed for the formation of mesostructured organized silica, where the key step is the formation of silica prepolymers. The initial  $C_{16}TMA^+X^-$  ( $X = Br$  or  $Cl$ ) aqueous solution (Figure 17A) contains spherical micelles, in equilibrium with surfactant cations and free counteranions. Upon addition of a highly alkaline solution of silicate species (step 1), a small fraction of  $Br^-$  anions located on the micelle surface is exchanged for  $HO^-$  or silicate anions (Figure 17B). The lowering of the initial pH (step 2) triggers silica polymerization, leading to silica prepolymers, presenting a low degree of polymerization (Figure 17C). These prepolymers begin to interact with free template ions ( $C_{16}TMA^+$ ). This behavior is similar to the one found in polyelectrolyte/surfactant systems bearing opposite charges. Upon pH decrease, the silica prepolymers grow along time (step 3), and each oligomer is able to interact with a greater number of surfactant molecules, performing a very efficient cooperative effect. In this stage, silica–surfactant hybrid micellar aggregates are formed, in agreement with what has been postulated by Huo et al.<sup>33</sup> (Figure 17D). The surfactant micelles play the role of a surfactant

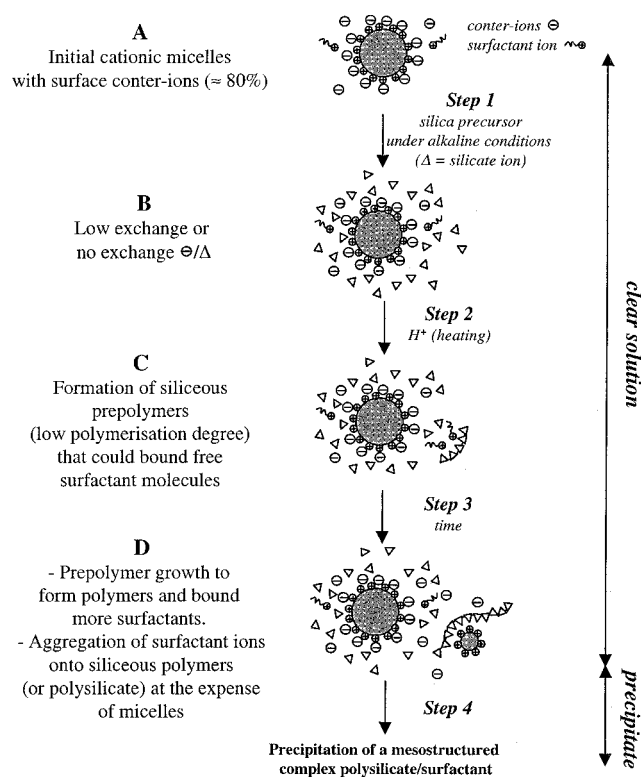


**Figure 17.** Proposed mechanism of mesoporous silica formation (adapted from Zana et al.<sup>197</sup>).

monomer reservoir, which is progressively used up. Figure 17D shows the system just before precipitation of the mesostructured polymer/surfactant com-

plex (step 4). Polymerization of the micellar/silica complexes takes place along the precipitation–aging sequence, leading to ordered mesoporous silica.

The presented models that tend to present the formation of MCM-41 like a succession of events that homogeneously take place in aqueous solution are relatively simple. The first work, based on cryo-TEM and SAXS experiments, shows that there is a possibility that the MCM-41 phase forms in a heterogeneous fashion. Intermediate structures, formed by rodlike shaped micellar clusters covered by silicate species, were observed before silica precipitation.<sup>198</sup> Along the reaction, the silicate species present on the cluster surface diffuse into the inner part of the micellar arrangement and are deposited on the individual micelle surfaces. Subsequent complete coverage of the cylindrical micelles leads to a mesostructure; the micellar clusters thus serve as nucleation sites of the MCM-41 phase.

**Summary of Silica Mesostructure Formation and Transformation.** In all published mechanistic studies, it clearly appears that the interaction between the inorganic precursor and the template is the key factor in the control of the mesostructured materials. All mechanisms presented in this section are adequately supported by experimental evidence; however, it must be kept in mind that none of them provides an exclusive or definitive answer. The analyzed reaction systems are sufficiently intricate as they involve numerous and complex species and equilibria, diffusion, nucleation and growth processes, and other features that can be very sensitive to factors such as temperature, reaction time, pH, and concentration. Moreover, some of the limitations of the characterization techniques are also evident: sampling, exposure time, sample modification, etc. It is important to note that most “discontinuous” characterization techniques sample only a fraction of the systems in a given time. The dynamics of these systems can be generally developed in three main steps: solution state (precursors), intermediate state (solid/liquid, onset of precipitation), and solid state (final material). The last stage is the easiest to study: the system evolution is practically “frozen”, and several available techniques permit a thorough characterization. The liquid states are more difficult to analyze, with a high number of thermodynamic, kinetic, and processing parameters in competition. The task is even more complicated when one is dealing with colloidal systems in evolution, in which a quantitative response is quite difficult to attain. This is remarkable for the onset of precipitation, where the surfactant-rich hybrid polymers, which are precursors of the precipitate, are formed, triggering the development of a heterogeneous system. In most of the synthesis methods reported, this heterogeneity and the organization appear simultaneously. In these conditions it has been difficult to retrieve sufficient robust information in a precise way, which would permit construction of a formation model over a solid basis. In-situ XRD studies permit a close view of mesostructure formation;<sup>191,192</sup> in the future, more light will be shed by combining these structural tools with time-resolved spectroscopic studies (NMR, FTIR,

Raman, etc.) that can provide information on the phenomena taking place at the molecular level. This has been accomplished for mesostructured materials shaped as films, where suitable in-situ techniques (grazing incidence SAXS, ellipsometry, TEM, fluorescence, or mass spectrometry) have been adapted to give a more complete panorama of the processes taking place during formation and processing of these solids.<sup>199–202</sup>

As-synthesized mesostructured hybrids are often weakly condensed, which permits substantial structural evolution upon processing. In a recent series of papers, Tolbert and co-workers studied the phase transformations that occur along hydrothermal treatment by in-situ XRD. Depending on the treatment imposed to mesostructured hybrids (temperature, pH), hexagonal ( $p6mm$ ) → cubic ( $Ia3d$ ),<sup>95a</sup> hexagonal ( $p6mm$ ) → lamellar,<sup>95b</sup> or lamellar → hexagonal ( $p6mm$ )<sup>95b</sup> were observed. In the ( $p6mm$ ) → ( $Ia3d$ ) transition, there is an epitaxial relationship between the axis of the two-dimensional hexagonal channels and the (111) direction of the cubic cell (body diagonal). The transformation is mainly driven by the surfactant; as-synthesized silicate walls are still flexible enough to undergo rearrangement and follow the phase transformation. In the case of lamellar–hexagonal transformations, a complex interplay of surfactant packing and silica charge density (and thus charge matching) results in different activation barriers that direct a given mesophase.<sup>203</sup> In these one-dimensional transitions (the two-dimensional channels evolve into lamellar structures or vice versa), pH is an essential variable, as it controls framework flexibility and surfactant loss. Under basic conditions (pH 11), with a low degree of silica polymerization (i.e., extended silica condensation is “off”) and minimal surfactant loss, changes in surfactant curvature are the main driving force for hexagonal to lamellar transformations.<sup>204</sup> In less basic conditions (pH 7–9), the main activation barriers are related to the rearrangement of the silica framework, which depends on silica hydrolysis and condensation. These processes affect in turn the surfactant density at the hybrid interface.<sup>205</sup> By a careful evaluation of the activation parameters for different paths, it has been possible to separate the effects of precondensation (i.e., inherent to the synthesis of the hybrid mesostructure) from the post-condensation that occurs during hydrothermal treatment. Both processes have a decisive influence on the characteristics of the final material and its ability to transform.

In a related work, Che et al. observed that a two-dimensional hexagonal phase ( $p6mm$ ) precursor is also involved in the synthesis of a  $Pm3n$  cubic mesostructure.<sup>206</sup> A detailed XRD and HRTEM study<sup>207</sup> shows an epitaxial relationship between the {211} plane of the cubic phase and the channels along the (01) direction of the hexagonal bidimensional arrangement. These findings indicate an epitaxial transformation from  $p6mm$  to  $Pm3n$  involving silica restructuring along the cylinder axis of the hexagonal phase.

### 3.3.4. Stability of the Inorganic Network

To create an ordered porous framework, the organic template has to be removed. This is generally carried out by extraction or thermal treatment. However, these treatments affect the mesostructure. Thermal treatment of the hybrid materials results in an important contraction of the inorganic network, in parallel with the exothermic processes associated with template elimination; these two linked processes can seriously deteriorate the mesostructure. In particular, it is of utmost importance to ensure the rigidity of the inorganic walls previous to template elimination. Mesostructured silica synthesized in alkaline conditions with cationic templates generally presents thin and relatively fragile walls. Structures synthesized from cationic surfactants in neutral or acid media, albeit slightly less organized, present thicker walls, being more robust in the face of thermal treatment. A good compromise is attained by resorting to triblock copolymers ABA, which lead to well-defined and organized large pores, thick walls, and, hence, an excellent thermal stability.

The long-term performance of these materials is often poor after template removal, limiting their use in extreme operation conditions. The inorganic framework can be affected by the hydrolysis of siloxane bridges by water present in the environment. This mechanical drawback is probably linked to the hydrophilic character of the internal pore surface, given by the presence of silanol (Si–OH) groups. One of the strategies aimed at the improvement of structural stability consists of grafting methyl organosilanes, to provide a partial hydrophobic nature to the walls.<sup>208</sup>

The hydrothermal stability of the MCM-41 framework synthesized in the presence of fluoride anions was found to be remarkably improved because of the formation of Si–F bonds on the surface of the mesopores.<sup>209</sup>

A coteremplating approach for the synthesis of new mesoporous aluminosilicates of ordered hexagonal structure with high acidity and excellent hydrothermal stability at high temperature has been recently reported via self-assembly of aluminosilicate nanoclusters with templating micelles.<sup>210</sup>

### 3.3.5. Thermal Treatment and Porosity

Mesoporous silica is typically obtained by thermal treatment of the hybrid phases, although extraction in acid ethanol has proven to be useful. The thermal stability of the organized materials depends on factors such as the final temperature and the conditions of calcination (heating ramp, atmosphere, etc.); all of these influence silica condensation and rearrangement and, thus, wall porosity and strength.<sup>211</sup> Surfactant elimination proceeds in several steps; a thorough study of the thermal treatment has determined that the hydrophilic/hydrophobic nature of the pore surfaces changes during heating.<sup>212</sup> For the final MCM-41, walls are typically 8 Å thick, and thus the material is fragile in hydrothermal conditions; this has somehow limited the initial enthusiasm regarding catalysis applications. For ABC templated materials, walls are thicker, enhancing the stability of the material. However, SBA-15 can present residual

microporosity, which is also a stability drawback. A careful analysis of XRD patterns of SBA-15 concluded that the pore walls are composed by a dense core and a less dense corona, where silica and the template polymer are intimately intertwined.<sup>213</sup> Strong interactions of the silica/silanol species with the ethylene oxide (hydrophilic) fraction of the template are responsible for this lack of definition of the hybrid interface. The nature of these interactions has been thoroughly studied in related silica–Pluronic monoliths by Chmelka and co-workers, by using CP-MAS NMR.<sup>214a</sup> A partition of low-weight silica polymers between the solvent and the solvent–template interface has been demonstrated. This silica–polymer entanglement results in a residual microporosity once the template is eliminated. In a remarkable series of pioneering papers, Wiesner and coworkers described a similar behavior in organoaluminosilica/PEO-PI organized nanocomposites.<sup>214b–e</sup> Galarneau et al. have clearly shown that the pore structure of SBA-15 depends on the synthesis and processing (i.e., thermal treatment) of the initial hybrid phases. The microporosity arising from the “comblike nature” of the hybrid interface can be controlled by modifying the silica–template interactions (i.e., modifying the polymerization degree of the inorganic species while enhancing the segregation between the template and the inorganic phase upon thermal treatment).<sup>215</sup>

## 3.4. Non-Silica Mesostructured Materials

Short after the discovery of periodically organized mesoporous silica, a number of efforts were devoted to extending the mesoporous family to non-silicate materials. These systems concern mainly oxides or phosphates of transition metals (TM), aluminum, tin, chalcogenides, etc. These materials are interesting because of their varied framework properties, which should permit development of a plethora of applications, particularly in catalysis, photocatalysis, sensors, optics, separation techniques, smart coatings, etc. However, the reported work on transition metal mesostructured materials is ~1 order of magnitude lower than its silica counterpart. Several main reasons can account for the slower advancement in this field:

- (1) The pioneer groups in mesoporous materials have a scientific background related to zeolites; therefore, they are mainly familiar with silicon and aluminum chemistry.

- (2) The high reactivity toward hydrolysis and condensation of transition metal oxide precursors increases the extent of uncontrolled phase separation between organic and inorganic components, yielding non-mesostructured materials, but porous gels.

- (3) The redox reactions, the possible phase transitions, and the crystallization processes are often accompanied by the collapse of the structural integrity.

- (4) Synthesis procedures are extremely sensitive to many external parameters, leading in some cases to irreproducible results.

Therefore, most reviews covering overall synthesis and characterization of porous and mesoporous materials are mainly focused on silica- and alumina-based systems; however, recent reviews cover specif-

ically non-silica systems.<sup>11–14</sup> In this section, we will focus on non-silica-based oxides and oxophosphates, stressing the chemistry involved in the synthesis paths. Other non-silica structures, such as mesoporous carbon,<sup>216a</sup> siliconitrides, metals,<sup>216b</sup> and polymers, have been recently reviewed by Schüth.<sup>14</sup>

This section is divided into several subsections: the first one summarizes the general chemical strategies that are necessary to construct meso-organized hybrids and oxides by soft chemistry processes. The most relevant work produced in this field, from the mid-1990s to the present, will be then presented. Subsequently, the presentation will be focused on three aspects: synthesis routes to hybrid mesophases, thermal treatment leading to non-silica mesoporous oxides, and a thorough discussion of the formation mechanisms presented so far.

### 3.4.1. Synthesis Strategies for Non-Silica Oxide-Based Structures: Evolution of the Research

The first studies concerning non-silica mesostructured materials have been presented by researchers of the University of Santa Barbara;<sup>33,96,217,218</sup> nowadays, research groups all over the world are developing this field. A great variety of oxide-based hybrids containing surfactant templates and metal cations have been synthesized in the form of powders or “bulk gels”: non-silica main block (Al,<sup>100,101,219–223</sup> Ga,<sup>224</sup> Sn,<sup>110,225–228</sup> Sb, Pb), transition metals (TM: Ti,<sup>111,229–239</sup> V,<sup>240–245</sup> Fe,<sup>246,247</sup> Mn,<sup>248,249</sup> Zr,<sup>250–254</sup> Hf,<sup>255</sup> Nb,<sup>113,256</sup> Ta,<sup>114</sup> W<sup>257</sup>), Y<sup>258</sup>, and rare earths.<sup>259</sup> Some methods can even be generalized for more than one metal cation<sup>173,260,261</sup> or mixed oxides.<sup>261,262,263</sup> Production of organized films is also possible for Al,<sup>264,265</sup> Ti,<sup>266–269</sup> Zr,<sup>270</sup> V<sup>271</sup>, and W<sup>272</sup> systems; films present the paramount advantage to be directly shaped in any substrate for a targeted application. The pioneering and/or relevant publications between 1994 and 2001 for each system are summarized in Tables 6 (salt precursors) and 7 (alkoxide precursors). Both tables include the nature of the precursors (molecular species, clusters, nanoparticles), surfactants, synthesis conditions, nature of the obtained phases, post-treatment, specific surface, and pore diameter. The information here presented permits a global estimation of synthesis methods at a glance. It is important to point out that the reported synthesis conditions are sometimes difficult to attain, leading to a lack of reproducibility. Indeed, most syntheses are kinetically controlled, and solids with amorphous inorganic walls are obtained. Uncontrolled (i.e., very fast) inorganic polymerization can “freeze” a metastable mesostructure (even a nonorganized one) in an “irreversible” fashion. As a consequence, this is an emerging field, and scarce work has been devoted to the formation mechanisms of these materials.<sup>186</sup>

Figure 18 displays selected TEM micrographs of non-silica mesostructured and mesoporous materials (powders or films), obtained by different pathways: precipitation or solvent evaporation. Generally, hexagonal or wormlike mesophases are obtained, cubic symmetry being less frequent (cf. Tables 6 and 7).

The differences between silica- and non-silica oxide-based systems with regard to their synthesis and processing can be summarized as follows:

(1) Metallic (TM, Al, Sn) alkoxide precursors are more reactive toward hydrolysis and condensation than Si alkoxides.

(2) Because of this high reactivity, inorganic polymerization has to be partially blocked. In some cases, clusters or nanoparticles may result, which aggregate upon drying. Thermal treatment of these randomly ordered aggregates can lead to textural mesoporosity, even if the overall solid presents little or no order at the mesoscopic scale.

(3) The mesostructure quality and the extension of the organized domains are often lower for TM than for silica-based systems.

(4) The obtained structures are often unstable toward template removal. This is particularly marked for metals capable of presenting various oxidation states (V, W).

(5) After hydrolysis and condensation, metal centers mostly present a higher coordination than tetrahedral silicon.

The subsequent discussion will be based on these features, which result in the marked differences of behavior observed for these systems.

### 3.4.2. Control of the Formation of the Inorganic Network

**Control of the Precursor Reactivity.** This is the first fundamental issue. **Inorganic hydrolysis and condensation have to be mastered, to avoid the instantaneous formation of an inorganic network,** which would irreversibly “freeze” an ill-organized structure. **The reactivity of the precursors can be efficiently controlled by different means:**<sup>16</sup> (1) by carefully adjusting the pH and dilution of metal salt solutions, (2) by using alkoxides or other salts in the presence of condensation inhibitors (**acids, complexing agents**), (3) by working in nonaqueous solvents and limited quantities of water, (4) by resorting to evaporation-induced self-assembly, (5) by modifying the redox state, or (6) by using preformed nano-objects. Some of the reported synthesis methods use a combination of two or more of these concepts; **the most general approach implies a combination of a condensation inhibitor with a nonaqueous solvent.**

(1) *Mineral Precursors.* The earliest approach, an extension of the methods applied for mesostructured silica, consisted in the dissolution of mineral salts in aqueous solutions containing surfactants (carrying ammonium, sulfate, or phosphate heads), in conditions of controlled pH. The use of these ionic templates produces mostly lamellar hybrid mesophases (Table 6). Highly charged metals [W, Sb(V)] known to yield polyoxometalates (POM) are capable of forming hexagonal or cubic meso-organized phases.<sup>33,96,217</sup> In the case of Sb<sub>2</sub>O<sub>5</sub>/C<sub>18</sub>TABr, for a metal/template ratio of 10, decreasing the pH of a KSb(OH)<sub>6</sub> solution to ~7 yields a cubic (*Ia3d*) phase; lowering the pH to 6.2–6.5 leads to a hexagonal mesophase. The change in pH permits a correct charge and curvature matching at the hybrid interface (cf. section 5). An increase in the template contents results in lamellar hybrids, between pH 6 and 7. For pH values <6, nonorganized amorphous phases are obtained.<sup>33</sup> Interestingly, this limit is coincident with the appearance of highly polycondensed species, such as Sb<sub>12</sub>(OH)<sub>67</sub><sup>7–</sup>.<sup>273</sup>

**Table 6. Mesoporous Non-Silica Oxide-, Oxopolymer- or Metal Oxophosphate-Based Materials, Obtained from Mineral Precursors (Except Silica or Silica-Based Binary Systems)**

mineral precursors (M) template (T)	conditions <sup>a</sup> solvent = H <sub>2</sub> O pH, temp	T:M	textured phases distances (XRD or (TEM) <sup>b</sup>	template removal treatment <sup>c</sup>	porous material distances XRD or TEM ( $\phi_{\text{pores}}$ , S) <sup>d</sup>	ref
[M <sup>2+</sup> (NO <sub>3</sub> <sup>-</sup> ) <sub>2</sub> ], [M <sup>3+</sup> (NO <sub>3</sub> <sup>-</sup> ) <sub>3</sub> ] M = Co, Ni, Zn, Mn, Mg, Fe, Al, Ga C <sub>12</sub> H <sub>25</sub> OPO <sub>3</sub> H <sub>2</sub> , n = 12–18	pH 3–4.5 100 °C/5–13 days	≈1	L/27–31 Å	550 °C	unstable	33
[M <sup>2+</sup> (NO <sub>3</sub> <sup>-</sup> ) <sub>2</sub> ] M = Fe, Co, Ni, Mn C <sub>n</sub> H <sub>2n+1</sub> OSO <sub>3</sub> Na	pH <3 RT/18 h	0.1	L/21–31 Å, n = 12–18	550 °C	unstable	33
[(NH <sub>4</sub> ) <sub>6</sub> H <sub>2</sub> W <sub>12</sub> O <sub>40</sub> ] [(NH <sub>4</sub> ) <sub>6</sub> Mo <sub>7</sub> O <sub>24</sub> , 4H <sub>2</sub> O] C <sub>n</sub> H <sub>2n+1</sub> (CH <sub>3</sub> ) <sub>3</sub> NBr, n = 12–18	pH 4–8 pH >9 pH 1–13	0.33	L+H/28–30 Å/40 Å L/28.3 Å/ L/20–25 Å	500 °C	unstable	33, 217
K[SbOH <sub>6</sub> ] C <sub>18</sub> H <sub>37</sub> (CH <sub>3</sub> ) <sub>3</sub> NBr (C <sub>18</sub> TABr)	pH 6.7–6.8 pH 6.2–6.5 pH 6–7	0.1 0.1 0.2	C (Ia3d)/42.9 Å H/46 Å L/37.5 Å	550 °C	unstable	33
SnCl <sub>4</sub> sodium dioctylsulfosuccinate (AOT)	RT/1 day	1–2	H, 31.5 Å	400 °C	unstable	225
Pb(NO <sub>3</sub> ) <sub>2</sub> C <sub>16</sub> H <sub>33</sub> SO <sub>3</sub> H	pH 7–8 90 °C/3 days	0.17	H/45.8 Å L/38.5 Å	550 °C	unstable	33, 217
ZrOCl <sub>2</sub> , 8H <sub>2</sub> O (C <sub>n</sub> TABr) C <sub>n</sub> H <sub>2n+1</sub> (CH <sub>3</sub> ) <sub>3</sub> NOH	pH 11.48 pH 11.60	0.25–0.08 0.25 0.17	textured phases 17.2–33.7 Å, n = 8–18 25.8–32 Å, n = 8–18	450 °C	(240–360 m <sup>2</sup> /g)	250
ZrOCl <sub>2</sub> , 8H <sub>2</sub> O, ZrO(NO <sub>3</sub> ) <sub>2</sub> , Zr(COOCH <sub>3</sub> ) <sub>4</sub> , ZrOSO <sub>4</sub> , xH <sub>2</sub> O, carboxymethyl trimethyl- ammonium hydroxide	(1) 70 °C/3–5 h (2) pH 6–8 6 days betaine as cosurfactant	0.8–3	H/41 Å	250 °C 250 °C	(320–380 m <sup>2</sup> /g) (240 m <sup>2</sup> /g)	251
Al(NO <sub>3</sub> ) <sub>3</sub> ·9H <sub>2</sub> O or Al <sub>2</sub> (SO <sub>4</sub> ) <sub>3</sub> ·16H <sub>2</sub> O C <sub>12</sub> H <sub>25</sub> OSO <sub>3</sub> Na (SDS)	urea (homogeneous alkalinization) pH 3.6–7/7.5 several anions	2	H/43 Å	600 °C	unstable (20 m <sup>2</sup> /g)	219
Al <sub>13</sub> (AlO <sub>4</sub> Al <sub>12</sub> (OH) <sub>24</sub> (H <sub>2</sub> O) <sub>12</sub> <sup>7+</sup> ) GaAl <sub>12</sub> (GaO <sub>4</sub> Al <sub>12</sub> (OH) <sub>24</sub> (H <sub>2</sub> O) <sub>12</sub> <sup>7+</sup> ) SDS	a-NaH <sub>2</sub> PO <sub>4</sub> / Na <sub>2</sub> HPO <sub>4</sub> pH 4.25 b-pH 3	0.6	PH/39 Å aluminophosphate galloaluminophosphate	exch CH <sub>3</sub> COO <sup>-</sup>	(630 m <sup>2</sup> /g, <30 Å)	298, 299
SnCl <sub>4</sub> , [Sn(OH) <sub>6</sub> ] <sup>2-</sup> C <sub>18</sub> H <sub>37</sub> (CH <sub>3</sub> ) <sub>3</sub> NBr (C <sub>18</sub> TABr)	pH 10 75 °C/1 day 90 °C/1 day		PH/38 Å	500 °C	32 Å (143 m <sup>2</sup> /g)	227
ZrOSO <sub>4</sub> ·xH <sub>2</sub> O Zr(SO <sub>4</sub> ) <sub>2</sub> ·4H <sub>2</sub> O C <sub>n</sub> TABr, n = 16, 18, 20	100 °C/2 days H <sub>3</sub> PO <sub>4</sub> /2 h	2	H 41.6 Å/46.2 Å/ 49 Å	500 °C	28.1 Å; 33.8 Å; 38.6 Å (230 m <sup>2</sup> /g; 320 m <sup>2</sup> /g; 340 m <sup>2</sup> /g)	218 274
HfCl <sub>4</sub> , (NH <sub>4</sub> ) <sub>2</sub> SO <sub>4</sub> C <sub>18</sub> TABr	pH 2.1 100 °C, 1 day	0.25	PH/40 Å	500 °C	(11 Å, 204 m <sup>2</sup> /g)	255
V <sub>2</sub> O <sub>5</sub> ·H <sub>2</sub> WO <sub>4</sub> Na <sub>2</sub> MoO <sub>4</sub> or H <sub>2</sub> MoO <sub>4</sub> C <sub>12</sub> TABr	pH 6–8 pH 2.6–6.6 HT: 3–5 h	1 0.5	L/21.34 Å L/22 Å		unstable unstable	240
V <sub>2</sub> O <sub>5</sub> /V <sup>0</sup> C <sub>16</sub> TABr	H <sub>3</sub> PO <sub>4</sub> pH 1.2/H <sub>2</sub> O <sub>2</sub>	0.2–0.6	H/37–40 Å V–P–O phases	400 °C	unstable	244
V <sub>2</sub> O <sub>5</sub> /V <sup>0</sup> C <sub>16</sub> TACl or C <sub>16</sub> TAOH	H <sub>3</sub> PO <sub>4</sub> pH 2.6–4.5	0.5	H/36 Å C/33 Å L/35–40 Å V–P–O phases	400 °C	unstable cation exch in L	245
FeCl <sub>3</sub> ·6H <sub>2</sub> O C <sub>16</sub> H <sub>33</sub> SO <sub>3</sub> Na (SHS)	OH:Fe = 1.5 H <sub>2</sub> O/PrOH 80 °C		PH/65 Å	300 °C	(250 m <sup>2</sup> /g) mesoporous	246
Fe(NO <sub>3</sub> ) <sub>3</sub> SHS	Na <sub>2</sub> HPO <sub>4</sub> /HF	≈0.3	WL	exch CH <sub>3</sub> COO <sup>-</sup>	26 Å (250 m <sup>2</sup> /g)	247
Y and Zr glycolates C <sub>18</sub> TABr	NaOH 80 °C/5 days		MS, 42 Å	450 °C 600 °C	18–21 Å (150–250 m <sup>2</sup> /g) unstable	258
Ln(NO <sub>3</sub> ) <sub>3</sub> or LnCl <sub>3</sub> Ln = La, Pr, Nd, Sm, Gd, Dy, Er, Yb, Lu, Eu SDS	urea (homogeneous alkalinization) 80 °C, >20 h	2	PH/49–51 Å	exch CH <sub>3</sub> COO <sup>-</sup>	49 Å (20–30 Å, 250–350 m <sup>2</sup> /g)	259

<sup>a</sup> RT, room temperature. <sup>b</sup> TEM, transmission electronic microscopy; H, hexagonal; PH, pseudo-hexagonal; L, lamellar; C, cubic; WL, wormlike; MS, mesostructure, not necessarily ordered. S, specific surface. <sup>c</sup> exch, exchange. <sup>d</sup>  $\phi_{\text{pores}}$  = pore diameter.



**Table 7. Mesostructured Non-silica Oxide-, Oxopolymer-, or Metal Oxophosphate-Based Materials, Obtained from Alkoxide or Chloroalkoxide Precursors (Except Silica or Silica-Based Binary Systems)**

alkoxide precursors (M) template (T) additives (complexing)	conditions (H <sub>2</sub> O/M) pH, temp <sup>a</sup>	M/T	textured phases distances (XRD or TEM) <sup>b</sup>	template removal treatment	porous material distances XRD or TEM ( $\varnothing_{\text{pores}}$ , S) <sup>c</sup>	ref
Al(OBu <sup>s</sup> ) <sub>3</sub> , Triton, Igepal, Tergitol Pluronic [(POE) <sub>13</sub> (POP) <sub>30</sub> (POE) <sub>13</sub> ]	(2) RT/16 h 100 °C/6 h	0.1	WL/68 Å WL/80–96 Å	500 °C	48 Å (420 m <sup>2</sup> /g) 40–80 Å (420–535 m <sup>2</sup> /g)	100, 101
Al(OBu <sup>s</sup> ) <sub>3</sub> C <sub>n</sub> H <sub>2n+1</sub> COOH, <i>n</i> = 11, 17	(3) alcohols RT/1 day 110 °C/2 days	0.33	MS 33 Å ( <i>n</i> = 11)	430 °C	30 Å, <i>n</i> = 11 (19 Å, 710 m <sup>2</sup> /g)	219
Sn(OPr <sup>i</sup> ) <sub>4</sub> C <sub>14</sub> H <sub>29</sub> NH <sub>2</sub> (TDA)	RT/2 days	5	WL/46 Å with SnO <sub>2</sub> nano- crystals	washing EtOH + 300 °C + 350 °C + 400 °C	46 Å (14 Å, 314 m <sup>2</sup> /g) 56 Å (18 Å, 300 m <sup>2</sup> /g) N/O (43 Å, 99 m <sup>2</sup> /g)	225
Sn(OPr <sup>i</sup> ) <sub>4</sub> TDA	80 °C/24 h		PH/48 Å	500 °C	34 Å (107 m <sup>2</sup> /g) unstable	227
Ti(OPr <sup>i</sup> ) <sub>4</sub> , acetylacetone C <sub>12</sub> H <sub>25</sub> OPO <sub>3</sub> H <sub>2</sub>	(160) pH 4–6 80 °C/5 days	1	H/36 Å	350 °C acid wash	~34 Å (200 m <sup>2</sup> /g) (24 Å, 603 m <sup>2</sup> /g)	111 313
Ti(OEt) <sub>4</sub> , H <sub>2</sub> O <sub>2</sub> , C <sub>16</sub> TACl	aq soln pH 11.5 100 °C/15 days	1	L/31.5 Å H/40.5 Å	300 °C	30–36 Å (275–310 m <sup>2</sup> /g)	232
Ti(OPr <sup>i</sup> ) <sub>4</sub> C <sub>16</sub> H <sub>33</sub> NH <sub>2</sub>	(30) 90 °C–RT/18 h	0.3	WL 32 Å	430 °C	unstable	110
Ti(OPr <sup>i</sup> ) <sub>4</sub> C <sub>n</sub> TABr, <i>n</i> = 16, 18, 20	(400) H <sub>2</sub> SO <sub>4</sub> RT, H <sub>3</sub> PO <sub>4</sub>	0.3	H/45 Å (C <sub>16</sub> ) H/51 Å (C <sub>18</sub> ) H+L/48 Å (C <sub>20</sub> )	350 °C 400 °C	32 Å (21 Å, 340 m <sup>2</sup> /g) 39 Å (28 Å, 360 m <sup>2</sup> /g)	110
Zr(OPr <sup>n</sup> ) <sub>4</sub> , acetylacetone C <sub>16</sub> H <sub>33</sub> NH <sub>2</sub>	(39) RT/5 days H <sub>2</sub> SO <sub>4</sub>	0.3	MS 41 Å	extr 110 °C 550 °C	18.5 Å (347 m <sup>2</sup> /g) 18.7 Å (216 m <sup>2</sup> /g)	252
Zr(OPr <sup>n</sup> ) <sub>4</sub> Zr(OEt) <sub>4</sub> C <sub>n</sub> H <sub>2n+1</sub> COO <sup>-</sup> , <i>n</i> = 1–18 C <sub>12</sub> H <sub>25</sub> SO <sub>4</sub> <sup>-</sup> , C <sub>12</sub> H <sub>25</sub> SO <sub>3</sub> <sup>-</sup> C <sub>n</sub> H <sub>2n+1</sub> OPO <sub>3</sub> <sup>2-</sup> , <i>n</i> = 4, 8, 12, 16	80 °C/4 days	1 1 1	L/14, 6 Å – 33.1 Å <i>n</i> = 1–18 L/38.3 Å L+PH/16.6–38.4 Å, <i>n</i> = 4–16	400 °C amorphous phases	unstable 15–26 Å (233–361 m <sup>2</sup> /g), <i>n</i> = 4–16	253
VO(OPr <sup>i</sup> ) <sub>3</sub> C <sub>12</sub> H <sub>25</sub> NH <sub>2</sub>	(52), RT 1 day 100 °C/1 day	0.5–1	L 23 Å H 30 Å L 28 Å			241
Nb(OEt) <sub>5</sub> C <sub>n</sub> H <sub>2n+1</sub> NH <sub>2</sub> , <i>n</i> = 12, 18	(442) RT/1–3 days 100 °C/1 day 180 °C/7 days	2 0.67	H H (P63 mmc)	washing PrOH/HNO <sub>3</sub>	28–40 Å, <i>n</i> = 12–18 (23 Å, 617 m <sup>2</sup> /g)*	256
Ta(OEt) <sub>5</sub> , C <sub>18</sub> H <sub>37</sub> NH <sub>2</sub> C <sub>n</sub> H <sub>2n+1</sub> NH <sub>2</sub> , <i>n</i> = 12, 18	(113) RT/1–3 days 80 °C/1 day 100 °C/1 day 180 °C/7 day	0.5	H		29–39 Å, <i>n</i> = 12–18 22–32 Å  (510 m <sup>2</sup> /g), <i>n</i> = 12–18	114
MCl <sub>n</sub> in EtOH M = Zr, Ti, Sn, Nb, Ta, W, Hf, Ge, V, Zn, Cd, In, Sb, Mo, Re, Ru, Ni, Fe, Cr, Mn, Cu, ... and mixed ZrTi, Al <sub>2</sub> Ti, ...	40–60 °C 1–7 days EISA, open recipients	<0.01	Zr H/115 Å Ti H/123 Å Nb H/106 Å Ta H/110 Å W H/110 Å Sn H/124 Å Hf H/124 Å Al H/120 Å ZrTi H/110 Å SiAl H/120 Å Al <sub>2</sub> Ti H/112 Å (P123)	400 °C	106 Å (58 Å, 150 m <sup>2</sup> /g) 101 Å (65 Å, 205 m <sup>2</sup> /g) 80 Å (50 Å, 196 m <sup>2</sup> /g) 70 Å (35 Å, 165 m <sup>2</sup> /g) 95 Å (50 Å, 125 m <sup>2</sup> /g) 106 Å (68 Å, 180 m <sup>2</sup> /g) 105 Å (70 Å, 105 m <sup>2</sup> /g) 186 Å (140 Å, 300 m <sup>2</sup> /g) 103 Å (80 Å, 130 m <sup>2</sup> /g) 95 Å (60 Å, 310 m <sup>2</sup> /g) 105 Å (80 Å, 270 m <sup>2</sup> /g)	260, 261
(PEO) <sub>m</sub> (PPO) <sub>70</sub> (PEO) <sub>m</sub> Pluronic P123 ( <i>m</i> = 20) Pluronic F127 ( <i>m</i> = 106)						
Al(OBu <sup>s</sup> ) <sub>3</sub> , TEA	(131–185)	0.33	WL/28–57 Å	300 °C	aluminophosphates	222

Table 7 (Continued)

alkoxide precursors (M) template (T) additives (complexing)	conditions (H <sub>2</sub> O/M) pH, temp <sup>a</sup>	M/T	textured phases distances (XRD or TEM) <sup>b</sup>	template removal treatment	porous material distances XRD or TEM ( $\varnothing_{\text{pores}}$ , S) <sup>c</sup>	ref
H <sub>3</sub> PO <sub>4</sub>	pH 10–11		(P/Al = 0.12–0.74)	400 °C	28–57 Å	
C <sub>12</sub> TABr	pH 8–9 after H <sub>3</sub> PO <sub>4</sub> P/Al = 0.12–0.74			500 °C	(13–37 Å, 480–650 m <sup>2</sup> /g) with P/Al = 0.12–0.74	
Al(OBu <sup>s</sup> ) <sub>3</sub> , TEA	pH 10, 11 60 °C/3 days	0.5	WL/69–95 Å	500 °C	69–95 Å (33–60 Å, 340–250 m <sup>2</sup> /g) for H <sub>2</sub> O/TEA range 7.4–44.5	222
C <sub>12</sub> TABr						
Ti(OBu <sup>n</sup> ) <sub>4</sub> TAMOH C <sub>12</sub> TABr	(285) Ti/TAM = 1.22 115 °C/3–6 days	0.6	L/30 Å	350 °C	unstable	234
Ti(OBu <sup>s</sup> ) <sub>3</sub> , C <sub>12</sub> TABr	TEA pH 10, 11 60 °C/3 days	0.3	WL-PH/69–95 Å	500 °C	69–95 Å (33–60 Å, 340–250 m <sup>2</sup> /g) for H <sub>2</sub> O/TEA range 7.4–44.5	173
Ti(OPr <sup>i</sup> ) <sub>4</sub> Nb(OEt) <sub>5</sub> Zr(OPr <sup>n</sup> ) <sub>4</sub> EG CTA <sub>1,2</sub> [M(EGo) <sub>3</sub> ] M = Ti, Zr, Nb C <sub>16</sub> TABr or C <sub>16</sub> TACL	a-M(OR) <sub>4</sub> in NaOH/EG 80 °C/5 days b-H <sub>2</sub> O RT/3–4 h	0.45–0.5	Ti, PH/50 Å Zr, H/37 Å Nb, H/37 Å	silanation/ 600 °C	WL, 40 Å 31 Å (277 m <sup>2</sup> /g) 32 Å (180 m <sup>2</sup> /g)	231
Ti(OEt) <sub>4</sub> C <sub>16</sub> TABr	(10–100), 50–70 °C EISA 3–7 days in EtOH/HCl	0.16	H/47 Å	350 °C	20–25 Å (280–370 m <sup>2</sup> /g)	283
Ti(OEt) <sub>4</sub> or Ti(O- <i>n</i> Bu) <sub>4</sub> PEO-based nonionic	(<1–10), 50–70 °C EISA 1–10 days in ROH/HCl	0.01–0.05	WL/~30–35 Å ( <i>h</i> < 1) H/50–167 Å ( <i>h</i> > 1)	350 °C	WL (250 m <sup>2</sup> /g)	239, 290
Ti(OEt) <sub>4</sub> PEO-based nonionic (P123)	(6), EISA films in ROH/HCl	0.005–0.02	L/d <sub>100</sub> = 100 Å H/d <sub>100</sub> = 90 Å C/d <sub>100</sub> = 81 Å	400 °C		269
TiCl <sub>4</sub> nonionic surfactants Brij 58 C <sub>16</sub> H <sub>33</sub> (PEO) <sub>20</sub> F127 (PEO) <sub>100</sub> (PPO) <sub>70</sub> (PEO) <sub>100</sub>	(1–20) EtOH EISA films	0.01–0.05	H/150 Å (F127) H/50 Å (B58)	300 °C	rectangular 53 Å rectangular 36 Å	266
TiO <sub>2</sub> (Anatase) nanoparticles Brij 58 C <sub>16</sub> H <sub>33</sub> (PEO) <sub>20</sub>	(15) EtOH EISA films aging 10 °C	0.083	pseudo-C/58 Å	450 °C	43 Å	268
ZrCl <sub>4</sub> Brij 58	(20) EtOH EISA films	0.05	H/50 Å (B58)	300 °C/ O <sub>3</sub>	rectangular 35 Å (28 Å, 192 m <sup>2</sup> /g)	270
VCl <sub>4</sub> /VCl <sub>5</sub> Brij 56 or 58	(5–10) EtOH EISA films	0.05	H/50–80 Å (B58)	220 °C/	monoporous, unstable <i>T</i> > 250 °C	271
AlCl <sub>3</sub> Brij 58	(40)-EtOH–NH <sub>3</sub> EISA films	0.08	H/67 Å (B58)	O <sub>3</sub> /220 °C	rectangular 36 Å	265
WCl <sub>6</sub> P123 (PEO) <sub>20</sub> (PPO) <sub>70</sub> (PEO) <sub>20</sub>	(0)-EtOH EISA films	0.017	WL/40–60 Å	solv extr 400 °C	(50 Å, 155 m <sup>2</sup> /g) (106 Å, 45 m <sup>2</sup> /g)	272
mixed alkoxides Zr/Si; Ta/Si; Fe/Si Al/P F127 (PEO) <sub>100</sub> (PPO) <sub>70</sub> (PEO) <sub>100</sub>	(0)-toluene nonhydrolytic 135 °C 3–24 h	0.04	WL/~150 Å	500 °C	100–110 Å (15–20 Å, ~500 m <sup>2</sup> /g)	262, 263

<sup>a</sup> RT, room temperature; EISA, evaporation-induced self-assembly. <sup>b</sup> TEM, transmission electronic microscopy; h, hexagonal; PH, pseudo-hexagonal; L, lamellar; C, cubic; WL, wormlike; MS, mesostructure, not necessarily ordered. <sup>c</sup> S, specific surface;  $\varnothing_{\text{pores}}$  = pore diameter.

Another recurrently observed feature is that the hybrid phases stemming from acidic aqueous solutions present a relatively low stability to thermal treatment, due to incomplete condensation of the inorganic network because of the low initial pH values. Detailed structural and in-situ characterization shows that the immediately formed mesostructured hybrids are composed of an incompletely con-

densed inorganic framework that can evolve upon aging.<sup>235</sup> An extra cross-linking induced by ion exchange with phosphate can overcome this problem, and Ti and Zr mesoporous oxosulfates and oxophosphates have been successfully synthesized this way.<sup>235,274</sup> A closely related preparation permits zirconium oxochromate (Cr/Zr = 0.5), stable to thermal treatment up to 550 °C,<sup>275</sup> to be obtained.

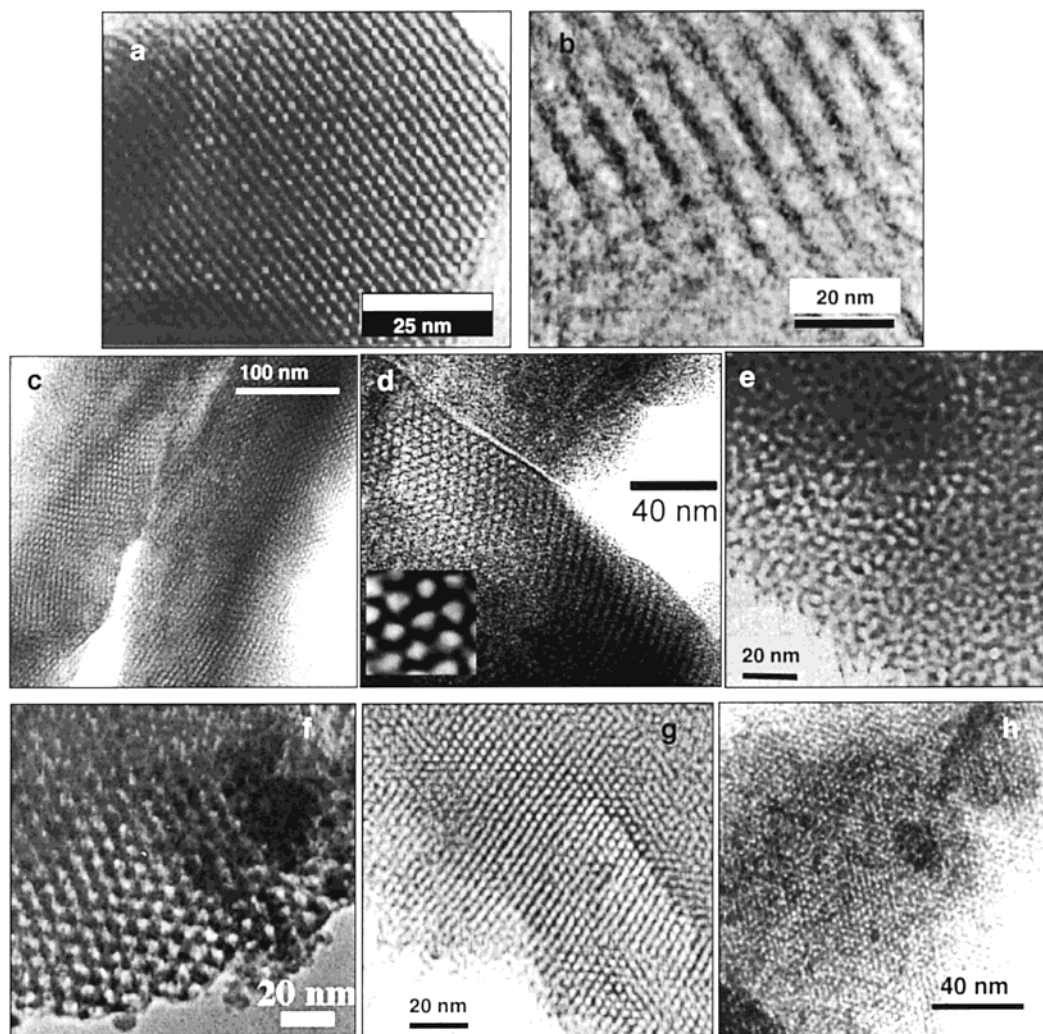


**Figure 18.** TEM micrographs of non-silica hybrid or oxide phases: (a) dodecylamine-templated  $\text{Nb}_2\text{O}_5$ ;<sup>256</sup> (b) diblock copolymer-templated ( $\text{EO}_{75}\text{BO}_{45}$ ) cubic  $\text{ZrO}_2$ ;<sup>261</sup> (c)  $\text{ZrO}_2$  hexagonal hybrid film (reprinted with permission from ref 270; copyright 2001 Royal Society of Chemistry); (d)  $\text{TiO}_2$  hexagonal film (reprinted with permission from ref 266; copyright 2001 Wiley-VCH); (e)  $\text{Zr/Si}$  mixed oxide;<sup>263</sup> (f) triblock copolymer-templated hexagonal  $\text{SnO}_2$  oxide;<sup>261</sup> (g) hybrid  $\text{TiO}_2/\text{CTAB}$  composite;<sup>283</sup> (h) same as (g), calcined to  $350\text{ }^\circ\text{C}$ .<sup>283</sup> Micrographs b–e were prepared using  $(\text{H}_{33}\text{C}_{16})_{10}(\text{OCH}_2\text{CH}_2)_n\text{OH}$  nonionic surfactants.

A homogeneous alkalization method (urea hydrolysis at  $T > 60\text{ }^\circ\text{C}$ )<sup>276</sup> has been introduced by Yada and co-workers, with the aim of a gentle and homogeneous pH rise. The higher pH attained should improve the condensation in M(III) systems ( $\text{M} = \text{Al}$ ,<sup>219,277</sup>  $\text{Ga}$ ,<sup>224</sup>  $\text{Y}$ , rare earths<sup>259</sup>), which are not as acidic as typical M(IV). Mesoporous  $\text{MO}_x/\text{alkyl-sulfates}$  [typically, sodium dodecyl sulfate (SDS)] have been synthesized in this way, which are regularly fragile upon thermal treatment.<sup>278</sup> The introduction of Y(III) stabilizes these networks, permitting mixed mesoporous oxides to be obtained by anion exchange with acetate.<sup>279–281</sup>

Hudson and Knowles<sup>250</sup> developed an approach based on the ion exchange properties of amorphous  $\text{ZrO}_2$  in highly alkaline medium ( $\text{pH} > \text{pH}_{\text{iepZrO}_2}$ ), followed by dissolution–reprecipitation. As a result, hexagonal mesoporous  $\text{ZrO}_2/\text{CTA}^+$  composites are synthesized, which can be subsequently transformed in mesoporous oxides. The “scaffolding” mechanism presented in this and following work<sup>253</sup> will be discussed later.

**(2) Inhibition of the Hydrolysis–Condensation Process.** There are two extensively used methods to control the hydrolysis and condensation processes of reactive alkoxides or chloroalkoxides, which usually lead to immediate precipitation: (a) Complexation of the metal centers (by means of phosphate, carboxylic acids,  $\beta$ -diketones, polyethanolamines, polyols, amines, etc.) was the first concept applied, which led to mesoporous  $\text{TiO}_2$ .<sup>111</sup> Complexation can be directly performed by the polar head of the surfactant; this is the case of phosphates, poly(alkylene oxide)-based block copolymers, or amines in the ligand-assisted templating approach (see below). (b) Mineral acids are added in an important  $\text{H}^+/\text{M}$  ratio. In alkoxide/alcohol-based synthesis, protons generated by hydrolysis are transferred to the alkoxide leaving groups.



In aqueous solutions, the hydrolysis of the metal cation will naturally lead to acidic pH.



(2a) *Complexation* of alkoxide precursors  $\text{M}(\text{OR})_n$  ( $\text{M} = \text{Ti}, \text{Al}, \text{Zr}, \text{Nb}, \dots$ ) by acetylacetone (*acac*), ethylene glycol (EG), triethanolamine (TEA), or other chelating agents permits control of the reactivity by avoiding fast hydrolysis/condensation of the precursors in contact with water.<sup>282</sup> These strong chelating agents also restrain the condensation reactions, thus favoring the presence of low-weight oligomeric species (aggregates, clusters, and nanoparticles) in solution. The high surface-to-volume ratio of these small entities makes them ideal to interact with surfactant molecules or aggregates in the self-assembly process. The choice of the complexing agent permits the pH to be adjusted, which is a supplementary degree of freedom. This aspect is indeed useful in the control of the subsequent step, in which extended condensation reactions between the oligomers take place, forming a continuous inorganic network. For example, in the case of alumina- or TM-based ( $\text{Ti}, \text{Zr}, \text{Nb}, \dots$ ) oxide mesostructures, *acac* is used as an inhibitor in neutral or slightly acidic medium in the presence of alkyl phosphate templates.<sup>111,230,256</sup> On the other hand, TEA<sup>173,222,236,244</sup> is employed in strongly basic media, to form chelates. In the presence of  $\text{C}_{16}\text{-TMA}^+$  cations, a great variety of oxide and oxophosphate networks are formed (alumina, titania,  $\text{Al/Si}, \text{Ti/Si}$  with important non-silica contents), which present wormlike porosity. Tris (ethylene glycolate)  $\text{Y}, \text{Ti},$  and  $\text{Zr}$  complexes have been used as starting species to create mesoporous yttria, titania, and zirconia in alkaline medium, using alkylammonium templates, as discussed below.<sup>231,258</sup> The isoelectric point of these oxides is located between 6 and 9. Consequently, the presence of positively charged polar heads in alkaline media (conversely, anionic templates in low pH) promotes strong electrostatic interactions between the surfactant (*S*) and the developing inorganic framework (*I*). These interactions ( $\text{S}^- \text{I}^+$ , and  $\text{S}^+ \text{I}^-$ , respectively, see Figure 10) favor the self-assembly process. Diols have been used to apparently complex  $\text{Ti}(\text{IV})$  at pH 5–8, generating anionic species as precursors; in this case, an  $\text{S}^- \text{M}^+ \text{I}^-$  type of interface (mediated by  $\text{K}^+$  cations) is proposed.<sup>231</sup> The same mediator role is attributed to sulfate anions, in the production of  $\text{Zr}$  oxophosphates.<sup>218</sup> Another interesting and simple approach has been developed, by combining soluble peroxytitanates  $[\text{Ti}(\text{O}-\text{O})(\text{OH})(\text{H}_2\text{O})](\text{OH})$  with cationic  $\text{C}_{16}\text{-TMACl}$ .<sup>232</sup> The synthesis takes place in alkaline medium, giving rise to lamellar and hexagonal titania, depending on the base used (TMAOH or NaOH, respectively).

Surfactants with complexation ability constitute a particular case of inhibition agents. In the case of titania–phosphate mesophases, the complexing power of the template heads is important enough to believe that coordination interactions already take place in the initial steps of the surfactant–mineral self-assembly process. These interactions are enhanced upon drying and thermal treatment, processes that entail dehydration and further condensation. Indeed, phosphate groups are difficult to remove either by extraction or calcination, which may be a major

drawback in many applications concerning the free access of a target molecule to the oxide surface.

Similar complexation reactions should take place in analogous systems that use alkylcarboxylates, alkylamines, neutral surfactants presenting poly(ethylene oxide) (PEO) groups, and hydroxy-capped polar heads, such as  $\text{C}_n\text{H}_{2n+1}[\text{EO}]_m\text{OH}$  (Tergitol, Triton, Igepal, Brij) or  $[\text{PEO}]_n[\text{PPO}]_m[\text{PEO}]_n$  (Pluronics, Synperonics). The complexing properties of the polar heads have been advantageously used in the synthesis of several mesostructured oxides ( $\text{Al}, \text{Nb}, \text{Ta}, \text{Sn},$  and  $\text{Ti}$ , see Table 7) presenting hexagonal, quasi-hexagonal (short-range hexagonal order), or wormlike bicontinuous pore arrangements. Complexation can take place before hydrolysis–condensation of the inorganic precursors, as in the case of niobium alkoxide tetradecylamine or tantalum alkoxide tetradecylamine, that yields hexagonal mesophases.<sup>113,256</sup> Titanium seems to show weaker H-bonding interactions with alkylamines; however, previous interaction of the metal species and the template seems to be essential for template effect to take place.<sup>232</sup>

For weaker chelating agents, such as PEO/PPO groups, complexation can take place during the drying stage; in fact, water, chloride, or small alcohols are far better nucleophiles. However, during solvent evaporation, hydrolysis and transalcoholysis equilibria can be displaced, and TM cations can attach to the polar heads.<sup>238</sup> In particular, the condensation of titanium alkoxides  $[\text{Ti}(\text{OR})_4]$  in the presence of Pluronic-type polymers and sub-stoichiometric water amounts ( $h = [\text{H}_2\text{O}]/[\text{M}] \leq 2$ ) yields porous materials presenting wormlike channels with an ill-defined symmetry.<sup>238</sup> This result can be explained in terms of relatively strong interactions between the template and hydrophobic oligomers, which have a detrimental effect on the polymer folding (vide infra, in the mechanism section).<sup>239</sup>

(2b) *Acid Inhibition.* Strongly acidic conditions (pH < 1, adjusted with HCl or  $\text{HNO}_3$ ) also permit the reactivity of TM alkoxides  $\text{M}(\text{OR})_4$  ( $\text{M} = \text{Ti}, \text{Zr}, \text{Nb}, \dots$ ) to be controlled. Under these conditions, generally associated with high hydrolysis ratios ( $h > 2$ ), condensation is hindered by protonation of the  $\text{M}-\text{OH}$  nucleophilic species present in the medium. At the same time, depolymerization processes (the inverse of condensation) are promoted. Both processes generally lead to the formation of small hydrophilic oligomers: clusters or nano-objects. As a result, both organic and mineral building blocks present a hydrophilic character, due to the presence of water, which favors micelle formation. This procedure of “matching the hydrophilic domains” permits hybrid mesostructured phases that present hexagonal symmetry to be obtained, using neutral or cationic templates, upon solvent evaporation or precipitation.<sup>238,239,283</sup>

Addition of a strong Lewis acid such as  $\text{TiCl}_4$  to an alcoholic solution produces chloroalkoxide and HCl in situ, according to



This is also a suitable way to introduce acid into the

initial solutions without adding water and slow the condensation process.<sup>260,261</sup>

(3) *Nonaqueous Solvents and Controlled Water Contents.* One of the alternatives to avoid massive precipitation of nonstructured phases is to conduct the synthesis in nonaqueous media, in the absence of water, or low  $h$  values. A classical example is the first synthesis of mesostructured alumina phases, developed by Bagshaw and Pinnavaia, using nonionic surfactants as templates, in alcohol/water mixtures.<sup>101</sup> The presence of low water quantities ( $h \approx 1-2$ ) will have decisive effects, not only in the kinetics of the formation of the mineral phase but also in the chemical compatibility at the hybrid interface; this central topic will be discussed in the mechanisms section.

A successful nonaqueous approach has been developed by Stucky and co-workers, in ethanolic medium.<sup>260,261</sup> A great variety of mesostructured and mesoporous metal oxides (Al, Ti, Zr, Nb, Ta, Sn, ...) and mixed oxides (Ti/Al, Ti/Zr, Zr/W, ...) have been obtained, by using ethanolic solutions of  $MCl_n$  and PEO-based triblock copolymers. After solvent evaporation (evaporation-induced self-assembly, see next section), hexagonal or cubic mesostructures were formed, depending on the surfactant. Moreover, thick inorganic walls are obtained, which convey toughness to the inorganic framework. The resulting mesoporous oxides present nanocrystalline walls, which is indeed interesting for eventual applications. This synthesis path combines an essentially nonaqueous medium, high acidity, and the formation of an ordered liquid crystalline phase by evaporation; all of these features will be discussed below. An alternative two-step method was developed by Ozin and co-workers, using glycolate complexes (Ti, Zr, and Nb) in ethylene glycol as solvent.<sup>231</sup> The addition of CTAC promotes the precipitation of a layered hybrid phase,  $CTA_{1,2}(M(EGO)_3)$  ( $EGO = EG^{2-}$ ). Once this precursor is hydrolyzed in water, two-dimensional hexagonal mesostructures are formed. The resulting hybrid phases are not completely condensed, and silanization is a previous step to obtain mesoporous silica-containing TM oxides.

Nonaqueous solvents with low polarity tend to assist the production of inverse micelles and, therefore, to change the curvature of the hybrid interface. A clear example is present in work by Tiemann et al.<sup>284</sup> Lamellar aluminophosphate is synthesized in water/alkyl phosphates; when ethanol is used as solvent, an ordered dispersion of aluminophosphate particles is formed, rather than an ordered array of pores in a continuous matrix. An extreme case is given in synthesis of titania nanoparticles from a nonionic Triton TX-100/cyclohexane titanium isopropoxide system, presenting mesoporous behavior.<sup>285</sup> In this case, both the shape of the surfactant and the solvent employed cooperate to obtain a nanoparticle dispersion.

A recently developed synthesis route makes use of mixed molecular precursors and PEO-based block copolymers in toluene, under hydrothermal conditions (90–150 °C, sealed vessels).<sup>262,263</sup> This method permits mixed oxides such as  $ZrO_2 \cdot 4SiO_2$ ,  $Ta_2O_5 \cdot$

$6SiO_2$ ,  $Fe_2O_3 \cdot 6SiO_2$ , and  $AlPO_4$  to be obtained, presenting tailored regular pore size and a wormlike mesostructure. Under these temperature and pressure conditions, a nonhydrolytic condensation is likely to occur, as will be discussed in the next section.<sup>286</sup>

(4) *Evaporation-Induced Self-Assembly (EISA).* The so-called EISA process, initially proposed by Brinker and colleagues,<sup>187</sup> is based on the processes that take place upon the formation of mesostructured silica films.<sup>287,288</sup> Starting from dilute solutions, a liquid crystalline (LC) mesophase is gradually formed upon solvent evaporation. The formation of an inorganic network around this LC phase permits well-defined mesostructured hybrids to be obtained, which present a segregation of organic and mineral domains at the nanoscale. This procedure permits one to avoid the diffusion problems encountered when infiltrating a real LC structure with a metal precursor (Figure 7, route A). Subsequently, inorganic condensation can be “turned on”, giving birth to a condensed inorganic framework. This procedure permits the material in the shape of powders (aerosols<sup>289</sup>), gels, monoliths,<sup>214</sup> or films to be processed. The hybrid structure is quite flexible as-synthesized, due to incomplete inorganic polymerization. Therefore, a subsequent “locking” step is necessary (by a chemical process, for example, inorganic or organic polymerization, or by mild thermal treatment) in order to obtain a robust mesostructure. This is an interesting procedure for TM-based materials, because starting solutions are relatively dilute, and the inorganic polymerization can be readily controlled by an acid, which is subsequently eliminated by evaporation.

In the conditions developed by Stucky's group for a general route,<sup>260,261</sup> upon dissolution of the metal chlorides in alcohol, HCl is released and metal-chloro-alkoxo species are produced in situ. Following solvent evaporation, the systems travel along the (solvent, polymer, inorganic precursor) phase space, until a mesostructured dry gel is formed. In the first interpretation of this synthesis route, a nonhydrolytic condensation path was considered to be responsible for the formation of the mineral framework. However, in the reported synthesis conditions (40 °C, open recipients), it is unlikely that a nonhydrolytic condensation could successfully compete with ordinary condensation, water being provided by air moisture. There is sufficient evidence that permits this path to be discarded in Ti(IV) and Zr(IV) systems as the main process. Studies on EISA-based systems (precursor solutions, “bulk” gels<sup>239,283</sup> or powders, or thin films<sup>202,266,270</sup>) stress the role of water in the mesoscopic organization of the obtained phases. As an example, titania–nonionic surfactant hybrid composites have been synthesized by EISA in alkoxide–alcohol–water–HCl mixtures, using block copolymers.<sup>234,239</sup> In addition, the use of preformed hydrophobic clusters to generate mesostructured  $TiO_2$  in low-water conditions results in wormlike structures (see below).<sup>290</sup> As shown in other systems (vide supra), nonhydrolytic condensation requires strict absence of water and more drastic temperature and pressure conditions.<sup>262,263</sup>

Hexagonal  $\text{TiO}_2/\text{CTAB}$  hybrids that lead to mesoporous  $\text{TiO}_2$  upon thermal treatment were obtained by combining EISA with acid inhibition of the condensation with  $\text{HCl}$ .<sup>283</sup> In this case, a flexible “titanotropic” hybrid LC phase is formed by amorphous Ti-oxo subunits that assemble around an organic template; an  $I^+X^-S^+$  type of hybrid interface (cf. section 5) is formed. The formation of a well-defined mesostructure depends critically on factors such as the synthesis temperature, which controls two processes in competition: solvent evaporation (and, thus, self-assembly) versus inorganic polymerization. The effects of the inhibitor and metal concentrations and solvent composition have also been stressed.<sup>283</sup> The hybrid titania-CTAB mesostructure has to be thermally reinforced, to assist inter-NBB condensation, leading to robust hybrid precursors at  $T > 70$  °C. Thermal treatment of these precursors leads to high-area ( $250\text{--}380\text{ m}^2\text{ g}^{-1}$ ) phosphate-free  $\text{TiO}_2$ .

This approach has also been extended to films, which are indeed interesting in view of applications as selective electrodes, sensors, photocatalytic, or electrochromic devices.<sup>291</sup> Titania, zirconia, and aluminum oxhydroxide mesoporous films presenting hexagonal texture and high stability toward thermal treatment have been recently reported.<sup>265,266,269,270</sup> Mesostructured tungsten oxide films presenting a wormlike aspect have demonstrated superior electrochemical and optical performances compared to ordinary sol-gel-derived thin films.<sup>272</sup>

(5) *Tuning of the Redox State.* Following the first models proposed by Stucky and co-workers,<sup>33,96</sup> one of the keys for the formation of a well-defined hybrid mesostructure is the charge matching between the inorganic framework and the polar heads of the surfactants (see below). In the case where variable oxidation states of the metallic centers are possible (e.g., V, W, Mn), important changes are associated with the  $[\text{Red}]/[\text{Ox}]$  ratio. A well-documented case is the synthesis of oxovanadium  $[\text{V}(\text{IV})/\text{V}(\text{V})]$  phosphates, in which the  $\text{V}(\text{IV})/\text{V}(\text{V})$  ratio is tuned by making use of  $\text{V}(\text{V})$ ,  $\text{V}^0$ , and  $\text{H}_2\text{O}_2$ . Hexagonal phases are obtained within a wide range of compositions; optimal structural features are achieved when  $\text{V}(\text{IV})/\text{V}(\text{V}) \approx 0.5$ . The template ( $\text{C}_{16}\text{TMA}^+$ ) cations are associated with  $\text{V}(\text{IV})$  centers.<sup>244</sup> Mixed-valence oxovanadium phosphates have been recently obtained as lamellar, hexagonal, and cubic phases, depending on the synthesis pH, again by combining  $\text{V}^0$  and  $\text{V}_2\text{O}_5$ . Mesostructured vanadium oxide films stable up to 220 °C can be synthesized by carefully tuning the  $\text{V}(\text{IV})/\text{V}(\text{V})$  ratio; the presence of the  $\text{V}=\text{O}$  bond seems to block the three-dimensional growth of the inorganic framework and favor the development of lamellar vanadium oxide.<sup>271</sup> It seems that the presence of  $\text{V}(\text{IV})$  is also essential for the formation of vanadium oxide-based hybrid nanotubes.<sup>292–294</sup>

Mesostructured hexagonal and cubic mixed-valence (average oxidation state of 3.55) manganese oxides (MOMS)<sup>295</sup> have been obtained by means of the oxidation of a  $\text{Mn}(\text{OH})_2$  slurry under oxygen flow. Hexagonal MOMS display a hexagonal array of pores with an open porous structure, thick walls ( $\approx 2$  nm), and thermal stability up to 1000 °C.<sup>248</sup> Reduction of

a ( $\text{C}_{12}\text{TMA}^+$ )( $\text{MnO}_4^-$ ) intermediate with ethanol and further aging leads to a mesostructured precursor; a transformation from lamellar birnessite to a hexagonal mesophase is an alternative way to obtain an organized hybrid.<sup>249</sup> The mechanism of formation of these interesting mesophases is not clear.

(6) *Organization of Preformed Nano-objects: Assembly of Nanobuilding Blocks (ANBB).* The organization of nanometric objects by means of hybrid interfaces is a recently opened route, which should lead to control of the nature of the inorganic network in a more precise way. The assembly of mineral species of a given nature (clusters, aggregates, or nanocrystalline particles) permits other features, such as the reactivity of the inorganic precursors (“bricks”) or the conservation of a pre-existent geometry, to be tailored. These can form an extended network, acting either as preformed nanobuilding blocks (NBB),<sup>4</sup> which can be assembled around a hybrid interface, or as a mineral source, via dissolution-recondensation processes, according to their reactivity and the physical-chemical features of the reacting systems. Mesostructured silica has been synthesized from precondensed siloxane precursors.<sup>85,296</sup>  $\text{Ti}(\text{IV})$  clusters, aluminate, galloaluminate, or W-based polyoxometalates (POM) are the most used non-silica nano-objects so far.

Hybrid mesostructured phases can be obtained from  $\text{W}(\text{VI})$  polyanions and  $\text{C}_{16}\text{TAB}$  templates; however, syntheses based upon polyoxotungstates often lead to hybrid salts that do not yield mesoporous oxides.<sup>257,297</sup> Thermal treatment of these hybrids results in the destruction of these phases. This may be due to several reasons: (1) The mineral walls are constituted of weakly connected polyanions, resulting in an overall fragile structure. (2) Thermal treatment of the hybrid phases is associated with redox reactions between the surfactant and the metal centers. The resulting changes in coordination symmetry and the subsequent rearrangements may lead to the destruction of the inorganic framework.


In the “salt-gel” process, developed by Stein and co-workers, preformed Keggin ions ( $\text{Nb}_x\text{W}_{6-x}\text{O}_{19}^{(2+x)-}$ ) are initially assembled with an oppositely charged surfactant, leading to lamellar cluster/surfactant salts. These preordered NBBs are further linked by silicate into a three-dimensional network.<sup>257</sup> Partially condensed  $\text{Al}_{13} [\text{AlO}_4\text{Al}_{12}(\text{OH})_{24}(\text{H}_2\text{O})_{12}^{7+}]$  or  $\text{GaAl}_{12} [\text{GaO}_4\text{Al}_{12}(\text{OH})_{24}(\text{H}_2\text{O})_{12}^{7+}]$  clusters have also been used as NBBs to yield hybrid assemblies with SDS. Subsequent acidic treatment in the presence of phosphate leads to mesostructured aluminophosphate or galloaluminophosphates. Upon aging at low pH ( $\sim 3$ ), the clusters break apart into smaller fragments and a suitable curvature is obtained. The resulting hybrids can be rendered mesoporous by extraction/ion exchange.<sup>298</sup> The connection can also be achieved by using silicate linkers.<sup>299</sup> These phases are interesting, as they join high surface area, mesoporosity, and anion exchange possibilities.<sup>300</sup>

$\text{Ti}(\text{IV})$  clusters such as  $\text{Ti}_{16}\text{O}_{16}(\text{OEt})_{32}$  ( $\text{Ti}_{16}$ ) have also been used as NBBs to produce textured mesophases. Two strategies have been reported so far, using ABC templates [block copolymers ( $\text{POE}$ ),-


(POP)<sub>m</sub>(POE)<sub>n</sub> or PS–PA). Pluronic–Ti16 hybrids presenting bicontinuous wormlike textures are obtained by EISA. The clusters are connected by hydrolysis–condensation reactions. Thermal treatment of these hybrids yields porous materials with surface areas of ~250–300 m<sup>2</sup>/g.<sup>290</sup> A similar process in PS–PA–Ti16 systems in toluene leads to hexagonal hybrid mesophases.<sup>301</sup> Functionalized dendrimers have also been used as preformed texturing agents, yielding ordered cluster dispersions. Hybrid textured dendrimer–Ti16 phases where the cluster integrity is preserved have been obtained upon solvent evaporation.<sup>302</sup>

Recent examples report highly condensed walls, composed of nanometric size titania particles, either preformed or formed in situ. The first strategy has been applied to generate mesoporous titania thin films, presenting hexagonal or pseudo-cubic mesostructure.<sup>268</sup> This route is interesting because of the higher control of the condensation degree of the metal centers. Although an amorphous inorganic wall is reported, titania nanocrystalline particles should be indeed interesting for photocatalytic applications. Mixed Ti/Zr oxide wormlike powders have been synthesized, in which an overall amorphous zirconia matrix presents embedded anatase nanodomains;<sup>303</sup> these crystalline NBBs are formed during solution aging.



**Coordination Polyhedra, Flexibility, and Curvature.** Silica, silicates, and silicones are well-known for the great structure diversity they present, as well as for their complex topologies. The flexibility of these structures, which can adopt a great variety of Si–O–Si angles, is due to the  $\mu_2$ –O connection between corner-sharing SiO<sub>4</sub> (or R<sub>x</sub>SiO<sub>2-x/2</sub>) tetrahedra. This geometrical versatility permits silica to attain practically every possible curvature and explains the multiplicity of structures and morphologies of silica-based synthetic or natural materials.

In the case of non-silica oxides (TM, Al, Sn, ...), the charge, size, valence, and coordination criteria impose polyhedra of higher coordination number. For example, Ti or Sn present usually hexacoordination, Zr is often hepta- or octacoordinated, and Al accepts environments with four to six oxide neighbors; the flexibility of the latter is one of the reasons for the great structural diversity of aluminosilicates. Apart from corner-sharing connections, metal–oxo coordination polyhedra of TM often display edge- or face-sharing structures. The presence of  $\mu_i$ –O oxygen bridges ( $i = 1$ –6) directs a more rigid linkage between hedra, which leads to less versatile “network nuclei”, less adapted to a variety of shapes and curvatures.

Which chemical parameters can be thus modified to attain a higher topological flexibility in non-silica systems? The following is a nonexhaustive list of possible strategies:

- Limit the size of the first oligomers obtained after hydrolysis, rendering them less compact and more linear, by means of inhibitors or mono bridging anions. 
- Resort to nonhydrolytic condensation processes in the first stages of texturing; typically, these

processes favor lo  coordination polyhedra.

- Perform synthesis in ext  pH conditions, in which the connectivity between  coordination polyhedra may be more versatile.

- Combine metal cations with metal centers that accept tetrahedral coordination [Si, Al, V(IV), Ga], which can give rise to *more flexible species*. This can be done by mere insertion (e.g., metal-substituted mesostructured silica networks, displaying excellent order) or by varying the oxidation state [a typical example is V(V), vide supra], thus generating mixed-valence networks. It has been suggested that cations able to form glasses should favor a better curved inorganic network, by presenting corner-shared polyhedra (rather than edge- or face-shared)<sup>84,173</sup> in agreement with the well-known Zachariasen rules.<sup>304</sup>

- Insert other type of anions in the inorganic network, these anions being polyatomic (phosphate, carboxylate, ...) or being forced to bridge a limited number of cations. These two features tend to decrease the average number of bonds and multiply the possible bonding angles, which may impart a greater flexibility to the mineral framework.

The last two ideas are relatively classical in solid state chemistry and helped to develop a great number of microporous and mesoporous solids: zeolites, aluminosilicates, metasilicates, etc.<sup>305</sup>

### 3.4.3. Formation Mechanisms

Concerning TM-based materials, four types of mechanisms have been proposed in the literature, based on crossing different spectroscopical characterization techniques, such as NMR, fluorescence, RPE, or UV–vis absorption: charge matching (CM), ligand-assisted templating (LAT), ion exchange/scaffolding, and modulation of the hybrid interface (MHI). These will be described and discussed in the following section. A point that is emphasized in most publications is the matching between the micellar arrangement and the inorganic phase. Therefore, a great deal of attention has been focused on the development of the hybrid interface, which has to generate “favorable interactions between the inorganic species and the surfactant”.<sup>14</sup>

**Charge Matching.** This mechanism, based on the cooperative formation of LC hybrids, was first proposed by Monnier et al. for the formation of silica mesophases.<sup>84</sup> In the original paper, it was suggested that an extension could be made to non-silica materials. Subsequently, the cooperative organization in solution of anionic mineral species and cationic surfactants has been proposed to explain the formation processes of mesophases based on W or Sb.<sup>33,84,96</sup> In water-rich media, when charged oxopolymers, polyanions (X<sup>−</sup>), or polycations (C<sup>+</sup>) are put into contact with ionic surfactants, the self-assembly pathways leading to textured materials are described in a similar way to those involved in the construction of silica networks (vide supra). These assembly mechanisms rely on the cooperative association between surfactant molecules and mineral oligomers in solution. At moderate (ambient) temperatures, hybrid LC phases are formed (Figure 16).<sup>193</sup> This cooperative mechanism is preferred over the classical

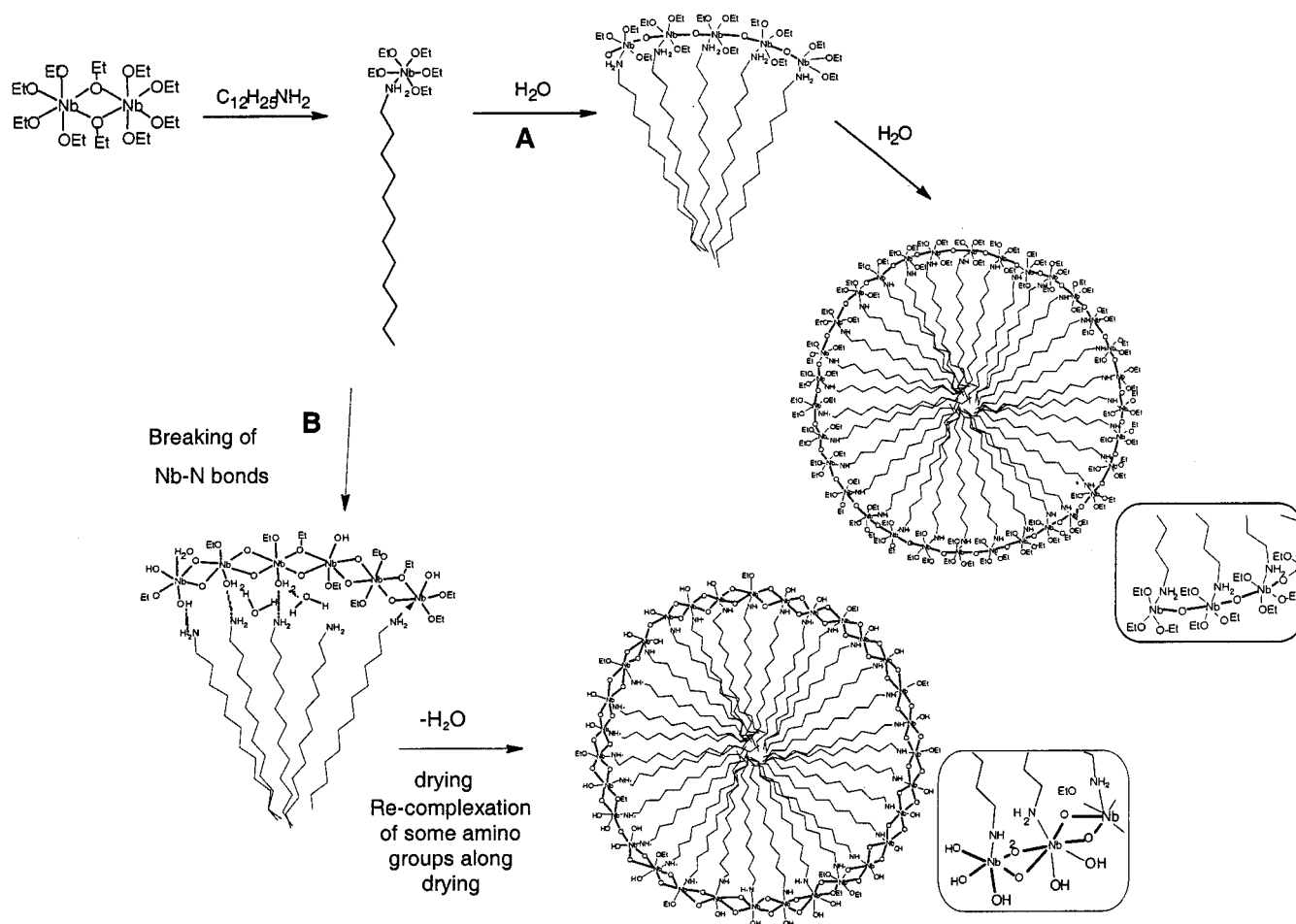


**Figure 19.** Ligand-assisted templating (LAT) mechanism, proposed by Ying et al. See references 5 and 113.

Mobil approach, based on the mineralization of preformed micellar arrangements, because of the low template concentrations, usually lower than the cmc; this cooperative assembly has been also observed in the case of V mesophases.<sup>306</sup> The hybrid interface is built up via electrostatic interactions between the ionic polar heads of the surfactants ( $S^+$  or  $S^-$ ) and the charged molecular inorganic moieties ( $I^+$  or  $I^-$ ). The resulting hybrid oligomers self-assemble into lyotropic LC. The interactions at the hybrid interface (Figure 10) can be direct ( $S^+I^-$  or  $S^-I^+$ ), or the matching can be adapted by the counterions that are associated with the surfactant ( $X^-$  or  $M^+$ ), giving rise to a composite interface, ( $S^+X^-I^+$ ) or ( $S^-M^+I^-$ ). However, the role of counterions seems to be more important, although still not completely clear, as recently suggested by Leontidis.<sup>307</sup>

**Ligand Assisted Templating.** This mechanism is based on the formation of chemical coordination bonds between the template and the precursor inorganic species from the first stages of the synthesis path (Figure 19). This chemical bond is a Lewis acid–base reaction between the amine head of the template and the metallic center (e.g.,  $R-NH_2 \rightarrow Nb$ ). This was shown by  $^{14}N$  NMR of the initial complex and the mesostructured dried material.<sup>113,256</sup>

The “ $Nb(OR)_5$ –alkylamine” complex thus formed is hydrophobic and cannot form micelles in alcoholic media. Subsequent mixing of this complex in excess of water yields a gel; aging of this gel at 100–180 °C

for some days leads to hexagonal materials. Two reaction paths can be proposed, which are schematically shown in Figure 19.

The first path (A) depends on the stability of the  $N: \rightarrow Nb$  bond, which has to be kept along all the steps that lead to the mesostructured material, without being hydrolyzed. Excess water permits the remaining alkoxy groups to be hydrolyzed, triggering the condensation of the Nb atoms fixed on the amine polar heads, and helps the micellization process. Nitrogen coordinated to the metal center increases the coordination number (i.e., no protons of the alkoxy are exchanged upon amine coordination) and probably decreases the probability of forming mineral aggregates by olation reactions. Under this hypothesis, the number of highly coordinated O atoms (i.e., oxo bridges  $\mu_i-O$  with  $i > 2$ ) should be minimized, and therefore less rigid connections between Nb polyhedra should be favored. These “supple” connections should permit a higher angular variation between metal centers, and the improved flexibility of the inorganic framework should lead to a better texturing.

The second possible path is summarized in Figure 19B. If hydrolysis and condensation of niobium alkoxides is very fast, a great fraction of the amine complex should be destroyed. However, hydrolysis produces hydrophilic Nb–oxo oligomers; these species can in turn associate with the surfactant heads via H-bonding interactions. Excess water induces a more



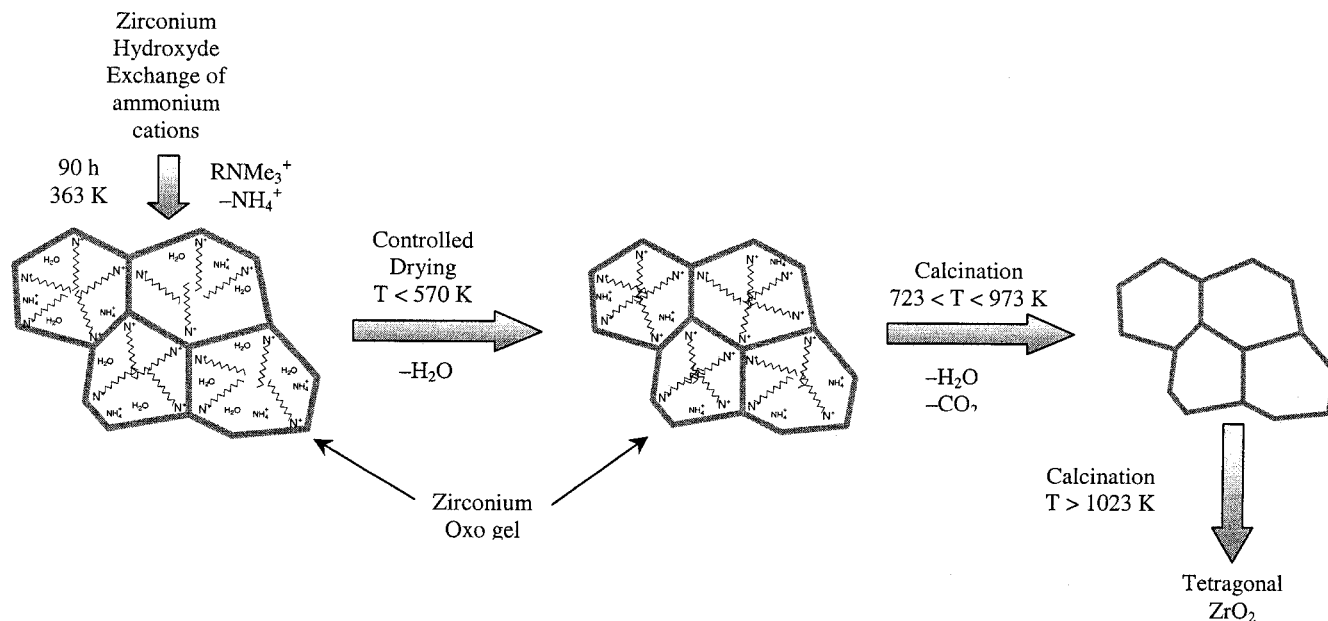


**Figure 20.** Ion exchange mechanism, followed by scaffolding, proposed by Hudson and Knowles (adapted from ref 250b).

extended condensation of the mineral network and simultaneously encourages the segregation of the aliphatic chains of the surfactant into micellar domains. Upon drying, residual solvent is eliminated, and certain niobium sites that are not coordinatively saturated may interact with the surfactant polar heads. Careful regulation of the surfactant/precursor ratio permits hexagonal hybrid phases to be obtained.

**Ion Exchange Followed by Scaffolding.** This mechanism has been proposed to explain the formation of mesostructured zirconia in alkaline conditions, in the presence of alkylammonium templates. No LC-like templating could be stated in these conditions, as the variation of the interpore distance measured after gel formation is independent of the organic chain length. On the other hand, after an adequate thermal treatment during gel drying ( $T < 570 \text{ K}$ ), the interpore distance varies linearly with the length of the alkyl chain. This is explained by a two-stage mechanism. The first stage involves the exchange of ammonium ions present in the precursor zirconium hydrated gel by alkylammonium species (Figure 20). The latter are adsorbed on the mineral surface, decreasing surface tension of the solution and minimizing gel deterioration upon solvent removal. It has been found that the diminution of the surface tension depends in an approximately linear fashion of the chain length, for a homologous series of surfactants. The surface tension at the pore interface is decreased independently of the network organization; therefore, the surface area and the pore size of the dried and calcined materials are only proportional to the chain length.<sup>250</sup>

This model has been further discussed by Fripiat and co-workers, who considered a modified scaffolding process for the formation of poorly organized materials.<sup>253b</sup> Particular attention is paid to the interaction between the zirconia oligomers and the surfactant, in the low pH synthesis conditions used to slow the inorganic hydrolysis–condensation processes. The first step in the gel formation involves

aggregation of surfactant–oligomer complexes in a tail-to-tail fashion. It is suggested that H-bonding interactions are responsible for the inorganic–surfactant link. These hybrid building units subsequently associate in poorly organized tactoids that contain the “organic voids”. The forces responsible for this association arise from gradual Zr–oxo condensation. The scaffolding effect begins to be evident when gels are thermally treated at low temperature (0.2–0.6 mL/g at 150 °C); porosity begins to arise when solvent is released upon drying; this process does not destroy the mesostructure.<sup>308</sup> The condensation and aggregation of the Zr–oxo oligomers upon drying and further thermal treatment result in crystallization and sintering above 400 °C. A partial enhancement of the network order goes in parallel with a decrease in the pore volume.

**Modulation of the Hybrid Interface.** This mechanism has been proposed to explain the different mesostructured  $\text{TiO}_2$ -based hybrid materials that can be obtained by hydrolysis–condensation of titanium alkoxides, in the presence of neutral PEO-based surfactants (PEO–PPO–PEO block copolymers or PEO–alkyl surfactants). The model is focused on the competition between the hydrophobic/hydrophilic character of the inorganic precursor and the template and the complexing power of the latter.<sup>238,239</sup>

In organic media (alcohol, THF, and toluene), presenting low  $h = [\text{H}_2\text{O}]/[\text{Ti}]$  ratios, bicontinuous worm-like textured phases are systematically obtained. The distance between inorganic walls rather depends on the quantity of template added rather than on template size; in this way, the polymer acts as a separator, but in no way does segregation of an ordered phase take place. An excess of acid water ( $h = 5\text{--}100$ ; pH  $\sim 0$ ) gives rise to hybrid hexagonal phases; in these conditions, the mesostructure parameters depend on template size. The two proposed pathways are schematized in Figure 21.

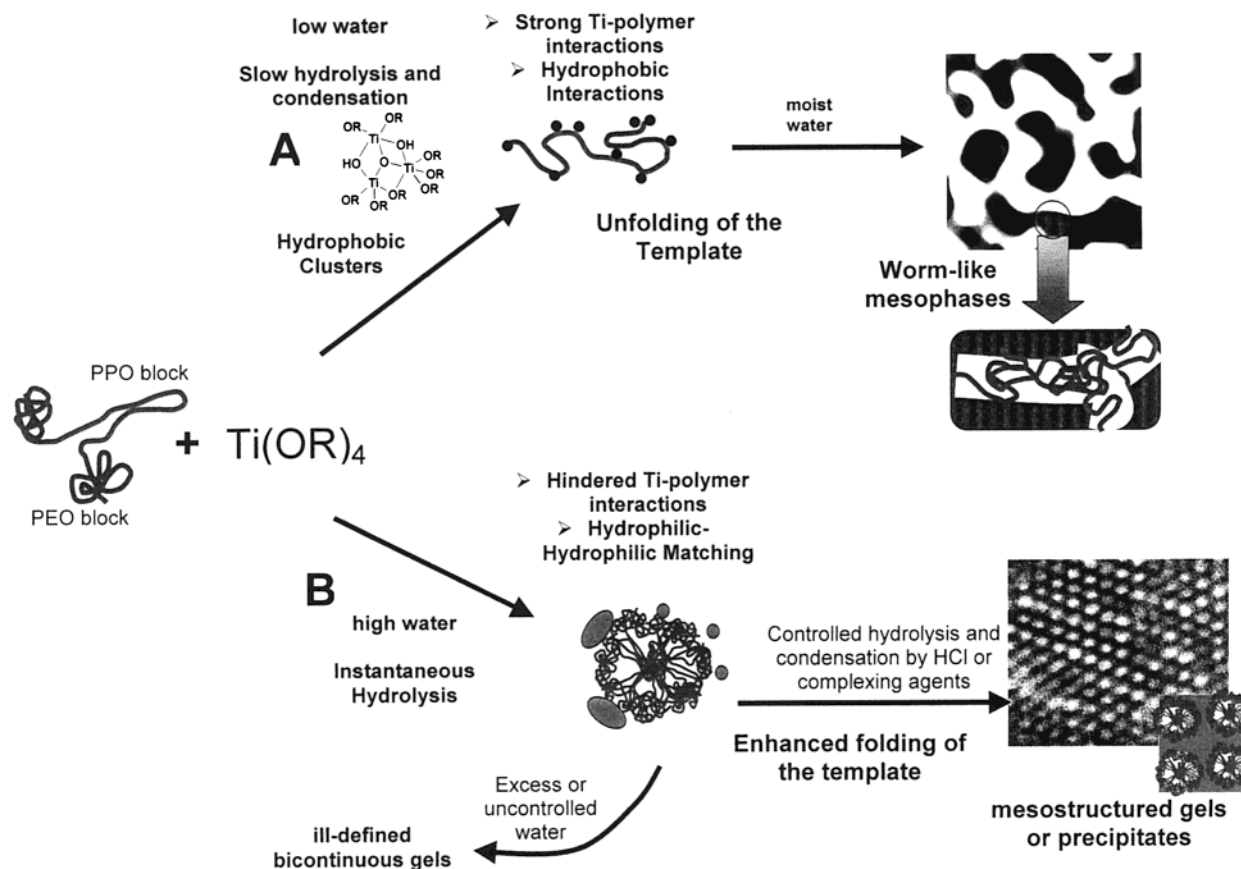


**Figure 21.** Modulation of the hybrid interface (MHI) mechanism, proposed by Sanchez and Soler-Illia. Reprinted with permission from ref 238. Copyright 2000 Royal Society of Chemistry (RSC) and CNRS. See references 238 and 239.

In path A, scarce water is present, and the metal cations can be chelated by the polar head of the surfactant ( $-OCH_2CH_2OH$ ) or by the ether functions of the PEO or PPO chains; this has been validated by NMR and UV-vis spectroscopy.<sup>238</sup> These metal cations can belong to alkoxide monomers or oligomers, hydrophobic moieties (arising from incomplete condensation), or even well-defined clusters.<sup>290</sup> These transalcoholysis or complexation reactions are strongly favored in apolar or aprotic solvents (THF or toluene), alcohol or water being efficient competitors for nucleophilic substitution. Therefore, complexation phenomena are enhanced upon drying or solvent evaporation. The binding of the polar heads or chain segments to the metallic centers favors the formation of  $Ti(OR)_{n-x-y}(OEt)_x(O-Surf)_y$  ( $0 \leq x + y \leq n$ ) species. As a result, the relative solubility difference between the PEO and the PPO blocks is diminished. This modification of the relative solubility of both blocks alters the micellization behavior, hindering the proper folding of these polymers. Moreover, hydrophobic metal-oxo-alkoxo species can attach to the hydrophobic fraction of the polymers, also helping to deploy the template. Mineralization advances along the wormlike spaces left over by a poor polymer-mineral phase segregation. As a consequence, the thickness of the organic domains (measured by TEM and XRD) is independent of the polymer size but is correlated to polymer quantity. This effect has also been reported when using nonhydrolytic conditions, which lead to small pore size, even with bulky polymers such as F127 [(PEO)<sub>106</sub>(PPO)<sub>70</sub>(PEO)<sub>106</sub>].<sup>262,263</sup> The

lack of segregation should be less marked with (PEO-alkyl) templates, although their maximum pore range is somewhat restrained (up to  $\sim 60$  Å); this should be not surprising, in view of the lack of interactions between the alkyl chain and the inorganic oligomers.

In contrast, through the *aqueous* route (Figure 21, path B), rapid condensation processes lead to the formation of hydrophilic oxo oligomers. In the presence of HCl, condensates of general formula  $TiX_x(OH)_yO_{2-(x+y)/2}$  ( $X = OR$  or  $Cl$ ,  $x \approx 0.3-0.7$ , and  $y \approx 0-0.2$ ) are obtained; the size of these oligomeric species has been determined by SAXS to be on the order of 20 Å.<sup>309</sup> In the first stages of the texturing process, complexation by the polymer is discouraged and the interaction between the hydrophilic subunits and the polymers is mostly by H-bonding. These relatively loose interactions permit a more flexible adjustment of the curvature at the interface level. Upon drying, improved segregation is promoted, and a few  $M-(OSurfactant)$  chelating bonds can possibly have a role in the nucleation of structured precipitates. The co-condensation of the hydrophilic clusters around the micelles leads to the formation of the inorganic network. The overall hydrophilic conditions assist polymer folding, the hydrophilic Ti-oxo-hydroxo species and PEO groups match together at the hybrid interface, whereas PPO segments migrate to the micelle interior, creating the conditions for an adequate phase segregation at the mesoscale. In this case, hexagonal or cubic mesostructures are obtained, and the interpore distances depend on the polymer

size. The important acid quantities hinder a complete condensation; therefore, a subsequent solidification treatment is often needed.

This “hydrophilic matching” approach has been successfully extended to  $\text{TiO}_2$ –CTAB mesophases, where the surfactant/mineral interactions are in principle of a different nature. However, strongly acid conditions in both cases blur the specific template/inorganic bonding, and the essential interactions are focused on the compatibilization of the hydrophilic character of the polar head and the inorganic polymeric precursors at the hybrid interface.<sup>263</sup> These simple concepts have been successfully applied in the design of synthesis methods for non-silica oxide mesostructured films,<sup>265,266,270,271</sup> and aerosols<sup>271c</sup> where an adequate control of the competition between evaporation and stiffening of the as-deposited gel-like phase determines the order of the final structure.<sup>202a</sup> Although proposed for transition metals, this model can be also valid for silica systems, where the quality of the mesostructure also depends on the adequate segregation of the inorganic and organic domains.<sup>271d</sup> From the side of the inorganic framework, the hydrophilicity of the silica interface depends on the extent of hydrolysis, and the water contents of the initial systems should be crucial for the final phase. A more general “hydrophilic matching” approach should also be valid under conditions different from EISA (i.e., precipitation).

#### 3.4.4. Stability of the Inorganic Network: from Consolidated Hybrids to Mesoporous Phases

An essential issue in the performance of non-silica mesoporous materials is the stability of the inorganic network. Most synthesis methods being based on avoiding fast and extended condensation, subsequent chemical, mild thermal, or hydrothermal processing is often needed to favor extended condensation. This postprocessing helps to consolidate the mineral walls. Phase transformations (for example, lamellar to hexagonal<sup>310,311</sup>) can take place during this process. Sonochemical treatment has been applied to reduce the treatment times.<sup>312</sup>

Template removal to obtain a porous oxide remains a fundamental issue, in view of promising applications: catalysis, sensors, and separation; postfunctionalization of the high pore surfaces opens the path to controlled nanocavities.<sup>157</sup> In principle, pore space can be liberated by thermal treatment (calcination) or repeated washing, as in silica systems. In the case of non-silica systems, an irreversible deterioration of the mesostructure is often associated with template elimination. However, high specific surface areas (in the order of the hundreds of  $\text{m}^2/\text{g}$ ) can be obtained, depending on the nature of the metal and the synthesis protocol (see Tables 6 and 7). Unfortunately, most of these oxides cannot support temperatures  $> 500\text{ }^\circ\text{C}$ , which is a serious limitation for most catalysis applications.<sup>270b,271c</sup> It is important to stress that mesoporous materials can be obtained by treating even ill-defined mesostructured hybrids at higher temperatures. In these cases, even if the resulting calcined materials are not necessarily organized, mesoporosity can arise from textural features (i.e.,

the one originated by a dispersion of nanoparticles, which arise from the irreversible deterioration of a mesostructured material).

The destruction of the mesoporous framework can be due to different reasons: the presence of an insufficiently condensed inorganic network, which bears residual stress or microporosity, modifications of the valence state via redox reactions, or crystallization of an inorganic phase being the most common examples. These drawbacks can be solved in a number of ways:

(1) Aging the as-prepared hybrid phases in mild hydrothermal conditions permits a better consolidation of the inorganic walls.

(2) Resorting to ABC templates gives rise to larger segregation domains; this permits thicker inorganic walls to be obtained. Commercially available  $[\text{PEO}]_n$ – $[\text{PPO}]_m$ – $[\text{PEO}]_n$  triblock copolymers are the most used in this case, and high-porosity TM-, Sn-, or Al-based mesoporous phases have been obtained from these templates (see Tables 6 and 7). The elaboration of tailored templates (specifically adapted to one type of cation) should open the way to the construction of novel multiscale architectures.

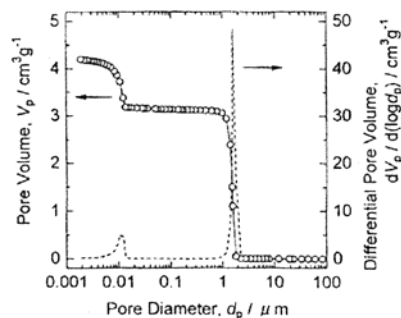
(3) A gradual and rational thermal treatment, composed of consecutive stages, separates the different decomposition steps of the template (control of temperature ramps, atmosphere, ...).

(4) Selective washing of the template can be done before thermal treatment. This approach has been applied in the case of amine-templated Nb mesoporous oxides, where a simple washing with acid ethanol suffices to remove most of the template, by protonation of the polar head, cleaving the amino–Nb Lewis complex.<sup>256</sup> Anion exchange (acetate in alkaline medium) has been used to remove anionic surfactants from mesostructures without altering the order.<sup>298</sup>

(5) Using additives delays the crystallization of the inorganic walls, such as cations or mineral anions (sulfates, phosphates, added before or after the synthesis, or coming from the template polar head). The thermal resistance of some oxo–metallic compounds is substantially improved by this procedure.<sup>235</sup>

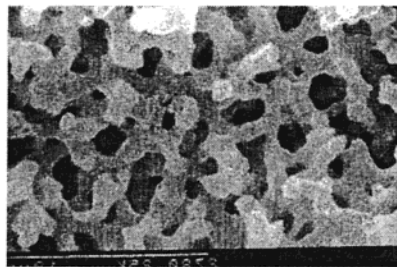
(6) An NBB approach, in which precrystallized nanoparticles are gathered around the organic mesophase, can be used. This should lead to lower contraction and structural change of the inorganic network upon thermal treatment.<sup>303</sup> This concept implies mastering of the colloidal interactions between the NBBs and the micelles or LC structures.

An interesting example is given by the nature and structure of titania-based mesophases, formed in the presence of alkyl phosphate templates, which has been a matter of debate.<sup>111,230,313</sup> Independently of the lamellar or hexagonal nature of these materials, the  $\text{TiO}_2$  obtained after partial template elimination presents two main features: mesoporosity (20–30 Å) and high specific surface area (200  $\text{m}^2/\text{g}$  at 350  $^\circ\text{C}$ , 600  $\text{m}^2/\text{g}$  after acid washing). It is important to note that a significant phosphate amount is present in the oxide phases, which probably contributes to a better



I

Pore size distribution measured by  
nitrogen and mercury volumetry



II

SEM micrograph

**Figure 22.** Bimodal pore distribution of a silica network (I) presenting mesopores (4–10 nm) and macropores (II, 1–3  $\mu\text{m}$ ). Application: chromatographic supports. Figure 22-I, reprinted with permission from ref 86. Copyright 1997 Kluwer Academic Publishers. Figure 22-II, reprinted with permission from Nakanishi and Soga, *J. Non-Cryst. Solids* **1992**, *139*, 1. Copyright 1992 Elsevier Science NL.

cohesion of the inorganic framework and retards the development of crystalline phases.

The most remarkable effect of phosphate anions has been found in Zr oxophosphates, where the mesoporous material is stable until 500 °C.<sup>235</sup> Zirconium or hafnium oxosulfate hexagonal hybrid mesophases do not stand template removal. In contrast, when these mesophases are treated with phosphoric acid or sodium phosphate at 250 °C, an oxometallophosphate hybrid compound is obtained via anion exchange. These compounds are resistant to thermal treatment, giving rise to mesoporous oxophosphates presenting 230–500  $\text{m}^2/\text{g}$  specific surface areas, depending on the template chain length.<sup>235</sup> Titanium oxophosphate of high surface area is stable until 400 °C.<sup>235</sup> Detailed and complete characterization of the thermal behavior of these phases has been recently presented by Kleitz et al.<sup>314a</sup> for powders and by Crepaldi et al. for films.<sup>314b</sup>

An improvement of the thermal behavior of some structures has also been observed in the presence of carboxylates, well-known for their ability to bridge metal centers. These anions arise from the polar head of the alkyl carboxylate templates, or of their moderate calcination in the case of PEO-based surfactants. Mesoporous alumina of 20 Å pore diameter and 710  $\text{m}^2/\text{g}$  specific surface area, stable to 430 °C, has been obtained from aluminum alkoxides and alkyl carboxylate templates.<sup>219</sup>

Alternative treatments for surfactant removal without resorting to high temperatures include ozone<sup>315</sup> or UV/O<sub>3</sub> treatment.<sup>316</sup> Although potentially very interesting, this procedure has not been applied so far to non-silica structures.

Organic functionalization of the mesoporous walls is an important added value for advanced TM-based mesostructures. Hybridization of the pore surface can be easily performed by postfunctionalization, once the oxide network of mesoporous material is consolidated. Organic molecules bearing interesting functions (chromophores, selective solubilization, trapping, etc.) have been anchored to the pore wall by means of complexing groups (carboxylates, phosphonates,  $\beta$ -diketonates, and allied derivatives).<sup>270</sup> An interest-

ing feature of TM-oxide walls is the availability of the grafting molecules and the quickness and completion of the grafting reactions. Silane-coupling agents can also be envisaged for functionalization purposes.

#### 4. Multiscale Texturation

Nature has been producing inorganic materials and hybrid composites with a remarkable efficiency for millions of years by making use of highly selective structures. The construction of materials presenting complex hierarchical structures is a particularly interesting challenge for the materials chemist. In general, two main approaches are envisaged, based on introducing macrotemplates (with size ranging from 1000 Å to several micrometers: latex or silica nanoparticles, large polymers, bacteria, etc.) directly in the reaction media or by combining these macrotemplates with usual mesoscale templates (surfactants, molecular agents, etc.).

Materials presenting multimodal or multiscale porosity present a major interest, particularly for catalysis and separation processes, where optimization of the diffusion and confinement regimes is required. Whereas micro- and mesopores provide the size and shape selectivity for the guest molecules, enhancing the host-guest interactions, the presence of macroporous channels should permit improved access to the active sites at the immediate smaller scale, avoiding pore blocking by reagents or products.

##### 4.1. Phase Separation, Cooperative Autoassembly, and Topological Defects

Mesoporous-macroporous silicas have been obtained in an original and simple fashion by adjusting sol-gel hydrolysis/condensation kinetics and solvent-mineral polymer interactions.<sup>86</sup> Macroporosity can be controlled by inducing a phase separation between a continuous solvent phase (hydrosoluble polymers or tuned solvent polarities) and a growing inorganic network. Mesoporosity can be controlled by solvent exchange and treatment in alkaline conditions. These silica phases (Figure 22) are being developed as

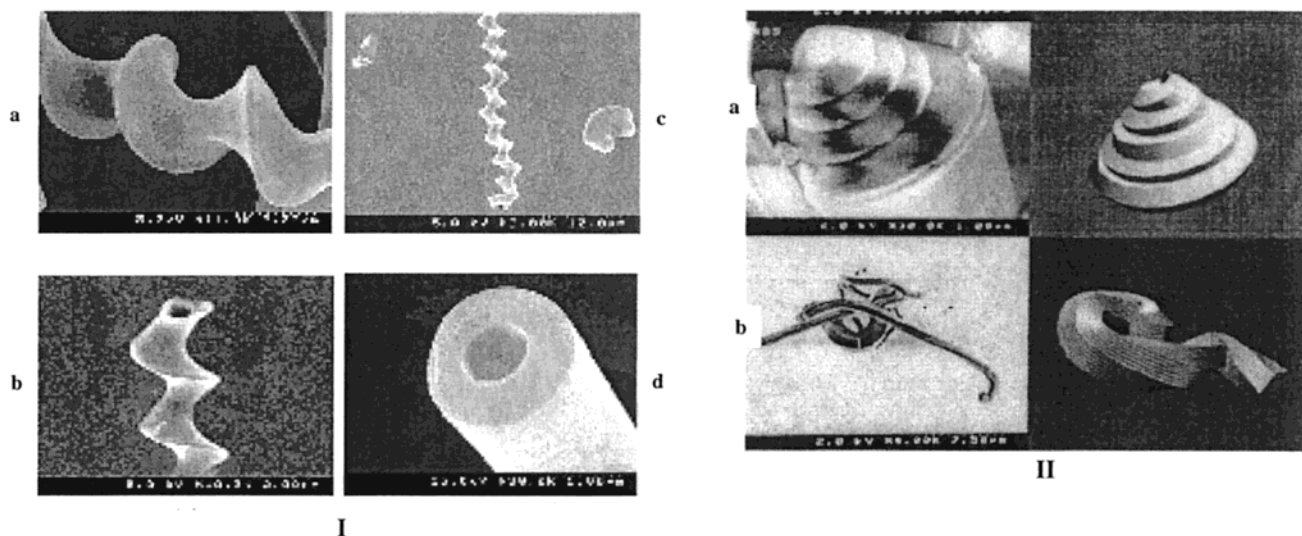


**Figure 23.** SEM micrographs of mesoporous silica presenting complex shapes, obtained by topological defects of an LC phase: (I) spiral (a) and fibrous morphologies (b) (SEM pictures to the left; schemes on the right); (II) helicoidally (a–c) and cylindrical (d) hollow shapes. Reprinted with permission from refs 318 and 319. Copyright 1998 and 1999, respectively, Wiley-VCH.

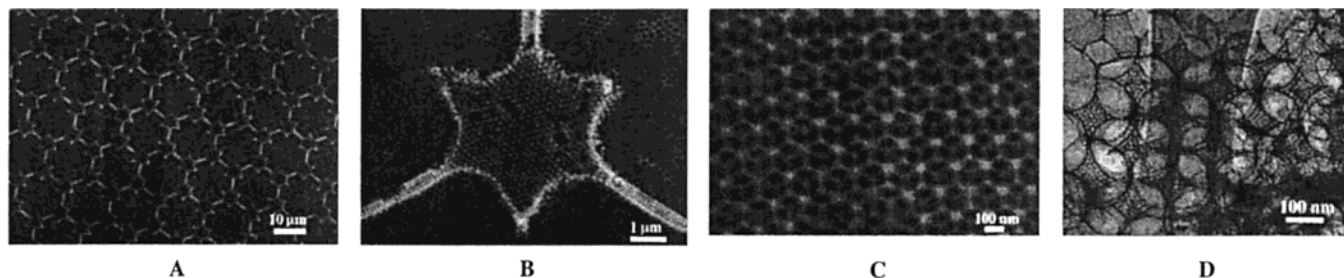


**Figure 24.** (A–C) SEM micrographs of hierarchically ordered multiscale porous silica, presenting a three-level organization. (D) TEM micrograph of the same sample, showing the cubic mesoporous symmetry within the macroporous walls ( $d_{100} \sim 11$  nm). Reprinted from Yang et al. *Science* **1998**, 282, 2244. Copyright 1998 American Association for the Advancement of Science.

chromatographic supports.<sup>86</sup> Segregation of aqueous droplets can also give rise to spongelike membranes, which also display mesopores.<sup>317</sup>

Recently, it has been shown that topological defects of LC phases (dislocations, disclinations, etc.) can act as templates to obtain silica with original and complex morphology (Figure 23).<sup>318</sup> The energy that is necessary to create a defect in LC phases is certainly lower than the one required to form a defect in a solid crystalline network. This energetic advantage of soft matter permits easily created extended defects, strongly distorting the director field.

In LC systems, surface interactions are of paramount importance; indeed, they can give rise to the stabilization of a certain kind of defect, favoring a particular anchoring of the director. On the other hand, additional fields, such as gravity, electrical, magnetic, and shear, can modify the nucleation and growth processes of the LC phase, structuring the director field in an original fashion.

For instance, dilute silica species in a water–formamide solution, in the presence of  $C_{16}$ TMABr lead to helicoidally twisted hollow silica fibers, presenting mesoporous walls.<sup>319</sup> These complex hierarchical structures are formed at the solution–air interface. Hollow mesoporous fibers have also been synthesized in two-phase static systems (acidic water/hexane or acidic water/ $CCl_4$ ).<sup>320</sup>

These examples illustrate the hypothesis that complex structures similar to those found in nature arise from the combination of self-assembly processes, topological defects, and external fields (i.e., symmetry breaking) associated with “open” systems.

## 4.2. Micromoulding and Cooperative Self-Assembly

A simple method that permits a double-texturing scale based on the use of latex nanoparticles and amphiphilic molecules (low-weight surfactants, or ABC) has been recently developed.<sup>19,152</sup> The precipitation of mesostructured silica has been performed within the empty spaces of a colloidal crystal of polystyrene (PS) beads. A similar approach has been developed from siloxane precursors. Micropatterned poly(dimethylsiloxane) (PDMS)<sup>321</sup> has been used as a macroscopic template, in which mesostructured silica is produced. The same procedure has been successfully extended to other PDMS/surfactant systems.

PEO block copolymers (PEO–PPO–PEO) have been employed to obtain triple-scale hierarchically ordered silica (Figure 24).<sup>151</sup> The micromolding is performed by patterning a PDMS template, and the submicronic texture is again formed by packed PS spheres. The mesoporous structure is generated in the voids of the PS colloidal crystal, via a cooperative

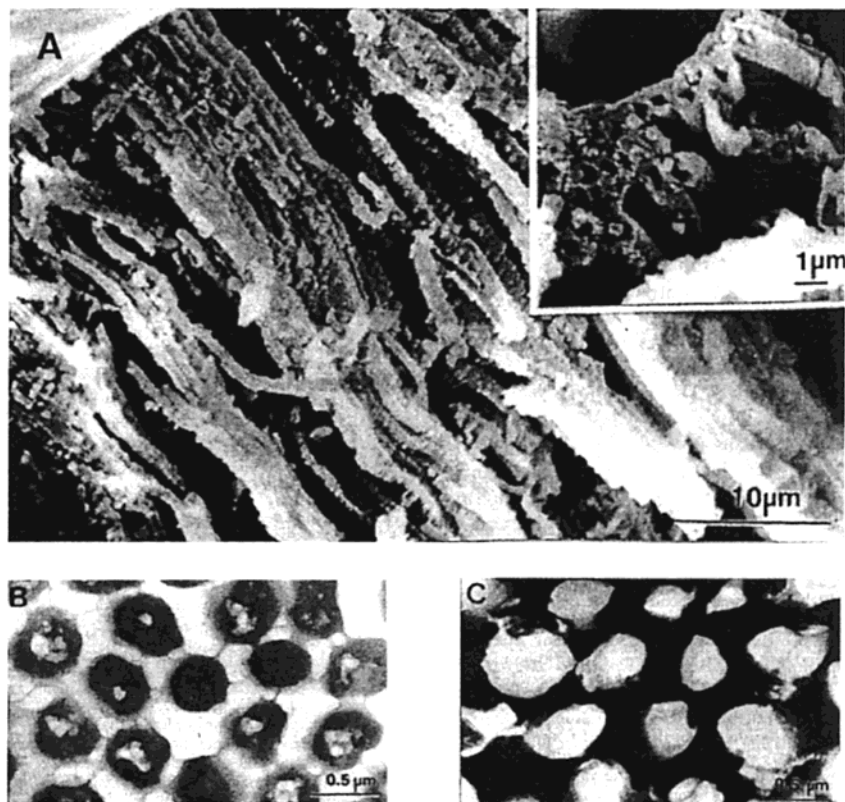


**Figure 25.** (A) SEM micrograph of a bacterial thread infiltrated by MCM-41 silica, thermally treated and fractured parallel to the fibers [hollow mesoporous silica cylinders can be observed (see inset)]; (B) TEM micrograph of a nonmineralized bacterial thread network, showing the empty spaces; (C) TEM image corresponding to the mineralized network, showing the development of continuous silica walls and encapsulated multicellular filaments. Reprinted with permission from ref 23. Copyright 1997 Macmillan Magazines Limited.

self-assembly of the inorganic species and the ABC template. These latex-based structuring methods have been extended to zeolitic structures.<sup>138,322</sup>

#### 4.3. Biotemplates and Cooperative Self-Assembly

Biological structures can also be used as templates.<sup>23</sup> *Bacillus subtilis* cells can produce long aligned filaments, formed by smaller coaligned fibrils of  $\sim 0.2 \mu\text{m}$  diameter. In culture media, a quasi-hexagonal superstructure is developed from multicellular filaments ( $0.5 \mu\text{m}$  in diameter). The bacterial superstructure is placed in contact with an aqueous silica sol, to fill the voids between the fibers with silica nanoparticles. Superstructure swelling by solvent water allows the silica nanoparticles to diffuse, giving rise to very well aligned hybrid silica-based channels. The organic component is eliminated by heating at  $600 \text{ }^\circ\text{C}$ , revealing a macroporous replica of the fibrillar network: parallel channels of  $0.5 \mu\text{m}$  diameter, aligned along the morphological axis of the fibers (Figure 25). The addition of  $\text{C}_{16}\text{TMABr}$  to the colloidal sol textures the walls that separate the bacterial filaments, the final material presenting a double-scale porosity.

Original and homogeneous macrottextures shaped with coral-like, helical, or macroporous sieve morphologies have been obtained following a nanotechnology approach based on the template-directed assembly by poly( $\gamma$ -benzyl-L-glutamate) (PBLG) of organically functionalized  $\text{CeO}_2$  crystalline nanoparticles. By adjusting a single parameter, such as the

template-to-inorganic ratio, a versatile tuning between templating effect and phase separation yields hierarchical porous materials presenting both micro- and macroporosity with inorganic walls constituted of nanocrystalline cerium oxide particles.<sup>323</sup>

#### 4.4. Organogel/Metal Oxide Hybrids

Organogelators open a great number of possibilities for multiscale texturing, the possible size scale being in the nanometer to a fraction of a millimeter range.<sup>324</sup> Molecules based on a steroidal or diaminocyclohexane skeleton, 2,3-bis(*n*-decyloxyanthracene) (DDOA) or 2,3-di-*N*-alkoxyphenazine (DAP), have been used as templates, due to the low concentration required to produce gels (between  $5 \times 10^{-4}$  and  $10^{-2} \text{ mol L}^{-1}$  in methanol) (see Figure 26). Cryofracture TEM analysis shows the presence of a three-dimensional dense matrix constituted by randomly arranged fiber bundles ( $60 \text{ nm}$ ). Methanol being a suitable sol-gel solvent, a silica matrix can be synthesized in situ, using DDOA and DAP as templates. In this way, a double-scale porosity silica can be obtained.<sup>325</sup>

In recent reports, two Japanese research teams<sup>156,326–333</sup> have shown that hydrolysis and condensation of silicon or titanium alkoxides in the presence of organogelators lead to hybrid metal oxide-based fibrous networks; the corresponding oxides are obtained upon calcination. Synthesis parameters such as the pH, the nature of the organogelator, and the interactions taking place between the template

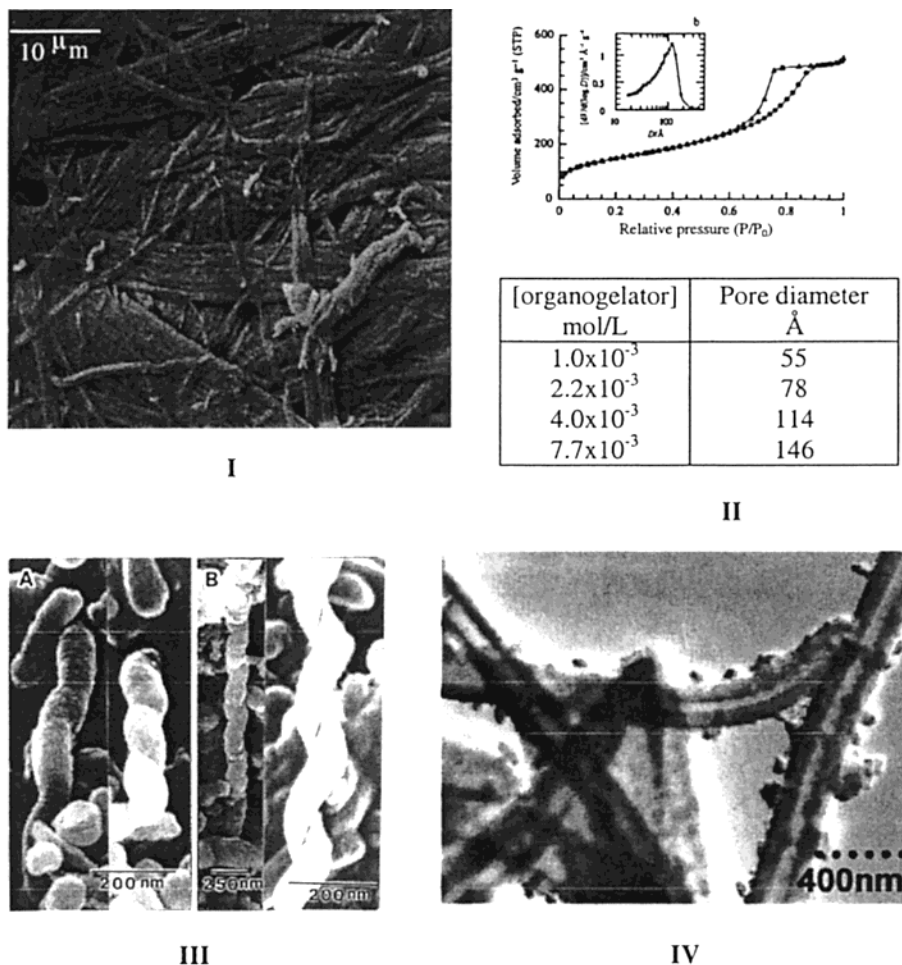


**Figure 26.** (I) SEM micrograph of entangled silica fibers, formed in the presence of organogelators; (II) nitrogen adsorption–desorption isotherm [inset, pore distribution; the table shows the dependence of pore size with the organogelator concentration (reprinted with permission from ref 325. Copyright 2000 Royal Society of Chemistry)]; (III) twisted silica fibers, obtained in the presence of a chiral organogelator (see Figure 11E): left-handed (A) and right-handed (B) helicoidal fibers;<sup>331</sup> (IV) hollow calcined TiO<sub>2</sub> fibers.<sup>330</sup>

and the developing mineral phase (H-bonding or electrostatic) permit control of the structure of the hybrid fibers and their integrity upon elimination of the template. Silica fibers (Figure 27) have been synthesized in the presence of cholesterol derivatives containing a crown ether group (see Figure 11J) or neutral or modified cyclohexanediamides.

Siliceous materials presenting novel morphologies and textures have been obtained by changing the nature of the organogelator: hollow silica tubes (Figure 27), presenting an aspect similar to the lamellar-like patterns observed in *spiculae*,<sup>333</sup> have been synthesized from the cholesteryl derivatives; chiral information has been transcribed to a mineral network by simple templating with organogelators E and H of Figure 11 [in particular, diaminocyclohexane derivatives permitted isolation of helical silica fibers;<sup>331</sup> chiral selectivity is attained by selecting templates with the adequate (*R* or *S*) configuration (Figure 26.III)]; novel organic–inorganic hybrids that present helical symmetries have been obtained by hydrolysis of organosilica derivatives bearing an *R,R* or *S,S* chiral diureidocyclohexane spacer (left- and right-handed helices are self-generated depending on the configuration of the chosen organic subunit).<sup>334</sup>

These first results are indeed encouraging, as they strongly suggest that the use of organogelators as templates will make possible the elaboration of novel materials presenting complex architectures.

All of the presented examples demonstrate that chemists already know to construct materials with original, complex, and unique architectures. These are the first steps of a naive albeit close approach to the construction methods observed in nature. Hierarchical structures can be obtained by making use of different templates (latex, bacteria, polymers, topological defects in LC, ...) and by combining this with self-assembly processes that associate inorganic precursors with amphiphilic molecules, acting in synergy at different length scales (from nanoscopic to the micrometer scale). A limited number of pioneering works have established that hierarchical structures can be generated from one type of molecule (surfactant, organogelator), which combines at the same time phase separation phenomena and local interactions, able to manage the organization at the mesoscopic scale. In the dawn of the third millennium, these promising results open a wide ocean of possibilities in the domain of materials construction and elaboration. A better understanding of the yet unknown construction rules and mechanisms and of the

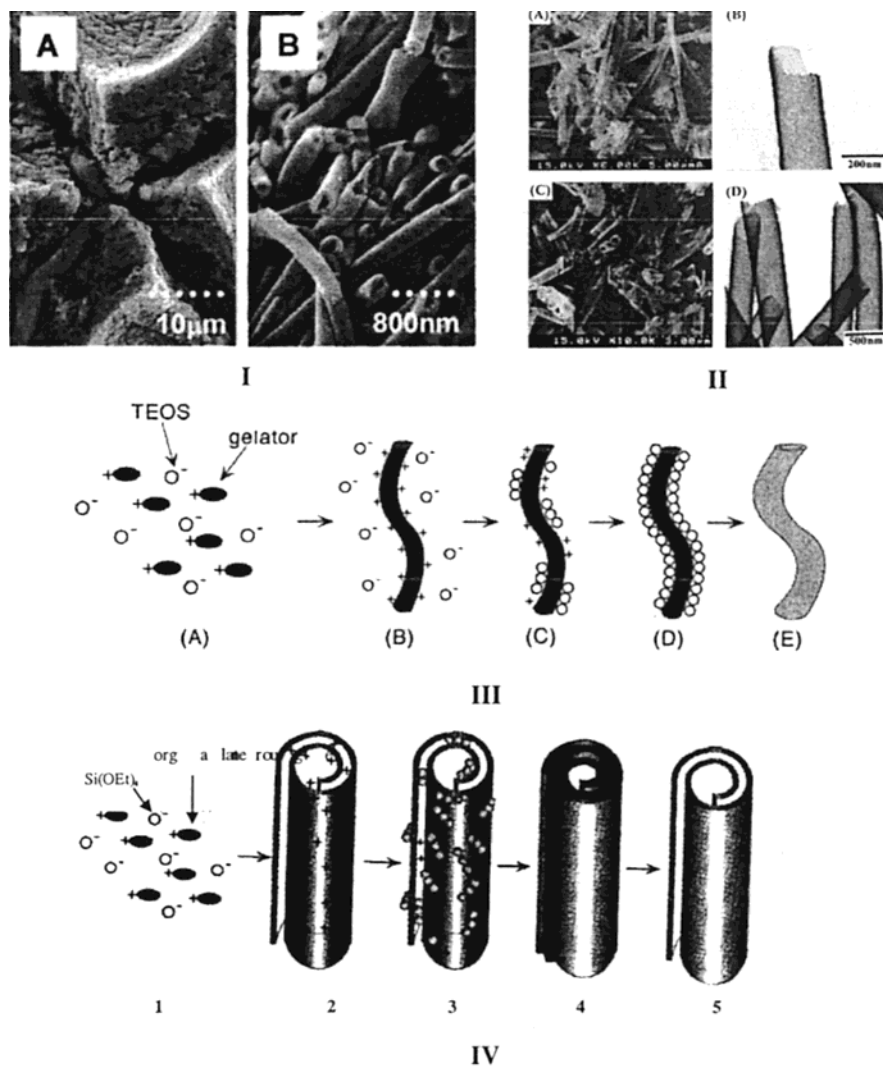


**Figure 27.** (I) SEM micrograph of macroporous silica (A) and hollow silica fibers (B) obtained from the same organogelator in acid or alkaline medium, respectively;<sup>330</sup> (II) SEM (A, C) and TEM micrographs (B, D) of hollow silica ribbons;<sup>333</sup> (III) formation mechanism of the hollow fibers;<sup>333</sup> (IV) formation mechanism of the silica ribbons.<sup>330</sup>

role of the hybrid interface and external stimuli (applied fields, fluxes, ...) on their formation processes will clear the track to totally tailored materials.

### 5. Perspectives and Concluding Remarks

Mesotextured materials constitute a challenging domain in materials chemistry, which is experiencing explosive growth.<sup>335</sup> The potential of these structures has been recognized in the domain of optical devices, catalysis, separation techniques, controlled delivery, adsorption, and sensors.<sup>35</sup> Optimization of the properties of these materials requires a sound knowledge of the structure–property relationships, as well as a deeper understanding of the formation mechanisms. In the past five years, the increasing number of successful synthesis methods for mesostructured and mesoporous silica, metal oxides, phosphates, etc. is the proof of the deeper knowledge and better design techniques available. The central synthetic ideas (schematized in Figure 28) are based on three fundamental issues:

(a) The condensation processes must be controlled, to avoid quick and indiscriminate growth of the inorganic network. At the same time, an extended

polymerization of the inorganic network has to be ensured.

(b) Phase segregation at the nanoscale must be promoted, by enhancing the organic–organic ( $\Delta G_{\text{org}}$  in eq (1), usually weak) interactions. This has to be adequately balanced by a good compatibility at the organic–inorganic interface ( $\Delta G_{\text{inter}}$ ), to balance the (usually strong) contribution of the inorganic–inorganic links.

(c) The resulting curvature must be managed. Silica polymerization leads to supply building blocks presenting tetrahedral ( $\text{SiO}_4$ ) environments, which can easily adapt to the curvature imposed by the template. In non-silica systems, control of hydrolysis and condensation usually involves obtaining dense metal–oxo clusters as precursors. The volume fraction of these building units has to be adapted to generate the desired “nanometric synthon”: a micellar-like arrangement, covered by an inorganic oxide layer (Figure 28, see below). In an excess of template, surfactants attached to the inorganic NBB generate the “negative” nanosynthon: well-dispersed organic-capped inorganic colloids, which give rise to LC dispersions of inorganic particles. The optimal cur-



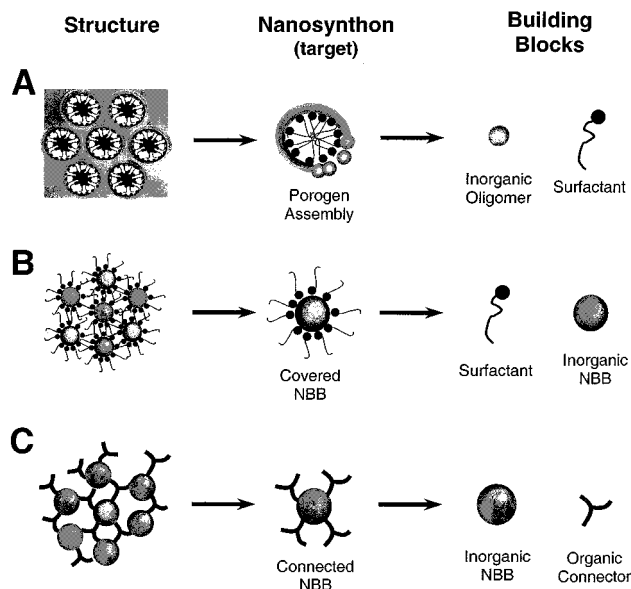


**Figure 28.** Illustrative examples of the nanosynthesis and retrosynthesis concepts applied to the design of nanostructured materials. In the case of a templated nanostructure (A), the target is composed of well-defined micelles wrapped by inorganic oligomers. The organic–organic interactions leading to micelle formation should be strong, as well as the compatibility at the hybrid interface. A low degree of inorganic condensation results in small oligomers as inorganic BB. The opposite curvature can be obtained (B) by varying the template/metal ratio; in this case, ordered nanoparticle dispersions can be obtained, see ref 4. The simplest example is given by the decomposition of a textured network into a “grafted particle” nanosynthon (C). The organic connectors and inorganic NBB can be chosen from a great variety of available nanoparticles, polymers, etc.

vature results from the optimization of template packing, flexibility of the inorganic construction units (branched oligomers or small dense NBB), and “interface matching”.

Materials chemists possess nowadays a set of efficient tools at hand, being able to smartly choose the texturing agents (surfactants, block copolymers, dendrimers, etc.), the starting mineral precursors (salts, alkoxides, NBB, etc.), and the reaction media (solvents, water contents, pH, complexing agents, aging conditions, etc.) to attempt a high control on the compatibility of the mineral and organic components and the self-assembly processes at hybrid interfaces. This control creates hybrid composites that are organized at the nanometric scale. The controlled creation of complexation, H-bonding, or electrostatic bonding between the organic and the mineral components, along with the tuning of the mineral network formation, permits a better management of the curvature and the interface matching (Figure 28A). These two intimately related features form the hybrid interface, which is the key issue that links the self-assembly and the sol–gel processes. Indeed, a hybrid *nanosynthon* (i.e., a “nanometric synthon”: a desired supramolecular element with a definite structure and symmetry at the nanometric scale) can be imagined aiming to a rational design of mesostructures. A retrosynthetic approach, akin to the one used in organic chemistry, can be developed; some examples are schematized in Figure 28A–C.

The assembly processes may be simultaneous or sequential, and the inorganic wall may be built up by polymerization of discrete or preformed species, in one or more condensation cascades. In particular, the comparison of systems obtained from structurally well-defined precursors of different condensation degree (molecules, clusters, nanoparticles, ...) is indeed important in order to improve the current understanding of the construction of TM-based mesostructures. These concepts are now currently extended to construct new self-assembled non-oxide systems.<sup>9,14</sup> Recent examples include helicoidally shaped chalcogenides<sup>336</sup> and smart functionalized mesostructured carbons.<sup>337</sup>

After a robust hybrid mesostructure is obtained, the hybrid interface may be modified or even destroyed in a subsequent step, to create materials of controlled porosity. This can be done by means of thermal or chemical procedures assisted by UV irradiation. In this step, the limitations arising from the high reactivity or tendency to yield low-surface crystalline phases of non-silica networks have to be taken into account. Block copolymer templates solve partially these problems by permitting thicker inorganic walls that enhance thermal stability. Indeed, a larger variety of microstructures presenting larger domains than those of conventional surfactant can be produced by an intelligent choice of the different blocks.

Hybridization of the pore network extended surface allows new functionalized materials to be implemented. Postfunctionalization of mesoporous transition metal oxide with organic moieties can be easily performed by taking advantage of available grafting groups, therefore opening the route to advanced oxide-based polyfunctional materials. Indeed, mesoporous materials can be used as templates for novel non-oxide materials.<sup>337</sup>

The chemical strategies offered by the coupling of sol–gel and self-assembly processes and the approaches based on functional well-defined NBBs (molecular clusters and colloids) will allow, through an intelligent and tuned coding, development of a new *vectorial chemistry*. By using these newborn concepts, materials chemists will be able to direct the assembling of a large variety of inorganic structures (from amorphous networks to structurally well-defined clusters or nanoparticles) into novel architectures. Many new combinations between inorganic or hybrid NBBs and an organic or biologic component are bound to appear in the future. In particular, original ordered materials presenting complex architectures will be designed<sup>338</sup> through the synthesis of new hybrid NBBs (acting as *nanosynthons*),<sup>4</sup> carrying chirality and/or dissymmetry, having complementary tuned connectivities, and allowing for the coding of hybrid assemblies.

The next step concerns the development of integrative synthesis pathways, clearing the track to tailored hierarchically ordered materials. In this growing field, current approaches include coupling of multi-scale templating (use of self-assembled or larger templates and controlled phase segregation) and morphosynthesis, associated with external stimuli

(applied fields, fluxes, mechanical constraints, imprinting, etc.). These multiscale structured hybrid or inorganic networks (from nanometer to millimeter, by resorting to larger templates, such as latex colloids<sup>25,339</sup> or organogelators<sup>330</sup>) will provide opportunities for designing new materials. Could these new synthesis strategies allow us to dream of a future possibility to build intelligent advanced materials, which will respond to external stimuli, adapt to their environment, self-replicate, self-repair, or self-destroy at the end of their fleeting lives?

## 6. References

- (1) WTEC Panel Report on Nanostructure Science and Technology: R & D Status and Trends in Nanoparticles, Nanostructured Materials, and Nanodevices; Siegel, R. W., Hu, E., Roco, M. C., Eds.; Kluwer: Dordrecht, The Netherlands, 1999; Web version <http://www.nano.gov>.
- (2) See, for example: (a) *Chem. Mater.* **2001**, *13* (special issue on Nanostructured and Functional Materials; Eckert, H., Ward, M., Eds.; and all articles therein). (b) *MRS Bull.* **2001**, No. 26 (special issue on Hybrid Materials; Loy, D. A., Ed.; and all articles therein). (c) Schubert, U.; Hüsing, N.; Lorenz, A. *Chem. Mater.* **1995**, *7*, 2010. (d) Loy, D. A.; Shea, K. J. *Chem. Rev.* **1995**, *95*, 1431. (e) Chujo, Y.; Saegusa, T. *Adv. Polym. Sci.* **1992**, *100*, 11. (f) Novak, B. M. *Adv. Mater.* **1993**, *5*, 422. (g) Corriu, R. J. P. *Polyhedron* **1998**, *17*, 925. (h) Corriu, R. J. P.; Leclercq, D. *Angew. Chem., Int. Ed.* **1996**, *35*, 1420. (i) Schmidt, H.; Seifering, B. *Mater. Res. Soc. Symp. Proc.* **1986**, *73*, 739.
- (3) (a) Sanchez, C.; Ribot, F. *New J. Chem.* **1994**, *18*, 1007. (b) Ribot, F.; Sanchez, C. *Comments Inorg. Chem.* **1999**, *20*, 327. (c) Judeinstein, P.; Sanchez, C. *J. Mater. Chem.* **1996**, *6*, 511. (d) Sanchez, C.; Ribot, F.; Lebeau, B. *J. Mater. Chem.* **1999**, *9*, 35. (e) Sanchez, C.; Soler-Illia, G. J. A. A.; Ribot, F.; Mayer, C.; Cabuil, V.; Lalot, T. *Chem. Mater.* **2001**, *13*, 3061.
- (4) Ying, J. Y.; Mehnert, C. P.; Wong, M. S. *Angew. Chem., Int. Ed.* **1999**, *38*, 57.
- (5) Ciesla, U.; Schüth, F. *Microporous Mesoporous Mater.* **1999**, *27*, 131.
- (6) Barton, T. J.; Bull, L. M.; Klemperer, W. G.; Loy, D. A.; McEnaney, B.; Isono, M.; Monson, P. A.; Pez, G.; Scherer, G. W.; Vartuli, J. C.; Yaghi, O. M. *Chem. Mater.* **1999**, *11*, 2633.
- (7) (a) Göltner, C. G.; Antonietti, M. *Adv. Mater.* **1997**, *9*, 431. (b) Polarz, S.; Antonietti, M. *Chem. Commun.* **2002**, in press.
- (8) Ozin, G. A. *Chem. Commun.* **2000**, 419.
- (9) Raimondi, M. E.; Seddon, J. M. *Liq. Cryst.* **1999**, *26*, 305.
- (10) Tiemann, M.; Fröba, M. *Chem. Mater.* **2001**, *13*, 3211.
- (11) Behrens, P. *Angew. Chem., Int. Ed.* **1996**, *35*, 515.
- (12) Sayari, A.; Liu, P. *Microporous Mater.* **1997**, *12*, 149.
- (13) Schüth, F. *Chem. Mater.* **2001**, *13*, 3184.
- (14) Brinker, C. J.; Scherrer, G. W. *Sol-Gel Science, The Physics and Chemistry of Sol-Gel Processing*; Academic Press: San Diego, CA, 1990.
- (15) Livage, J.; Henry, M.; Sanchez, C. *Prog. Solid State Chem.* **1988**, *18*, 259.
- (16) *Matériaux hybrides*; Arago 17; Masson: Paris, France, 1996.
- (17) Velev, O. D.; Jede, T. A.; Lobo, R. F.; Lenhoff, A. M. *Nature* **1997**, *389*, 447.
- (18) Holland, B. T.; Blandford, C. F.; Stein, A. *Science* **1998**, *281*, 538.
- (19) Krämer, E.; Förster, S.; Göltner, C.; Antonietti, M. *Langmuir* **1998**, *14*, 2027.
- (20) Velev, O. D.; Jede, T. A.; Lobo, R. F.; Lenhoff, A. M. *Chem. Mater.* **1998**, *10*, 3597.
- (21) Holland, B. T.; Blandford, C. F.; Do, T. O.; Stein, A. *Chem. Mater.* **1999**, *11*, 795.
- (22) Davies, S. A.; Burkett, S. L.; Mendelson, N. H.; Mann, S. *Nature* **1997**, *385*, 420.
- (23) Imhof, A.; Pine, D. J. *Nature* **1997**, *389*, 948.
- (24) Wijnhoven, J. E. G.; W. L. Vos, W. L. *Science* **1998**, *281*, 802.
- (25) (a) *Biomaterialization, Chemical and Biochemical Perspectives*; Mann, S., Webb, J., Williams, R. J. P., Eds.; VCH: Weinheim, Germany, 1989. (b) *Biomimétisme et Matériaux*, Arago 25; OFTA: Paris, France, 2001.
- (26) Mann, S.; Burkett, S. L.; Davis, S. A.; Fowler, C. E.; Mendelson, N. H.; Sims, S. D.; Walsh, D.; Whilton, N. T. *Chem. Mater.* **1997**, *9*, 2300.
- (27) Dujardin, E.; Mann, S. *Adv. Mater.* **2002**, *14*, 775.
- (28) Mann, S.; Ozin, G. A. *Nature* **1996**, *382*, 313.
- (29) (a) Yang, H.; Ozin, G. A.; Kresge, C. T. *Adv. Mater.* **1998**, *10*, 883. (b) Yang, S. M.; Solokov, I.; Coombs, N.; Kresge, C. T.; Ozin, G. A. *Adv. Mater.* **1999**, *11*, 1427.
- (30) Szostak, R. In *Handbook of Molecular Sieves*; Van Nostrand Reinhold: New York, 1992.
- (31) Kessler, H. In *Comprehensive Supramolecular Chemistry, Vol. 7, Solid-State Supramolecular Chemistry: Two- and Three-Dimensional Inorganic Networks*; Atwood, J. L., Davis, J. E. D., MacNicol, D. D., Vögtle, F., Eds.; Pergamon: London, U.K., 1996; p 425.
- (32) Huo, Q.; Margolese, D. I.; Ciesla, U.; Demuth, D. K.; Feng, P.; Gier, T. E.; Sieger, P.; Firouzi, A.; Chmelka, B. F.; Schüth, F.; Stucky, G. D. *Chem. Mater.* **1994**, *6*, 1176.
- (33) Corma, A. *Chem. Rev.* **1997**, *97*, 2373.
- (34) Schüth, F.; Schmidt, W. *Adv. Mater.* **2002**, *14*, 629.
- (35) Sing, K. S. W.; Everett, D. H.; W. Haul, R. A.; Moscou, L.; Pierotti, J.; Rouquerol, J.; Siemieniewska, T. *Pure Appl. Chem.* **1985**, *57*, 603.
- (36) Kresge, C. T.; Leonowicz, M. E.; Roth, W. J.; Vartuli, J. C.; Beck, J. S. *Nature* **1992**, *359*, 710.
- (37) Wilson, S. T.; Lok, B. M.; Flanigen, E. M. U.S. Patent 4310440, 1982.
- (38) Lok, B. M.; Messina, C. A.; Patton, R. L.; Gajek, R. T.; Cannan, T. R.; Flanigen, E. M. *J. Am. Chem. Soc.* **1984**, *106*, 6092.
- (39) Flanigen, E. M.; Lok, B. M.; Patton, R. L.; Wilson, S. T. In *Proceedings of the 7th International Zeolite Conference*; Murakami, Y. A., Iijima, Ward, J. W., Eds.; Kodansha Elsevier: Tokyo, Japan, 1986; p 103.
- (40) Parise, J. B. *Chem. Commun.* **1985**, 606.
- (41) Merrouche, A.; Patarin, J.; Kessler, H.; Soulard, M.; Delmotte, L.; Guth, J.-L.; Joly, J.-F. *Zeolites* **1992**, *12*, 22.
- (42) Férey, G. *J. Fluorine Chem.* **1995**, *72*, 187.
- (43) Harrison, W. T. A.; Martin, T. E.; Gier, T. E.; Stucky, G. D. *J. Mater. Chem.* **1992**, *2*, 2175.
- (44) Wallau, M.; Patarin, J.; Widmer, I.; Caulet, P.; Guth, J. L.; Huve, L. *Zeolites* **1994**, *14*, 402.
- (45) Harvey, G.; Meier, W. M. In *Proceedings of the 8th International Zeolite Conference*; Jacobs, P., van Santen, R. A., Eds.; Elsevier: Amsterdam, The Netherlands, 1989 (*Stud. Surf. Sci. Catal.* **1989**, *49A*, 411).
- (46) Soghomoniam, V.; Chen, Q.; Haushalter, R. C.; Zubieta, J. *Angew. Chem., Int. Ed. Engl.* **1993**, *32*, 610.
- (47) Debord, J. R. D.; Reiff, W. M.; Warren, C. J.; Haushalter, R. C.; Zubieta, J. *Chem. Mater.* **1997**, *9*, 1994.
- (48) *Atlas of Zeolite Framework Types*, 5th ed.; Meier, W. M., Olson, D. H., Baerlocher, C. H., Eds.; Elsevier: Amsterdam, The Netherlands, 2001; pp 1–302.
- (49) Website <http://www.iza-structure.org>.
- (50) Kessler, H.; Patarin, J.; Schott-Darie, C. *Stud. Surf. Sci. Catal.* **1994**, *85*, 75.
- (51) Bibby, D. M.; Dale, M. P. *Nature* **1985**, *317*, 157.
- (52) Huo, Q.; Xu, R.; Li, S.; Ma, Z.; Thomas, J. M.; Jones, R. H.; Chippindale, A. M. *Chem. Commun.* **1992**, 875.
- (53) Althoff, R.; Unger, K.; Schüth, F. *Microporous Mater.* **1994**, *2*, 557.
- (54) Bibby, D. M.; Baxter, N. I.; Grant-Taylor, D.; Parker, L. M. In *Zeolite Synthesis*; ACS Symposium Series 398; Occelli, M. L., Robson, H. E., Eds.; American Chemical Society: Washington, DC, 1989; p 209.
- (55) Flanigen, E. M.; Breck, D. W. *Abstracts*, 137th National Meeting of the American Chemical Society, Cleveland, OH; ACS: Washington, DC 1960; Abstr. 33M.
- (56) Barrer, R. M.; Buynham, J. W.; Bultitude, F. W.; Meier, W. M. *J. Chem. Soc.* **1959**, 195.
- (57) Vaughan, D. E. W. In *Catalysis and Adsorption by Zeolites*; Ohlmann, G., et al., Eds.; Elsevier: Amsterdam, The Netherlands, 1991; p 275.
- (58) Burkett, S. L.; Davis, M. E. *Microporous Mater.* **1993**, *1*, 265.
- (59) Feijen, E. J. P.; De Vadder, K.; Bosschaerts, M. H.; Lievens, J. L.; Martens, J. A.; Grobet, P. J.; Jacobs, P. A. *J. Am. Chem. Soc.* **1994**, *116*, 2950.
- (60) Oliver, S.; Kuperman, A.; Ozin, G. A. *Angew. Chem., Int. Ed.* **1998**, *37*, 46.
- (61) Vidal, L.; Marichal, C.; Gramlich, V.; Patarin, J.; Gabelica, Z. *Chem. Mater.* **1999**, *11*, 2728.
- (62) Vidal, L.; Gramlich, V.; Patarin, J.; Gabelica, Z. *Eur. J. Solid State Inorg. Chem.* **1998**, *35*, 545.
- (63) Delprato, F.; Delmotte, L.; Guth, J.-L.; Huve, L. *Zeolites* **1990**, *10*, 546.
- (64) De Witte, B.; Patarin, J.; Guth, J.-L.; Cholley, T. *Microporous Mater.* **1997**, *10*, 257.
- (65) Wiebcke, M. *Chem. Commun.* **1991**, 1507.
- (66) Price, G. D.; Pluth, J. J.; Smith, J. V.; Bennett, J. M. *J. Am. Chem. Soc.* **1982**, *104*, 5971.
- (67) Burkett, S. L.; Davis, M. E. *J. Phys. Chem.* **1994**, *98*, 4647.
- (68) de Moor, P. P. E. A.; Beelen, T. P. M.; Komanshek, B. U.; Beck, L. W.; Wagner, P.; Davis, M. E.; van Santen, R. A. *Chem. Eur. J.* **1999**, *5*, 2083.
- (69) Kirschhock, C. E. A.; Ravishankar, R.; Verspeurt, F.; Grobet, P. J.; Jacobs, P. A.; Martens, J. A. *J. Phys. Chem. B* **1999**, *103*, 4965.
- (70) Moscou, L. In *Introduction to Zeolites Science and Practice*; van Bekkum, H., et al., Eds.; Elsevier: Amsterdam, The Netherlands, 1991; p 1.

- (72) Marcilly, C. *Stud. Surf. Sci. Catal.* **2001**, *135*, 37.
- (73) Guggenbichler, J. P.; Hirsch, A. PCT Int. Appl. WO 01 09,229, 2000.
- (74) Liu, M.; Li, X.; An, C.; Li, P. *Faming Zhuanli Shenqing Gongkai Shuomingshu* CN 1,262,591, 2000.
- (75) Hölderich, W. F. *Pure Appl. Chem.* **1986**, *58*, 1383.
- (76) Hölderich, W. F.; Hesse, M.; Näumann, F. *Angew. Chem.* **1988**, *27*, 226.
- (77) Corma, A.; Climent, M. J.; Garcia, H.; Primo, J. *Appl. Catal.* **1989**, *49*, 109.
- (78) Taramasso, A.; Perego, G.; Notari, B. U.S. Patent 4410501, 1983.
- (79) Esposito, A.; Taramasso, M.; Neri, C. Buonuomo, F. U.K. Patent 2116974, 1985.
- (80) Nagy, J. B.; Bodart, P.; Hannus, I.; Kiricsi, I. *Synthesis, Characterization and Use of Zeolitic Microporous Materials*; DecaGen Ltd: Hungary, 1998; p 159.
- (81) Kresge, C. T.; Leonowicz, M. E.; Roth, W. J.; Vartuli, J. C.; Beck, J. S. *Nature* **1992**, *359*, 710.
- (82) Beck, J. S.; Vartuli, J. C.; Roth, W. J.; Leonowicz, M. E.; Kresge, C. T.; Schmitt, K. D.; Chu, C. T. W.; Olson, D. H.; Sheppard, E. W.; McCullen, S. B.; Higgins, J. B.; Schlenker, J. L. *J. Am. Chem. Soc.* **1992**, *114*, 10834.
- (83) Vallet-Regi, M.; Rámila, A.; del Real, R. P.; Pérez-Pariente, J. *Chem. Mater.* **2001**, *13*, 308.
- (84) Monnier, A.; Schüth, F.; Huo, Q.; Kumar, D.; Margolese, D.; Maxwell, R. S.; Stucky, G. D.; Krishnamurthy, M.; Petroff, P.; Firouzi, A.; Janicke, M.; Chmelka, B. F. *Science* **1993**, *261*, 1299.
- (85) Firouzi, A.; Atef, F.; Oertli, A. G.; Stucky, G. D.; Chmelka, B. F. *J. Am. Chem. Soc.* **1997**, *119*, 3596.
- (86) Nakanishi, K. *J. Porous Mater.* **1997**, *4*, 67.
- (87) Kim, J. M.; Han, Y.-J.; Chmelka, B. F.; Stucky, G. D. *Chem. Commun.* **2000**, 2437.
- (88) *The Colloidal Domain Where Physics, Chemistry, Biology and Technology Meet*; Evans, D. F., Wennerström, H., Eds.; VCH Publishers: Weinheim, Germany, 1994.
- (89) Laughlin, R. G. *The Aqueous Phase Behavior of Surfactants*; Academic Press: London, U.K., 1994; p 22.
- (90) Israelachvili, N.; Mitchell, D. J.; Niham, B. W. *J. Chem. Soc., Faraday Trans. 2* **1976**, *72*, 1525.
- (91) *Intermolecular and Surface Forces*, 2nd ed.; Israelachvili, J., Ed.; Academic Press: New York, 1992.
- (92) *Liaisons Intermoléculaires, Les Forces en Jeu dans la Matière Condensée*; Gerschel, A., Ed.; Savoires Actuels, Interéditions/CNRS Editions: Paris, France, 1995.
- (93) *La Juste Argile*; Daoud, M., Williams, C., Eds.; Les Editions de Physique: 1995.
- (94) Huo, Q.; Leon, R.; Petroff, P. M.; Stucky, G. D. *Science* **1995**, *268*, 1324.
- (95) (a) Landry, C. C.; Tolbert, S. H.; Gallis, K. W.; Monnier, A.; Stucky, G. D.; Norby, P.; Hanson, J. C. *Chem. Mater.* **2001**, *13*, 1600. (b) Tolbert, S. H.; Landry, C. C.; Stucky, G. D.; Chmelka, B. F.; Norby, P.; Hanson, J. C.; Monnier, A. *Chem. Mater.* **2001**, *13*, 2247.
- (96) Huo, Q.; Margolese, D. I.; Ciesla, U.; Feng, P.; Gier, T. E.; Sieger, P.; Leon, R.; Petroff, P. M.; Schüth, F.; Stucky, G. D. *Nature* **1994**, *368*, 317.
- (97) This notation has been introduced by Huo et al. to classify the interactions between the inorganic framework (I) and the surfactant (S). The + and - signs refer to their charge. X<sup>-</sup> and M<sup>+</sup> refer to oppositely charged anion or cations, respectively (see Figure 10). The charge matching model will be further discussed below.
- (98) Tanev, P. T.; Chibwe, M.; Pinnavaia, T. J. *Nature* **1994**, *368*, 321.
- (99) Tanev, P. T.; Pinnavaia, T. J. *Science* **1995**, *267*, 865.
- (100) Bagshaw, S. A.; Prouzet, E.; Pinnavaia, T. J. *Science* **1995**, *269*, 1242.
- (101) Bagshaw, S. A.; Pinnavaia, T. J. *Angew. Chem., Int. Ed.* **1996**, *35*, 1102.
- (102) Voegtlin, A.-C.; Ruch, F.; Guth, J.-L.; Patarin, J.; Huve, L. *Microporous Mater.* **1997**, *9*, 95.
- (103) Sayari, A. *Stud. Surf. Sci. Catal.* **1996**, *102*, 1.
- (104) Li, J.; Delmotte, L.; Kessler, H. *Chem. Commun.* **1996**, 1023.
- (105) Olivier, S.; Kupermann, A.; Coombs, N.; Lough, A.; Ozin, G. A. *Nature* **1995**, *378*, 47.
- (106) Feng, P.; Xia, Y.; Feng, J.; Bui, X.; Stucky, G. D. *Chem. Commun.* **1997**, 949.
- (107) Zhao, D.; Feng, J.; Huo, Q.; Melosh, N.; Fredrickson, G. H.; Chmelka, B. F.; Stucky, G. D. *Science* **1998**, *279*, 548.
- (108) Reddy, J. S.; Sayari, A. *Catal. Lett.* **1996**, *38*, 219.
- (109) Yada, M.; Machida, M.; Kijima, T. *Chem. Commun.* **1996**, 769.
- (110) Ulagappan, N.; Rao, C. N. R. *Chem. Commun.* **1996**, 1685.
- (111) Antonelli, D. M.; Ying, J. Y. *Angew. Chem., Int. Ed.* **1995**, *34*, 2014.
- (112) Attard, G. S.; Glyde, J. C.; Goltner, C. G. *Nature* **1995**, *378*, 366.
- (113) Antonelli, D. M.; Ying, J. Y. *Angew. Chem., Int. Ed.* **1996**, *35*, 426.
- (114) Antonelli, D. M.; Ying, J. Y. *Chem. Mater.* **1996**, *8*, 874.
- (115) van Esch, J. H.; Feringa, B. L. *Angew. Chem., Int. Ed.* **2000**, *39*, 2263.
- (116) Terech, P.; Furman, I.; Weiss, R. G.; Bouas-Laurent, H.; Desvergne, J. P.; Ramasseu, R. *Faraday Discuss.* **1995**, *101*, 345.
- (117) Scartazzini, R.; Luisi, P. L. *J. Phys. Chem.* **1988**, *92*, 829.
- (118) Wang, R.; Geiger, C.; Chen, L.; Swanson, B.; Witten, D. G. *J. Am. Chem. Soc.* **2000**, *122*, 2399.
- (119) Galliot, C.; Larré, C.; Caminade, A.-M.; Majoral, J.-P. *Science* **1997**, *277*, 1981.
- (120) (a) Tomalia, D. A.; Durst, H. D. In *Topics in Current Chemistry*; Weber, E., Ed.; Springer-Verlag: Berlin, Germany, 1993; p 193. (b) Issberner, J.; Moors, R.; Vögtle, F. *Angew. Chem., Int. Ed.* **1994**, *33*, 413. (c) Caminade, A.-M.; Majoral, J.-P. *Main Group Chem. News* **1995**, *3*, 14. (d) Aroin, N.; Astruc, D. *Bull. Soc. Chim. Fr.* **1995**, *132*, 876. (e) Newkome, G. R.; Moorefield, C. N.; Vogtle, F. *Dendritic Molecules*; Verlag-Chemie: Weinheim, Germany, 1996.
- (121) Fréchet, J. M. J. *Science* **1994**, *263*, 1710.
- (122) Caminade, A.-M.; Laurent, R.; Chaudret, B.; Majoral, J. P. *Coord. Chem. Rev.* **1998**, *178–180*, 793.
- (123) Knapen, J. W. J.; van der Made, A. W.; de Wilde, J. C.; van Leeuwen, P. W. N. M.; Wijkens, P.; Grove, D. M.; van Koten, G. *Nature* **1994**, *372*, 659.
- (124) Ko, E. I. *CHEMTECH* **1993**, *23*, 31.
- (125) Linder, E.; Kemmler, M.; Mayer, H. A.; Wegner, P. *J. Am. Chem. Soc.* **1994**, *116*, 348.
- (126) Kriesel, J. W.; Tilley, T. D. *Chem. Mater.* **1999**, *11*, 1190.
- (127) Larsen, G.; Lotero, E.; Marquez, M. *J. Phys. Chem. B* **2000**, *104*, 4840.
- (128) Förster, S.; Plantenberg, T. *Angew. Chem., Int. Ed.* **2002**, *41*, 688.
- (129) Förster, S.; Antonietti, M. *Adv. Mater.* **1998**, *10*, 195.
- (130) Cha, J. N.; Stucky, G. D.; Morse, D. E.; Deming, T. J. *Nature* **2000**, *403*, 289.
- (131) Rothen, F.; Pieranski, P. *La Recherche* **1986**, *175*, 313.
- (132) Meng, Q.-B.; Fu, C.-H.; Einaga, Y.; Gu, Z.-Z.; Fujishima, A.; Sato, O. *Chem. Mater.* **2002**, *14*, 83.
- (133) Yang, S. M.; Coombs, N.; Ozin, G. A. *Adv. Mater.* **2000**, *12*, 1940.
- (134) Jiang, P.; Bertone, J. F.; Colvin, V. L. *Science* **2001**, *291*, 5503, and references cited therein.
- (135) Meldrum, F. C.; Douglas, T.; Levi, S.; Arosio, P.; Mann, S. *J. Inorg. Biochem.* **1994**, *58*, 59.
- (136) Meldrum, F. C.; Douglas, T.; Levi, S.; Arosio, P.; Mann, S. *J. Inorg. Biochem.* **1994**, *58*, 59.
- (137) Shenton, W.; Douglas, T.; Young, M.; Stubbs, G.; Mann, S. *Adv. Mater.* **1999**, *11*, 253.
- (138) Ogasawara, W.; Shenton, W.; Davis, S. A.; Mann, S. *Chem. Mater.* **2000**, *12*, 2835.
- (139) Beckwith, D.; Christou, R.; Cook, G.; Göltner, C. G.; Timms, P. L. *Proceedings of Silica 2001*, Second International Conference on Silica, Sept 3–6, 2001, Mulhouse, France.
- (140) Sims, S. D.; Walsh, D.; Mann, S. *Adv. Mater.* **1998**, *10*, 151.
- (141) Imhof, A.; Pine, D. J. *Adv. Mater.* **1998**, *10*, 697.
- (142) Schmidt-Winkel, P.; Lukens, W. W., Jr.; Zhao, D.; Yang, P.; Chmelka, B. F.; Stucky, G. D. *J. Am. Chem. Soc.* **1999**, *121*, 254.
- (143) Ibanez, A.; Maximov, S.; Guiu, A.; Chaillout, C.; Baldeck, P. L. *Adv. Mater.* **1998**, *10*, 1540.
- (144) Yanagisawa, T.; Shimizu, T.; Kuroda, K.; Kato, C. *Bull. Chem. Soc. Jpn.* **1990**, *63*, 988.
- (145) Di Renzo, F.; Cambon, H.; Dutartre, R. *Microporous Mater.* **1997**, *10*, 283.
- (146) Chiola, V.; Ritsko, J. E.; Vanderpool, C. D. U.S. Patent 3,356,725, 1971.
- (147) Martin, T.; Galarneau, A.; Di Renzo, F.; Fajula, F.; Plee, D. *Angew. Chem., Int. Ed.* **2002**, *41*, 2590.
- (148) Zhang, W.; Glomski, B.; Pauly, T. R.; Pinnavaia, T. J. *Chem. Commun.* **1999**, 1803.
- (149) Ulagappan, N.; Rao, C. N. R. *Chem. Commun.* **1996**, 2759.
- (150) Khushalani, D.; Kuperman, A.; Ozin, G. A.; Tanaka, K.; Garces, J.; Olken, M. M.; Coombs, N. *Adv. Mater.* **1995**, *7*, 842.
- (151) Yang, P.; Deng, T.; Zhao, D.; Feng, P.; Pine, D.; Chmelka, B. F.; Whitesides, G. M.; Stucky, G. D. *Science* **1998**, *282*, 2244.
- (152) Antonietti, M.; Berton, B.; Göltner, C.; Hentze, H.-P. *Adv. Mater.* **1998**, *10*, 154.
- (153) Stein, A. *Microporous Mesoporous Mater.* **2001**, *44*, 227.
- (154) Holland, B. T.; Adams, L.; Stein, A. *J. Am. Chem. Soc.* **1999**, *121*, 4308.
- (155) Shimizu, K.; Cha, J.; Stucky, G. D.; Morse, D. E. *Proc. Natl. Acad. Sci. U.S.A.* **1998**, *95*, 6234.
- (156) Ono, Y.; Nanshima, K.; Sano, M.; Kanekiyo, Y.; Inoue, K.; Hojo, J.; Shinkai, S. *Chem. Commun.* **1998**, 1477.
- (157) Stein, A.; Melde, B. J.; Schroden, R. C. *Adv. Mater.* **2000**, *12*, 1403.
- (158) Macquarrie, D. J.; Jackson, D. B.; Tailland, S.; Utting, K. A. *J. Mater. Chem.* **2001**, *11*, 1843.
- (159) Maschmeyer, T.; Rey, F.; Sankar, G.; Thomas, J. M. *Nature* **1995**, *378*, 159.
- (160) Brunel, D.; Cauvel, A.; Fajula, F.; Di Renzo, F. *Stud. Surf. Sci. Catal.* **1995**, *97*, 173.

- (161) Anwander, R. *Chem. Mater.* **2001**, *13*, 4419.
- (162) Burkett, S.; Sims, S. D.; Mann, S. *Chem. Commun.* **1996**, 1367.
- (163) Lim, M. H.; Stein, A. *Chem. Mater.* **1999**, *11*, 3285.
- (164) (a) Prouzet, E.; Pinnavaia, T. *J. Angew. Chem., Int. Ed.* **1997**, *36*, 516. (b) Silva, F. H. P.; Pastore, H. O. *Chem. Commun.* **1996**, 833. (c) Schmidt-Winkel, P.; Yang, P.; Margolese, D. I.; Chmelka, B. F.; Stucky, G. D. *Adv. Mater.* **1999**, *11*, 303.
- (165) Boissière, C.; van der Lee, A.; El Mansouri, A.; Larbot, A.; Prouzet, E. *Chem. Commun.* **1999**, 2047.
- (166) Boissière, C.; Larbot, A.; van der Lee, A.; Kooyman, P.; Prouzet, E. *Chem. Mater.* **2000**, *12*, 2902.
- (167) Kim, J. M.; Han, Y.-J.; Chmelka, B. F.; Stucky, G. D. *Chem. Commun.* **2000**, 2437.
- (168) Reddy, K. M.; Moudrakovski, I.; Sayari, A. *Chem. Commun.* **1994**, 1059.
- (169) Sayari, A.; Danumah, C.; Moudrakovski, I. L. *Chem. Mater.* **1995**, *7*, 813S.
- (170) Gontier, S.; Tuel, A. *Appl. Catal. A* **1996**, *143*, 125C.
- (171) Cheng, F.; He, H.; Zhou, W. Z.; Klinowski, J.; Goncalves, J. A. S.; Gladden, L. F. *J. Phys. Chem.* **1996**, *100*, 390.
- (172) Corma, A.; Pérez-Pariente, M. T. *J. Chem. Commun.* **1994**, 147.
- (173) Cabrera, S.; El-Haskouri, J.; Guillem, C.; Latorre, J.; Beltrán-Porter, A.; Beltrán-Porter, D.; Marcos, M. D.; Amorós, P. *Solid State Sci.* **2000**, *2*, 405.
- (174) Gontier, S.; Tuel, A. *Chem. Mater.* **1996**, *8*, 114.
- (175) Klimova, T.; Rodríguez, E.; Martínez, M.; Ramírez, J. *Microporous Mesoporous Mater.* **2001**, *44–45*, 357.
- (176) Clark, J. H.; MacQuarrie, D. J. *Chem. Commun.* **1998**, 853.
- (177) Brunel, D. *Microporous Mesoporous Mater.* **1999**, *27*, 239.
- (178) MacQuarrie, D. J. *Chem. Commun.* **1996**, 1961.
- (179) Inagaki, S.; Guan, S.; Fukushima, Y.; Ohsuna, T.; Terasaki, O. *J. Am. Chem. Soc.* **1999**, *121*, 9611.
- (180) Melde, B. J.; Holland, B. T.; Blanford, C. F.; Stein, A. *Chem. Mater.* **1999**, *11*, 3302.
- (181) (a) Asefa, T.; MacLachlan, M. J.; Coombs, N.; Ozin, G. A. *Nature* **1999**, *402*, 867. (b) Yoshina-Ishii, C.; Asefa, T.; Coombs, N.; MacLachlan, M. J.; Ozin, G. A. *Chem. Commun.* **1999**, 2539. (c) Asefa, T.; MacLachlan, M. J.; Grondley, H.; Coombs, N.; Ozin, G. A. *Angew. Chem., Int. Ed.* **2000**, *39*, 1808. (d) Asefa, T.; Yoshina-Ishii, C.; MacLachlan, M. J.; Ozin, G. A. *J. Mater. Chem.* **2000**, *10*, 1751.
- (182) Lu, Y.; Fan, H.; Doke, N.; Loy, D. A.; Assink, R. A.; La Van, D. A.; Brinker, C. J. *J. Am. Chem. Soc.* **2000**, *122*, 5258.
- (183) Guan, S.; Inagaki, S.; Ohsuna, T.; Terasaki, O. *J. Am. Chem. Soc.* **2000**, *122*, 5660.
- (184) Inagaki, S.; Guan, S.; Ohsuna, T.; Terasaki, O. *Nature* **2002**, *416*, 304.
- (185) Corriu, R. J. P.; Mehdi, A.; Reyé, C.; Thieuleux, C. *Chem. Commun.* **2002**, 1382.
- (186) Patarin, J.; Lebeau, B.; Zana, R. *Curr. Opin. Colloid Interface Sci.* **2002**, *7*, 107.
- (187) Brinker, C. J.; Lu, Y.; Sellinger, A.; Fan, H. *Adv. Mater.* **1999**, *11*, 579.
- (188) Chen, C.-Y.; Burkett, S. L.; Li H.-X.; Davis, M. E. *Microporous Mater.* **1993**, *2*, 27.
- (189) Steel, A.; Carr, S. W.; Anderson, M. W. *Chem. Commun.* **1994**, 1571.
- (190) Stucky, G. D.; Monnier, A.; Schüth, F.; Huo, Q.; Margolese, D.; Kumar, D.; Krishnamurty, M.; Petroff, P.; Firouzi, A.; Janicke, M.; Chmelka, B. F. *Mol. Cryst. Liq. Cryst.* **1994**, *240*, 187.
- (191) Lindén, M.; Schunk, S. A.; Schüth, F. *Angew. Chem., Int. Ed.* **1998**, *37*, 821.
- (192) O'Brien, S.; Francis, R. J.; Fogg, A.; O'Hare, D.; Okazaki, N.; Kuroda, K. *Chem. Mater.* **1999**, *11*, 1822.
- (193) Firouzi, A.; Kumar, D.; Bull, L. M.; Besier, T.; Sieger, P.; Huo, Q.; Walker, S. A.; Zasadzinski, J. A.; Glinka, C.; Nicol, J.; Margolese, D.; Stucky, G. D.; Chmelka, B. F. *Science* **1995**, *267*, 1138.
- (194) Galarneau, A.; Di Renzo, F.; Fajula, F.; Mollo, L.; Fubini, B.; Ottaviani, M. F. *J. Colloid Interface Sci.* **1998**, *201*, 105.
- (195) Galarneau, A.; Lerner, D.; Ottaviani, M. F.; Di Renzo, F.; Fajula, F. *Mesoporous Molecular Sieves 1998*; Bonnevot, L.; Béland, F.; Danumah, C.; Giasson, S., Eds.; Kluwer Academic Publishers: Amsterdam, The Netherlands, 1998; *Stud. Surf. Sci. Catal.* **1998**, *117*, 405.
- (196) Frasch, J.; Zana, R.; Soulard, M.; Lebeau, B.; Patarin, J. *Langmuir* **1999**, *15*, 2603.
- (197) Frasch, J.; Lebeau, B.; Soulard, M.; Patarin, J.; Zana, R. *Langmuir* **2000**, *16*, 9049.
- (198) Regev, O. *Langmuir* **1996**, *12*, 4940.
- (199) Yao, N.; Ku, A. Y.; Nakagawa, N.; Lee, T.; Saville, D. A.; Aksay, I. A. *Chem. Mater.* **2000**, *12*, 1536, and references cited therein.
- (200) Ruggles, J. L.; Holt, S. A.; Reynolds, P. A.; White, J. M. *Langmuir* **2000**, *16*, 4613, and references cited therein.
- (201) Grosso, D.; Balkenende, A. R.; Albouy, P.-A.; Ayrál, A.; Amenitsch, H.; Babonneau, F. *Chem. Mater.* **2001**, *13*, 1848.
- (202) (a) Soler-Illia, G. J. A. A.; Grosso, D.; Crepaldi, E. L.; Cagnol, F.; Sanchez, C. *Mater. Res. Soc. Symp. Proc.* **2002**, *726*, Q 7.3. (b) Sanchez, C.; Crepaldi, E. L.; Grosso, D.; Soler-Illia, G. J. de A. A. *Mater. Res. Soc. Symp. Proc.* **2002**, *728*, S 1.2.
- (203) Grosso, A. F.; Ruiz, E. J.; Tolbert, S. H. *J. Phys. Chem. B* **2000**, *104*, 5448.
- (204) Grosso, A. F.; Le, V. H.; Kirsch, B. L.; Tolbert, S. H. *Langmuir* **2001**, *17*, 3496.
- (205) (a) Grosso, A. F.; Le, V. H.; Kirsch, B. L.; Riley, A. E.; Tolbert, S. H. *Chem. Mater.* **2001**, *13*, 3571. (b) Grosso, A. F.; Le, V. H.; Kirsch, B. L.; Tolbert, S. H. *J. Am. Chem. Soc.* **2002**, *124*, 3713.
- (206) Che, S.; Kamiya, H.; Terasaki, O.; Tatsumi, T. *J. Am. Chem. Soc.* **2001**, *123*, 12089.
- (207) For a remarkable HRTEM/electron crystallography study of cubic or three-dimensional mesostructured silica, please refer to: (a) Sakamoto, Y.; Kaneda, M.; Terasaki, O.; Zhao, D. Y.; Kim, J. M.; Stucky, G. D.; Shin, H. J.; Ryoo, R. *Nature* **2000**, *408*, 449. (b) Sakamoto, Y.; Díaz, I.; Terasaki, O.; Zhao, D. Y.; Pérez-Pariente, J.; Kim, J. M.; Stucky, G. D. *J. Phys. Chem. B* **2002**, *106*, 3118.
- (208) Koyano, K. A.; Tatsumi, T.; Tanaka, Y.; Nakata, S. *J. Phys. Chem. B* **1997**, *101*, 9436.
- (209) Xia, Q. H.; Hidajat, K.; Kawi, S. *Mater. Lett.* **2000**, *42* (1–2), 102.
- (210) Zhang, Z.; Han, Y.; Xiao, F. S.; Qiu, S.; Zhu, L.; Wang, R.; Yu, Y.; Zhang, Z.; Zou, B.; Wang, Y.; Sun, H.; Zhao, D.; Wei, Y. *J. Am. Chem. Soc.* **2001**, *123*, 5014.
- (211) A complete review in mesoporosity issues: Kruk, M.; Jaroniec, M. *Chem. Mater.* **2001**, *13*, 3169. See also Davidson, A. *Curr. Opin. Colloid Interface Sci.* **2002**, *7*, 92.
- (212) Keene, M. T. J.; Gougeon, R. D. M.; Denoyel, R.; Harris, R. K.; Rouquerol, J.; Llewellyn, P. L. *J. Mater. Chem.* **1999**, *9*, 2843.
- (213) Impéror-Clerc, M.; Davidson, P.; Davidson, A. *J. Am. Chem. Soc.* **2000**, *122*, 11925.
- (214) (a) Melosh, N. A.; Lipic, P.; Bates, S. F.; Wudl, F.; Stucky, G. D.; Fredrickson, G. H.; Chmelka, B. F. *Macromolecules* **1999**, *32*, 4332. (b) De Paul, S.; Zwanziger, J. W.; Ulrich, R.; Wiesner, U.; Spiess, H. W. *J. Am. Chem. Soc.* **1999**, *121*, 5727. (c) Finnefrock, A. C.; Ulrich, R.; Du Chesne, A.; Honeker, C.; Schumacher, K.; Unger, K. K.; Gruner, S.; Wiesner, U. *Angew. Chem. Int. Ed.* **2001**, *40*, 1208. (d) Templin, M.; Franck, A.; Du Chesne, A.; Leist, H.; Zhang, Y.; Ulrich, R.; Schädler, V.; Wiesner, U. *Science* **1997**, *278*, 1795. (e) For a thorough discussion of these works, refer to Simon, P. F. W.; Ulrich, R.; Spiess, H. W.; Wiesner, U. *Chem. Mater.* **2001**, *13*, 3464.
- (215) Galarneau, A.; Cambon, H.; Di Renzo, F.; Fajula, F. *Langmuir* **2001**, *17*, 8328.
- (216) (a) Ryoo, R.; Joo, S. H.; Jun, S. H. *J. Phys. Chem. B* **1999**, *103*, 7743. (b) Attard, G. S.; Bartlett, P. N.; Coleman, N. R. B.; Elliott, J. M.; Owen, J. R.; Wang, J. H. *Science* **1997**, *278*, 838. For a recent review on electrochemical deposition of periodic non-oxide materials, see: Braun, P. V.; Wiltzius, P. *Curr. Opin. Colloid Interface Sci.* **2002**, *7*, 116.
- (217) Ciesla, U.; Demuth, D.; Leon, R.; Petroff, P.; Stucky, G. D.; Unger, K. K.; Schüth, F. *Chem. Commun.* **1994**, 1387.
- (218) Ciesla, U.; Schacht, S.; Stucky, G. D.; Unger, K. K.; Schüth, F. *Angew. Chem., Int. Ed.* **1996**, *35*, 541.
- (219) Vaudry, F.; Khodabandeh, S.; Davis, M. E. *Chem. Mater.* **1996**, *8*, 1451.
- (220) Yada, M.; Hiyoshi, H.; Machida, M.; Kijima, T. *J. Porous Mater.* **1998**, *5*, 133.
- (221) Kimura, T.; Sugahara, Y.; Kuroda, K. *Chem. Mater.* **1999**, *11*, 508.
- (222) Cabrera, S.; El-Haskouri, J.; Alamo, J.; Beltrán, A.; Mendoroz, S.; Marcos, M. D.; Amorós, P. *Adv. Mater.* **1999**, *11*, 379.
- (223) Valange, S.; Guth, J.-L.; Kolenda, F.; Lacombe, S.; Gabelica, Z. *Microporous Mesoporous Mater.* **2000**, *35–36*, 597.
- (224) Yada, M.; Takenaka, H.; Machida, M.; Kijima, T. *J. Chem. Soc., Dalton Trans.* **1998**, 1547.
- (225) Severin, K. G.; Abdel-Fattah, T. M.; Pinnavaia, T. *Chem. Commun.* **1998**, 1471.
- (226) Qi, L.; Ma, J.; Cheng, H.; Zhao, Z. *Langmuir* **1998**, *14*, 2579.
- (227) Chen, F.; Liu, M. *Chem. Commun.* **1999**, 1829.
- (228) Hyodo, T.; Nishida, N.; Shimizu, Y.; Egashira, M. *Nippon Seramikkusu Kyokai Gakujutsu Ronbunshi* **2001**, *109*, 481.
- (229) Fröba, M.; Muth, O.; Reller, A. *Solid State Ionics* **1997**, *101–103*, 249.
- (230) Putnam, R. L.; Nakagawa, N.; McGrath, K. M.; Yao, N.; Aksay, I. A.; Gruner, S. M.; Navrotsky, A. *Chem. Mater.* **1997**, *9*, 2690.
- (231) Khushalani, D.; Dag, Ö.; Ozin, G. A.; Kuperman, A. *J. Mater. Chem.* **1999**, *9*, 1500.
- (232) Trong On, D. *Langmuir* **1999**, *15*, 8561.
- (233) Antonelli, D. M. *Microporous Mesoporous Mater.* **1999**, *30*, 315.
- (234) Lin, W.; Pang, W.; Sun, J.; Shen, J. *J. Mater. Chem.* **1999**, *9*, 641.
- (235) Lindén, M.; Blanchard, J.; Schacht, S.; Schunk, S.; Schüth, F. *Chem. Mater.* **1999**, *11*, 3002.
- (236) Cabrera, S.; El-Haskouri, J.; Beltrán-Porter, A.; Beltrán-Porter, D.; Marcos, M. D.; Amorós, P. *Solid State Sci.* **2000**, *2*, 513.
- (237) Blanchard, J.; Schüth, F.; Trens, P.; Hudson, M. *Microporous Mesoporous Mater.* **2000**, *39*, 163.

- (238) Soler-Illia, G. J. A. A.; Sanchez, C. *New J. Chem.* **2000**, *24*, 493.
- (239) Soler-Illia, G. J. A. A.; Scolan, E.; Louis, A.; Albouy, P.-A.; Sanchez, C. *New J. Chem.* **2001**, *25*, 154.
- (240) Abe, T.; Taguchi, A.; Iwamoto, M. *Chem. Mater.* **1995**, *7*, 1429.
- (241) Luca, V.; MacLachlan, D. J.; Hook J. M.; Withers, R. *Chem. Mater.* **1995**, *7*, 2220.
- (242) Doi, T.; Miyake, T. *J. Chem. Soc., Chem. Commun.* **1996**, 1635.
- (243) Liu, P.; Moudrakovski, I.; Liu, J.; Sayari, A. *Chem. Mater.* **1997**, *9*, 513.
- (244) El Haskouri, J.; Roca, M.; Cabrera, S.; Alamo, J.; Beltrán-Porter, A.; Beltrán-Porter, D.; Marcos, M. D.; Amorós, P. *Chem. Mater.* **1999**, *11*, 1446.
- (245) Mizuno, N.; Hatayama, H.; Uchida, S.; Aguchi, T. *Chem. Mater.* **2001**, *13*, 179.
- (246) Michot, L.; Mathieu, C.; Bouquet, E. *C. R. Acad. Sci. Paris, Ser. II C* **1998**, 167.
- (247) Guo, X.; Ding, W.; Wang, X.; Yan, Q. *Chem. Commun.* **2001**, 709.
- (248) **Tiang, Z.-R.; Tong, W.; Wang, J.-Y.; Duan, N.-G.; Krishnan, V. V.; Suib, S. L. *Science* **1997**, *276*, 926.**
- (249) **Luo J.; Suib, S. L. *Chem. Commun.* **1997**, 1031.**
- (250) (a) **Hudson, M. J.; Knowles, J. A. *Chem. Commun.* **1995**, 1083.** (b) Hudson, M. J.; Knowles, J. A. *J. Mater. Chem.* **1996**, *6*, 89.
- (251) Kim, A. Y.; Bruinsma, P. J.; Chen, Y. L.; Liu, J. *Mater. Res. Symp. Proc.* **1996**, 435, 131.
- (252) Huang, Y. Y.; McCarthy, T. J.; Sachtler, W. M. H. *Appl. Catal. A* **1996**, *148*, 135.
- (253) (a) Pacheco, G.; Zhao, E.; García, A.; Sklyarov, A.; Fripiat, J. J. *Chem. Commun.* **1997**, 491. (b) Pacheco, G.; Zhao, E.; García, A.; Sklyarov, A.; Fripiat, J. J. *J. Mater. Chem.* **1998**, *8*, 219. (c) Zhao, E.; Hernández, O.; Pacheco, G.; Hardcastle, S.; Fripiat, J. J. *J. Mater. Chem.* **1998**, *8*, 1635.
- (254) Wong, M. S.; Ying, J. Y. *Chem. Mater.* **1998**, *10*, 2067.
- (255) Liu, P.; Liu, J.; Sayari, A. *Chem. Commun.* **1997**, 577.
- (256) Antonelli, D. M.; Nakahira, A.; Ying, J. Y. *Inorg. Chem.* **1996**, *35*, 3126.
- (257) Stein, A.; Fendorf, M.; Jarvie, T. P.; Mueller, K. T.; Benesi, A. J.; Mallouk, T. E. *Chem. Mater.* **1995**, *7*, 304.
- (258) Mamak, M.; Coombs, N.; Ozin, G. A. *Adv. Mater.* **2000**, *12*, 198.
- (259) Yada, M.; Kitamura, H.; Ichinose, A.; Machida, M.; Kijima, T. *Angew. Chem., Int. Ed.* **1999**, *38*, 3506.
- (260) Yang, P.; Zhao, D.; Margolese, D. I.; Chmelka, B. F.; Stucky, G. D. *Nature* **1998**, *396*, 512.
- (261) Yang, P.; Zhao, D.; Margolese, D. I.; Chmelka, B. F.; Stucky, G. D. *Chem. Mater.* **1999**, *11*, 2813.
- (262) Kriesel, J. W.; Sander, M. S.; Tilley, T. D. *Adv. Mater.* **2001**, *13*, 331.
- (263) Kriesel, J. W.; Sander, M. S.; Tilley, T. D. *Chem. Mater.* **2001**, *13*, 3554.
- (264) Idrissi-Kandri, N.; Ayril, A.; Klotz, M.; Albouy, P.-A.; El Mansouri, A.; van der Lee, A.; Guizard, C. *Mater. Lett. (Gen. Ed.)* **2001**, *50*, 57.
- (265) Pidol, L.; Grosso, D.; Soler-Illia, G. J. A. A.; Crepaldi, E. L.; Sanchez, C.; Albouy, P.-A.; Amenitsch, H.; Euzen, P. *J. Mater. Chem.* **2002**, *12*, 557.
- (266) Grosso, D.; Soler-Illia, G. J. A. A.; Babonneau, F.; Sanchez, C.; Albouy, P.-A.; Brunet-Bruneau, A.; Balkenende, A. R. *Adv. Mater.* **2001**, *13*, 1085.
- (267) Yun, H.; Miyazawa, K.; Zhou, H.; Honma, I.; Kuwabara, M. *Adv. Mater.* **2001**, *13*, 1377.
- (268) Hwang, Y. K.; Lee, K.-C.; Kwon, Y.-U. *Chem. Commun.* **2001**, 1738.
- (269) Alberius-Henning, P.; Frindell, K. L.; Hayward, R. C.; Kramer, E. J.; Stucky, G. D.; Chmelka, B. F. *Chem. Mater.* **2002**, *14*, 3284.
- (270) (a) Crepaldi, E.; Soler-Illia, G. J. A. A.; Grosso, D.; Albouy, P.-A.; Sanchez, C. *Chem. Commun.* **2001**, 1582. (b) Crepaldi, E.; Soler-Illia, G. J. A. A.; Bouchara, A.; Grosso, D.; Durand, D.; Sanchez, C. *Angew. Chem. Int. Ed.* **2002**, in press.
- (271) (a) Crepaldi, E.; Grosso, D.; Soler-Illia, G. J. A. A.; Albouy, P.-A.; Amenitsch, H.; Sanchez, C. *Chem. Mater.* **2002**, *14*, 3316. (b) Crepaldi, E.; Soler-Illia, G. J. A. A.; Grosso, D.; Albouy, P.-A.; Amenitsch, H.; Sanchez, C. *Stud. Surf. Sci. Catal.* **2002**, *141*, 235. (c) Grosso, D.; Soler-Illia, G. J. A. A.; Crepaldi, E.; Sanchez, C. *Adv. Funct. Mater.* **2002**, in press. (d) Soler-Illia, G. J. A. A.; Crepaldi, E.; Grosso, D.; Sanchez, C. *Chem. Commun.* **2002**, in press.
- (272) Cheng, W.; Baudrin, E.; Dunn, B.; Zink, J. J. *J. Mater. Chem.* **2001**, *11*, 92.
- (273) Baes, C. F., Jr.; Mesmer, R. E. *The Hydrolysis of Cations*; Wiley: New York, 1976; p 374.
- (274) Ciesla, U.; Fröba, M.; Stucky, G. D.; Schüth, F. *Chem. Mater.* **1999**, *11*, 227.
- (275) Kim, J. M.; Shin, C. H.; Ryoo, R. *Catal. Today* **1997**, *38*, 221.
- (276) See, for example: Soler-Illia, G. J. A. A.; Jobbágy, M.; Candal, R. J.; Regazzoni, A. E.; Blesa, M. A. *J. Dispers. Sci. Technol.* **1998**, *19*, 207.
- (277) Yada, M.; Machida, M.; Kijima, T. *Chem. Commun.* **1996**, 769.
- (278) Yada, M.; Kitamura, H.; Machida, M.; Kijima, T. *Inorg. Chem.* **1998**, *37*, 6470.
- (279) Yada, M.; Ohya, M.; Machida, M.; Kijima, T. *Chem. Commun.* **1998**, 1941.
- (280) Yada, M.; Ohya, M.; Machida, M.; Kijima, T. *Langmuir* **2000**, *16*, 4752.
- (281) Yada, M.; Ohya, M.; Ohe, K.; Machida, M.; Kijima, T. *Langmuir* **2000**, *16*, 1535.
- (282) Sanchez, C.; Livage, J.; Henry, M.; Babonneau, F. *J. Non-Cryst. Solids* **1988**, *100*, 650.
- (283) Soler-Illia, G. J. A. A.; Louis, A.; Sanchez, C. *Chem. Mater.* **2002**, *14*, 750.
- (284) Tiemann, M.; Fröba, M.; Rapp, G.; Funari, S. S. *Chem. Mater.* **2000**, *12*, 1342.
- (285) Kluson, P.; Kacer, P.; Cajtami, T.; Kalaji, M. *J. Mater. Chem.* **2001**, *11*, 644.
- (286) See, for example: Vioux, A.; Leclerc, D. *Heterog. Chem. Rev.* **1996**, *3*, 65. These processes take place in anhydrous media, in mild hydrothermal conditions ( $T > 110$  °C). In the presence of metallo-organic precursors containing alkoxy (M-OR) or alkoxy and halogenide (M-X) groups, the following reactions lead to the formation of a continuous metal-oxo network:  $MCl_2(OR)_2 \rightarrow MO_2 + 2RCl$  ( $M = Ti, Zr, \dots$ ) (2). These "water-less" condensation reactions may also yield ether molecules (R-O-R) as a product. This is a "clean" reaction when water is to be avoided and should be an interesting route for the synthesis of TM-based mesostructures.
- (287) (a) Yang, H.; Coombs, N.; Kuperman, A.; Mamiche-Afara, S.; Ozin, G. A. *Nature* **1996**, 379. (b) Ozin, G. A.; Yang, H.; Coombs, N. *Nature* **1996**, *381*, 589.
- (288) Bruinsma, P. J.; Kim, A. Y.; Liu, J.; Baskaran, S. *Chem. Mater.* **1997**, *9*, 2507.
- (289) Lu, Y.; Fan, H.; Stump, A.; Ward, T. L.; Rieker, T.; Brinker, C. J. *Nature* **1999**, *398*, 223.
- (290) Sanchez, C.; Soler-Illia, G. J. A. A.; Rozes, L.; Caminade, A.-M.; Turrin, C.-O. Majoral, J.-P. *Mater. Res. Soc. Symp. Proc.* **2000**, *628*, CC 6.2.3.
- (291) Frindell, K. L.; Bartl, M. H.; Popitsch, A.; Stucky, G. D. *Angew. Chem., Int. Ed.* **2002**, *41*, 960.
- (292) Spahr, M. E.; Bitterli, P.; Nesper, R.; Müller, M.; Krumeich, F.; Nissen, H. U. *Angew. Chem., Int. Ed.* **1998**, *37*, 1263.
- (293) Muhr, H.-J.; Krumeich, F.; Schönholzer, U. P.; Bieri, F.; Niederberger, M.; Gauckler, L. J.; Nesper, R. *Adv. Mater.* **2000**, *12*, 231.
- (294) Chandrappa, G. T.; Steunou, N.; Cassaignon, S.; Livage, J. *J. Sol-Gel Sci. Technol.* **2003**, in press.
- (295) **Brock, S. L.; Duan, N.; Tian, Z. R.; Giraldo, O.; Zhou, H.; Suib, S. L. *Chem. Mater.* **1998**, *10*, 2619.**
- (296) (a) Fu, G.; Fyfe, C. A.; Schwiager, W.; Kokotailo, G. T. *Angew. Chem., Int. Ed.* **1995**, *34*, 1499. (b) Fyfe, C. A.; Fu, G. *J. Am. Chem. Soc.* **1995**, *117*, 9709.
- (297) Janauer, G. J.; Doble, A.; Guo, J.; Zavlij, P.; Wittingham, M. S. *Chem. Mater.* **1996**, *8*, 2096.
- (298) Holland, B. T.; Isbester, P. K.; Blanford, C. F.; Munson, E. J.; Stein, A. *J. Am. Chem. Soc.* **1997**, *119*, 6796.
- (299) Holland, B. T.; Isbester, P. K.; Munson, E. J.; Stein, A. *Mater. Res. Bull.* **1999**, *34*, 471.
- (300) Kron, D. A.; Holland, B. T.; Wipson, R.; Maleke, C.; Stein, A. *Langmuir* **1999**, *15*, 8300.
- (301) (a) Steunou, N.; Sanchez, C.; Florian, P.; Förster, S.; Göltner, C.; Antonietti, M. In *Sol-Gel Commercialization and Applications*; Feng, S., Klein, L. C., Pope, E. J. A., Komarneni, S., Eds.; Ceramic Transactions; American Ceramic Society: Westerville, OH, 2001; Vol. 123, p 49. (b) Steunou, N.; Förster, S.; Florian, P.; Antonietti, M.; Sanchez, C. *J. Mater. Chem.* **2002**, in press.
- (302) Soler-Illia, G. J. A. A.; Rozes, L.; Boggiano, M. K.; Sanchez, C.; Turrin, C.-O.; Caminade, A.-M.; Majoral, J.-P. *Angew. Chem., Int. Ed.* **2000**, *39*, 4250.
- (303) Elder, S. H.; Gao, Y.; Li, X.; Liu, J.; McCready, D. E.; Windisch, C. F., Jr. *Chem. Mater.* **1998**, *10*, 3140.
- (304) (a) Zachariasen, W. H. *J. Am. Chem. Soc.* **1932**, *54*, 3841. (b) West, A. R. *Solid State Chemistry and its Applications*; Wiley: Chichester, U.K., 1984; p 596.
- (305) Férey, G. *Chem. Mater.* **2001**, *13*, 3084.
- (306) Luca, V.; Hook, J. M. *Chem. Mater.* **1997**, *9*, 2731.
- (307) Leontidis, E. *Curr. Opin. Colloid Interface Sci.* **2002**, *7*, 81.
- (308) Pacheco, G.; Fripiat, J. J. *J. Phys. Chem. B* **2000**, *104*, 11906.
- (309) Blanchard, J.; Ribot, F.; Sanchez, C.; Bellot, P.-V.; Trokiner, A. *J. Non-Cryst. Sol.* **2000**, *265*, 83.
- (310) Neeraj, S.; Rao, C. N. R. *J. Mater. Chem.* **1998**, *8*, 1631.
- (311) Yagi, Y.; Zhou, H.; Miyayama, M.; Kudo, T.; Honma, I. *Langmuir* **2001**, *17*, 1328.
- (312) (a) Wang, Y.-Q.; Tang, X.; Ying, L.; Huang, W.; Rosenfeld-Hachoen, Y.; Gedanken, A. *Adv. Mater.* **2000**, *12*, 1183. (b) Wang, Y.-Q.; Chen, S.-G.; Tang, X.-H.; Palchik, O.; Zaban, A.; Koltypin, Y.; Gedanken, A. *J. Mater. Chem.* **2001**, *11*, 521.
- (313) Stone, V. F.; Davis, R. J. *Chem. Mater.* **1998**, *10*, 1468.
- (314) (a) Kleitz, F.; Schmidt, W.; Schüth, F. *Microporous Mesoporous Mater.* **2001**, *44-45*, 95. (b) Crepaldi, E.; Soler-Illia, G. J. A. A.; Grosso, D.; Sanchez, C.; *New J. Chem.* **2003**, *27*, in press.

- (315) Büchel, G.; Denoyel, R.; Llewellyn, P. L.; Rouquerol, J. *J. Mater. Chem.* **2001**, *11*, 589.
- (316) Clark, T.; Ruiz, J. D.; Fan, H.; Brinker, C. J.; Swanson, B. I.; Parikh, A. N. *Chem. Mater.* **2000**, *12*, 3879.
- (317) Zhao, D.; Yang, P.; Chmelka, B. F.; Stucky, G. D. *Chem. Mater.* **1999**, *11*, 1174.
- (318) Yang, H.; Ozin, G. A.; Kresge, C. T. *Adv. Mater.* **1998**, *10*, 883.
- (319) Yang, S. M.; Solokov, I.; Coombs, N.; Kresge, C. T.; Ozin, G. A. *Adv. Mater.* **1999**, *11*, 1427.
- (320) (a) Huo, Q.; Zhao, D.; Feng, J.; Weston, K.; Buratto, S. K.; Stucky, G. D.; Schacht, S.; Schüth, F. *Adv. Mater.* **1997**, *9*, 974. (b) Kleitz, F.; Wilczok, U.; Schüth, F.; Marlow, F. *Phys. Chem. Chem. Phys.* **2001**, *3*, 3486.
- (321) Trau, M.; Yao, N.; Kim, E.; Xia, Y.; Whitesides, G. M.; Aksay, I. A. *Nature* **1997**, *390*, 674.
- (322) Huang, L.; Wang, Z.; Sun, J.; Miao, L.; Li, Q.; Yan, Y.; Zhao, D. *J. Am. Chem. Soc.* **2000**, *122*, 3530.
- (323) Bouchara, A.; Soler-Illia, G. J. de A. A.; Chane-Ching, J.-Y.; Sanchez, C. *Chem. Commun.* **2002**, 1234.
- (324) Gronwald, O.; Snip, E.; Shinkai, S. *Curr. Opin. Colloid Interface Sci.* **2002**, *7*, 148.
- (325) (a) Clavier, G.; Pozzo, J. L.; Bouas-Laurent, H.; Lière, C.; Roux, C.; Sanchez, C. *J. Mater. Chem.* **2000**, *10*, 1725. (b) Llusar, M.; Pídol, L.; Roux, C.; Pozzo, J. L.; Sanchez, C. *Chem. Mater.*, in press.
- (326) Ono, Y.; Kanekiyo, Y.; Inoue, K.; Hojo, J.; Nango, M.; Shinkai, S. *Chem. Lett.* **1999**, 475.
- (327) Oishi, G. K.; Ishi-i, T.; Sano, M.; Shinkai, S. *Chem. Lett.* **1999**, 1089.
- (328) Ono, Y.; Nakashima, K.; Sano, M.; Hojo, J.; Shinkai, S. *Chem. Lett.* **1999**, 1119.
- (329) Kobayashi, S.; Hanabusa, K.; Susuki, M.; Kimura, M.; Shirai, H. *Chem. Lett.* **1999**, 1077.
- (330) Kobayashi, S.; Hanabusa, K.; Hamasaki, N.; Kimura, M.; Shirai, H. *Chem. Mater.* **2000**, *12*, 1523.
- (331) Jung, J. H.; Ono, Y.; Hanabusa, K.; Shinkai, S. *J. Am. Chem. Soc.* **2000**, *122*, 5008.
- (332) Jung, J. H.; Ono, Y.; Shinkai, S. *Angew. Chem., Int. Ed.* **2000**, *39*, 1862.
- (333) Jung, J. H.; Ono, Y.; Shinkai, S. *Langmuir* **2000**, *16*, 1643.
- (334) Moreau, J. E.; Vellutini, L.; Man, M. W. C.; Bied, C. *J. Am. Chem. Soc.* **2001**, *123*, 1509.
- (335) An idea of this is the increasing number of meetings or symposia dedicated to the field. See, for example: (a) *Nanoporous Materials III*, *Stud. Surf. Sci. Catal.* Sayari, A., Jaroniec, M., Eds.; Elsevier: Amsterdam, The Netherlands, 2002; Vol. 141. (b) Special Issue of *Microporous Mesoporous Mater.* **2001**, *44–45*, 1–812 (dedicated to the 13th International Zeolite Conference, Montpellier, 2001). (c) *Proceedings of the 3rd International Mesoporous Materials Symposium*; Korean Zeolite Association: Jengju, South Korea, 2002. (d) *Mater. Res. Soc. Symp. Proc.* **2002**, Vols 726 and 728, in press.
- (336) Sone, E. D.; Zubarev, E. R.; Stupp, S. *Angew. Chem., Int. Ed.* **2002**, *41*, 1706.
- (337) Ryoo, R.; Sang, H. Y.; Kruk, M.; Jaroniec, M. *Adv. Mater.* **2001**, *13*, 677.
- (338) Milic, T. N.; Chi, N.; Yablon, D. G.; Flynn, G. W.; Batteas, J. D.; Drain, C. M. *Angew. Chem., Int. Ed.* **2002**, *41*, 2117.
- (339) Yang, P.; Deng, T.; Zhao, D.; Feng, P.; Pine, D.; Chmelka, B. F.; Whitesides, G. M.; Stucky, G. D. *Science* **1998**, *282*, 5397.

CR0200062